INVESTIGATION OF ELECTRICAL PROPERTIES OF FIELD GRADING MATERIALS BASED ZNO MICROVARISTORS

A thesis submitted to Cardiff University in the candidature for the

degree of

Doctor of Philosophy

by

Hafisoh Ahmad, B.Eng., M.Eng.

School of Engineering, Cardiff University

United Kingdom

January 2017

DECLARATIONS AND

STATEMENTS

DECLARATION

This work has not previously been accepted in substance for any degree and is not

concurrently submitted in candidature for any degree.

Signed …………………….…… (Hafisoh Ahmad) Date………..……….

STATEMENT 1

This thesis is being submitted in partial fulfilment of the requirements for the degree

of Doctor of Philosophy (PhD).

Signed …………………….…… (Hafisoh Ahmad) Date………..……….

STATEMENT 2

This thesis is the result of my own independent work/investigation, except where

otherwise stated. Other sources are acknowledged by explicit references.

Signed …………………….…… (Hafisoh Ahmad) Date………..……….

STATEMENT 3

I hereby give consent for my thesis, if accepted, to be available for photocopying

and for inter-library loan, and for the title and summary to be made available to

outside organisations.

Signed …………………….…… (Hafisoh Ahmad) Date………..……….

ABSTRACT

Field grading material based microvaristors are widely used to minimise the localised field enhancement which could trigger corona and partial discharges in high voltage equipment. In this research, two different microvaristor powders, *A* and *B* are composed of silicone rubber matrix at certain filler concentration. The fabrication process of this composite is done by mixing the insulating matrix with filler using high shear mixer, follow by degassing and curing. The additional procedure, heat treatment, is introduced to avoid the agglomeration risk. Such challenges during running this process are well discussed.

The composites are subjected to three high voltage tests, alternating current (AC), direct current (DC) and impulse. The non-linearity behaviour of these composite is characterised as dependent on the microvaristor loading, material properties and voltage application. The microscopic evaluations are conducted to examine the effect of material properties toward the electrical properties of composites.

An 11 kV polymeric insulator has been modelled and simulated in COMSOL® platform. The performance of this insulator is assessed under a number of simulation scenarios. The potential voltage and field profile of this insulator are identified. Such improvement of field distribution along the insulator is required, therefore the electrical properties of field grading material is adopted into numerical simulation. The introduction of microvaristor material with an appropriate switching characteristic has led to a substantial improvement in the electric field and heat distributions along the insulator profile.

ACKNOWLEDGEMENTS

All praise is due to Allah, the most gracious, the most merciful.

Peace and blessings be upon our Prophet Muhammad s.a.w and upon his family and companions.

***

To :

My husband, Hafizul Azizi Ismail

My son, Aariz Rahil Azizi

My daughter, Aaira Raisya Aziza

My late father, Mr Ahmad (25th May 1944-8th December 2016)

and mother Mrs Rodziah

PUBLICATIONS

Conference Proceedings:

1) H. Ahmad, A. Haddad, H. Griffiths, S. Robson, T. Nishimura, N. Tsukamoto, "Electrical properties of field grading material", in 19th International Symposium on High Voltage Engineering, Pilsen, Republic Czech, 23-28 August 2015.

2) H. Ahmad, A. Haddad, H. Griffiths, S. Robson, T. Nishimura, N. Tsukamoto, "Electrical characterisation of ZnO microvaristor materials and compounds", in IEEE Conference on Electrical Insulation and Dielectric Phenomena (CEIDP) 2015, pp 688-692, Ann Arbor, Michigan, USA, 18-21 October 2015.

3) A. Haddad, H. Ahmad, D. Silva, "Current discrimination in ZnO surge arresters for circuit parameters and condition monitoring", in INMR-World Congress on Insulators, Arresters, Bushings & Cable Accessories 2015, Munich, Germany, 18-21 October 2015.

4) H. Ahmad, A. Haddad, H. Griffiths, S. Robson, "Electrical properties of field grading materials compounded silicone rubber", in UHVnet 2015, Staffordshire, UK, 14-15 January 2015   .

TABLE OF CONTENTS

LIST OF FIGURES

LIST OF TABLES

LIST OF ABBREVIATIONS

AC   Alternating current

BEM   Boundary Element Method

DAQ   Data acquisition

DC   Direct current

DSO   Digital signal oscilloscope

EDX   Energy Dispersive X-Ray Spectroscopy

EPDM   Ethylene Propylene Diene Monomer

FEM   Finite Element Method

GFRP   Glass Fibre Reinforced Plastic

HV   High voltage

LMW   Low molecular weight

POW   Point on Wave

PDE   Partial Differential Equations

SiC   Silicon carbide

SEM   Scanning Electron Microscopy

UHV   Ultra High Vacuum

XPS   X-ray Photoelectron Spectroscopy

ZnO   Zinc oxide

LIST OF SYMBOLS

ε_r	Relative permittivity
ε_o	Permittivity of free space, $0.8541878176... \times 10^{-12}$ F/m
σ	Conductivity
ρ	Resistivity
A	Surface area
E	Electrical field
E_o	Threshold electrical field
J	Current density
P_{area}	Dissipated power per unit area
P_{volume}	Dissipated power per unit volume
I	Current
I_t	Total leakage current
I_r	Resistive current
I_c	Capacitive current
V	Voltage
t_p	Thickness of pollution layer
C	Capacitance
°C	Degree Celsius
α	Constant value of the switching threshold
wt. %	Weight percentage
vol. %	Volume percentage

CHAPTER 1

INTRODUCTION

1.1   BACKGROUND

In the modern era, the introduction of polymer based composite material has been widely accepted by industry and academia, since these materials exhibit extraordinary mechanical, electrical and thermal properties. In their technical report [1], Momen et al. identified a number of fillers that can be used to improve the performance and resistance of polymeric materials. The filler mixture composites were produced by dispersing fillers homogenously in the host matrix at a certain percentage, according to weight (wt. %), or according to volume (vol. %).

Field grading material is an example of a composite material that consists of an insulating matrix, filled with semi-conductive or conductive fillers [2]. Zinc oxide (ZnO) microvaristor powder is an example filler which may be deployed in field grading systems. The compounding of this material with the host matrix allows it to be used in situations requiring high voltage protection, such as at the terminals of high voltage cables or to provide electrostatic discharge protection (ESD) to electronic equipment.

Microvaristors were originally developed in Japan [3], before their use spread to electrical protection in America. This ceramic material exhibits a nonlinear current-field characteristic that can be tuned for specific applications and, significantly, can

be used for electric field control in medium voltage (MV) and high voltage (HV) systems [4]–[6]. This material operates in a similar manner to the back-to-back Zener diode and has superior voltage-current (V-I) characteristics and energy handling capabilities.

Figure 1.1 shows a magnified optical image of silicone rubber filled with ZnO microvaristors and it can be seen that microvaristor grains are uniformly dispersed within the compound. In general, the structure of microvaristor grains is similar to a small electro ceramics, surrounded by thin electrically insulating barriers. Because of its nature, the boundary of each grain will contribute to a certain level of switching voltage and improve the V-I nonlinearity effect. In addition, the nonlinearity of this material can be tailored by doping the elements and controlling the sintering parameters [7], [8], which means that it can be readily engineered for specific needs.

200 μm
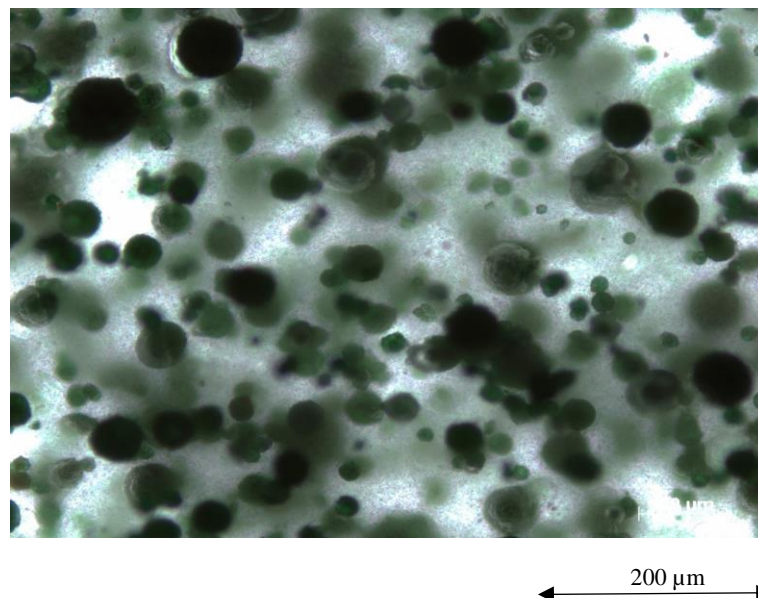
Figure 1.1: An optical micrograph of silicone rubber filled with ZnO microvaristors compound.

Conversely, the behaviour of other non-linear materials, such as silicon carbide (SiC) and carbon black, are based on particle contacts. The investigation carried out by Donzel et al. [9], [10] showed that these two materials exhibit many disadvantages, such as difficulty in controlling the material formulation, lower resistance, lower reproducibility and a propensity to lose electrical characteristics under transient conditions. Therefore, the opportunity has arisen to increase the potential of microvaristor powder and compound in power system applications.

1.2   MOTIVATION AND OBJECTIVES

In general, microvaristor compounds are extensively used in high voltage insulation, particularly in order to mitigate high electrical stress on high voltage equipment [8], [11], [12]. Microvaristor compound based polymers exhibit excellent non-linear material properties and offer flexibility of design, light weight and ease of installation. Research into microvaristor compounds is increasing due to its good potential compared to conventional methods.

A fundamental knowledge of the microvaristor powder is necessary to understand its non-linear characteristics. The electrical behaviour of the grain is directly transferred to the compound, thus, the optimization of the compound is greatly influenced by the amount of microvaristor loading, the nature of the host matrix and the properties of the grains [9], [14]–[16]. These beneficial properties give microvaristor compounds great potential to vary and adapt electrical characteristics.

The fabrication of microvaristor filled with silicone rubber is challenging, due to the different material properties of the filler and the host matrix. The amount of ZnO microvaristor required to allow the compound to exhibit non-linear behaviour is

3

considerable. Meanwhile, the compatibility of both materials offers good dispersion and prevents agglomeration in the compound. The choice of fabrication technique may aid the mixing process of microvaristor in the silicone rubber. A number of fabrication techniques are reviewed that highlight their advantages and drawbacks for implementation.

The non-linear electrical properties of the grading compound should provide homogenous field distribution in high voltage equipment. The application of field grading compound can minimise the dry band formation in outdoor insulation and prevent the occurrence of discharge activities, which would initiate flashover.

The specific objectives of this research are outlined below:

i. To review the current knowledge of field grading material, fabrication techniques and degradation of microvaristor compounds due to high voltage stresses.

ii. To evaluate the experimental set up relating to fabrication procedures, laboratory tests and microscopic studies.

iii. To investigate the method of fabricating microvaristor compounds which best ensures that there is adequate microvaristor loading to allow non-linear behaviour to occur.

iv. To develop and test in-house field grading compounds under different high voltage tests.

v. To investigate the potential use of in-house field grading material for controlling electric field distribution in high voltage outdoor insulation.

1.3   CONTRIBUTION OF THE PRESENT WORK

The major achievements and contribution of this research investigation can be summarised as follows:

i.   An extensive literature review on field grading materials and their applications was completed.

ii.   A new technique is developed for fabricating grading materials based on ZnO microvaristors hosted in a silicone rubber matrix by introducing heat treatment to overcome hydrophobicity incompatibility.

iii.   Physical examination techniques were introduced to quantify micro particle (microvaristor) size, their dispersion into the compound and their elemental content for two types of ZnO microvaristors.

iv.   Developed new test procedures for the electrical characterisation of microvaristor powder and non-linear compounds.

v.   Developed analysis technique for the full electrical parameter determination.

vi.   Using the characterisation technique, the electrical properties of microvaristor at different microvaristor concentrations (10 wt. %, 30 wt. %, 60 wt. % and 70 wt. % were identified. A 70 wt. % was found as the suitable mix of microvaristors with silicone rubber.

vii.   Application of fabricated grading material characteristics to electric field control, and a new proposal for outdoor insulator was achieved using numerical computations.

1.4   ORGANISATION OF THESIS

This thesis is divided into seven chapters:

CHAPTER 2 provides a review of the published literature relating to the work undertaken. The general review includes a consideration of the importance of non-linear grading material in controlling field distribution in a high voltage system. The methods of fabricating microvaristor compounds and the selection of materials are discussed. The degradation of the different varistor samples are reviewed, and the current monitoring techniques, particularly those used in AC systems are presented. An evaluation of potential field grading material to be deployed in real applications is considered.

CHAPTER 3 presents details of the experimental set up for this investigation. The laboratory procedures provide a guiding framework, starting with the fabrication process and ending with the performance evaluation of the composite. Three different high voltage tests were conducted (AC, DC and impulse) and all of the test conditions and procedures have been reviewed. The current monitoring technique is explained in order to differentiate the resistive component from the total leakage current during AC tests. The microscopic evaluation and processes, namely Scanning Electron Microscopy (SEM), X-ray Photoelectron Spectroscopy (XPS), XRD and Axio-Imager 2, are compared.

CHAPTER 4 presents the fabrication technique of microvaristor filled with silicone rubber, at differing microvaristor concentrations. There are two different types of microvaristor powder, and it is expected that each microvaristor compound will exhibit different non-linear properties. The observations and challenges encountered

during the fabrication process are highlighted. Also, in this chapter, the microscopic results are presented, detailing the material properties and microstructure evaluation of the compounds tested.

CHAPTER 5 provides the experimental results of different microvaristor powders and compounds, when subjected to high voltage stresses. The findings from the experimental tests are explained in detail, including the non-linear characteristics of samples from different tests. Observations made during testing are highlighted, such as the safety features employed and the methods of handling the samples.

CHAPTER 6 presents the computation model used to evaluate the potential of in-house field grading material to control field distribution in high voltage outdoor insulation. A case study is carried out on a typical 11 kV polymeric insulator to highlight its performance and the effectiveness of the proposed non-linear grading material. An analysis of equipotential and field distribution is conducted under different environments (dry-clean and wet-polluted conditions) on standard non-graded and on microvaristor graded insulators. The evaluation of insulator performance under transient conditions is discussed in this chapter. An assessment of the power dissipation profile is computed in order to examine the integration of the non-linear grading material with the insulator.

CHAPTER 7 presents some general conclusions based on the research findings in this investigation and outlines some recommendations for future improvements.

CHAPTER 2

FIELD GRADING MATERIALS:

A REVIEW

2.1   INTRODUCTION: STRESS CONTROL

Generally, in high voltage applications, the structure of cable accessories, machinery and outdoor insulation are composed of different types of materials that are attached to the metal electrodes. The implementation of different material properties and design concepts for such applications have initiated the high field development that specifically occur at the edges of triple points linked to metal, dielectric, gas or vacuum [17]. If these problems persist and occur under diverse service and environmental conditions, they will lead to material degradation and ageing. Materials, such as silicone rubber, that experience these problems will lose their hydrophobic properties, and this may trigger a partial discharge or a corona and may eventually cause flashover. Therefore, particular attention has been given to the determination of field distribution along the high voltage apparatus, and possible solutions to minimise the effect of field

stress in the vicinity are discussed. The degradation effect, due to the inhomogeneous field, is clearly seen near to the end terminals of the insulator.
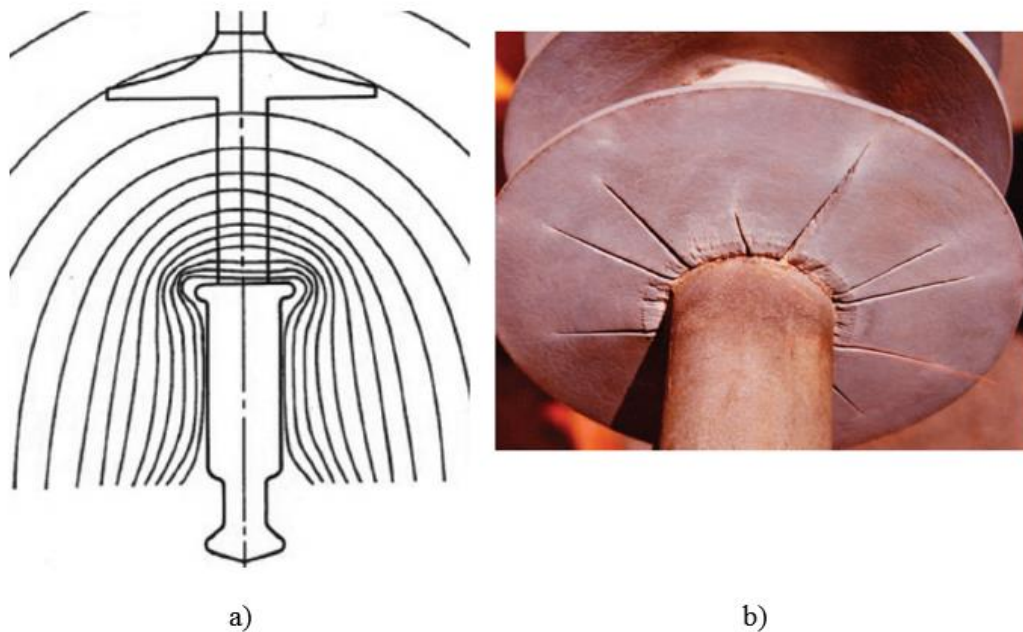
Figure 2.1: a) The non-uniformity of voltage distribution on the insulator which causes high field magnitudes near end fittings. b) The effect of the local field showing damage to a 115 kV suspension insulator [18].

This chapter presents a comprehensive review of field control through the displacement effects of field grading materials compared to conventional methods such as the use of a grading ring at the end terminals [21], improvements in the design of terminals [22], and the provision of extra hardware in high voltage equipment [23]. Compounding non-linear resistive materials with a polymer matrix has been identified as a potential solution to minimise field enhancement, and the ZnO microvaristor is

particularly focussed upon due to its intrinsic properties which allow for non-linear characteristics. The process of fabricating field grading materials is discussed in order to understand the procedure of mixing the non-linear material into the host matrix, where they appear incompatible.

Also, in this chapter some current discrimination techniques in high voltage applications are reviewed, with the aim of understanding how to extract the current components and to emphasize the effect of resistive current on material degradation. Further study has been done to evaluate the effectiveness of in-house field grading material in real applications. In this study, the performance monitoring of field control has been conducted by a computation method rather than by way of experiments. The finite element method has been applied and the procedure is explained in detail in the following chapter.

2.2   FIELD GRADING MATERIALS

Large-scale research investigations were conducted on different types of field grading materials which, specifically, mitigate field stress in high voltage applications. Generally, there are two techniques of field control using either capacitive or resistive grading systems [24]. The capacitive grading technique can be realised through application of condenser grading [13], refractive grading of high permittivity materials and geometrical design or a combination both of them [25]. Meanwhile, the resistive grading controls [26] the field distribution by embedding sufficient amount of non-

linear conductive materials into the insulating matrix. This technique will establish the path for current conduction within the compound. Both grading techniques show excellent results in re-distributing the field lines within a material structure, particularly, at the affected regions. Compared to the capacitive field grading system under nominal condition, the use of resistive field control is better, due to the flexibility of grading size that allows for a compact design at a low-cost of production [13].

2.2.1 NON-LINEAR RESISTIVE GRADING MATERIAL

Newnham et al. [27] highlighted that the performance of high voltage equipment can be improved if the system is equipped with an intelligent material that is able to operate based on the changes of its surroundings. Accomplishing this in a real system is quite challenging. Therefore, research has been carried out to investigate the potential of non-linear resistance materials [28], the methods of fabrication [15], [16] and the techniques of applying field grading layers [2], particularly in high voltage applications.

2.2.2 MATERIAL SELECTION

The stress control compound is based on a special ceramic powder that is dispersed into the matrix carrier at certain (wt. %) or (vol. %) material concentrations, which works effectively when the concentration is greater than the percolation threshold, in order to allow non-linear conductivity. A number of non-linear resistive materials have been identified as suitable for compounding with polymer matrices. They each

demonstrate promising results in electrical performance, but reveal drawbacks during the handling of the materials.

2.2.2.1 CONVENTIONAL MATERIALS

Silicon carbide (SiC) and carbon black are examples of non-linear materials that exhibit non-linear characteristics through particle – particle contacts. The nature of non-linear behaviour can be identified by any change of the band diagram occurring during particle – particle contacts, caused by filler structure and chemical formation on the surface. Transport mechanisms, such as tunnelling, hopping and thermal activation, will transfer electron particles over the potential barriers and can easily be disrupted by the presence of additional materials [9], [10], [29]. Figure 2.2 shows a microscopic picture of SiC powder and the field distribution result after the introduction of SiC composite in the high voltage insulators. Meanwhile, Figure 2.3 demonstrates the electrical properties of the new compound after loading SiC and carbon black in the matrix. The result is promising because the conductivity is increased based on filler concentration [30] in the EPDM matrix.

However, the conduction mechanism for both materials is quite complex, leading to difficulty in controlling the material formulation sand compounding process. Moreover, the materials are less resistant to external parameters and are susceptible to degradation, which greatly jeopardizes the electrical characteristics under elevated temperature and transient conditions. In addition, complex fabrication tools are required in material processing, which results in high manufacturing costs [9].

This disadvantage was eliminated when the investigation turned its attention to a new man-made material, microvaristor powder, which provides excellent electrical performance, robustness and allows for reproducibility.
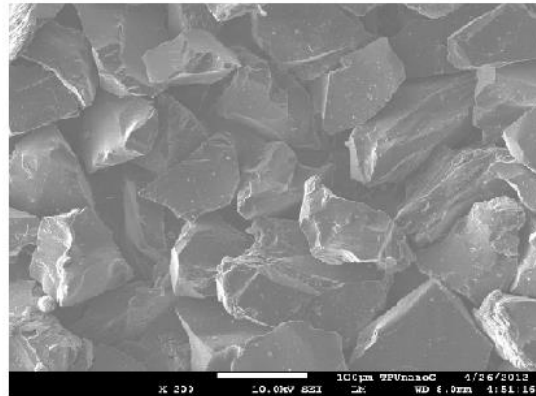
Figure 2.2: Scanning electron microscopy (SEM) image of SiC powder [31].
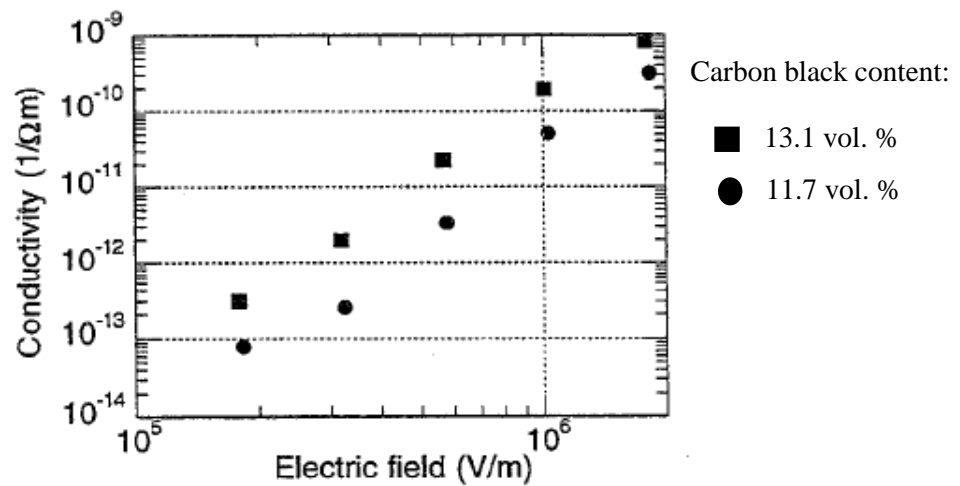
Figure 2.3: The conductivity of matrix at different amounts of carbon black at a constant amount 17.5 vol. % of silicon carbide [30].

2.2.2.2 ZnO MICROVARISTORS

ZnO microvaristor powder is an active smart material that excellently operates and adapts well to external change without assistance [27] as shown in Figure 2.4. This material is produced by the technique of spray drying aqueous slurry, which is discussed in [4], [9], in order to increase the resistance of particle contacts and its beneficial physical properties. The substances are subjected to a spray containing ZnO and other different metal oxide additives before the particles are sintered at a temperature of nearly 1200 $^{\circ}$C. At this high sintering temperature, additives melt and dissolve. Because of this unique manufacturing process, zinc oxide microvaristor exhibits a non-linear characteristics due to a low resistance between the particle contacts. A summary of publications related to ZnO varistors or microvaristors is shown in Figure 2.5.
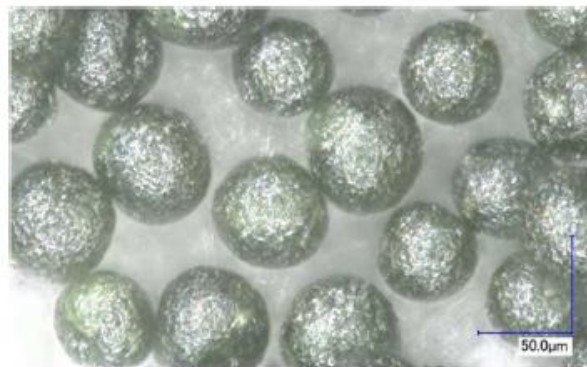
Figure 2.4: Microvaristor particles [33].
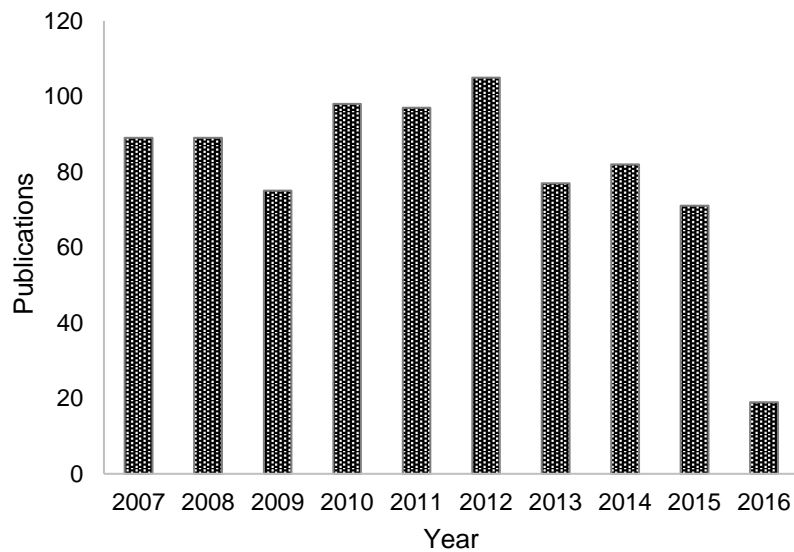
Figure 2.5: Citations using the terms microvaristors or ZnO varistors (Scopus research database, 2016).

The non-linear characteristic of ZnO varistors is governed by the double Schottky barrier that is formed at the boundaries of the ZnO grains and allows the varistors to operate similarly under both polarities. The formation of the depletion layer at the Schottky junction influences the capacitance profile which will decrease with the increase of input voltage [34]. According to Figure 2.6, the non-linear characteristic of ZnO based varistors is represented with three main regions or regimes.

During the pre-breakdown region, the potential voltage is distributed at the intergranular layers [35]. The current is composed of capacitive and resistive currents corresponding to a grain boundary resistor and capacitor. Generally, the leakage current consists primarily of capacitive current whose magnitude several times greater than the resistive component. When the voltage is increased, it will encourage the

15

tunnelling current across the grain boundary barriers. In this situation, the leakage current rises significantly, which shows thermal effects and degradation of zinc oxide varistors. The second phase is known as the breakdown region or nonlinear region. A small increase of voltage will encourage a large flow of current and allow the varistors to change from a high-value resistor to a good conductor after reaching the breakdown voltage. The current is mostly resistive and the degree of nonlinearity is governed by the flatness of this nonlinear region [34].
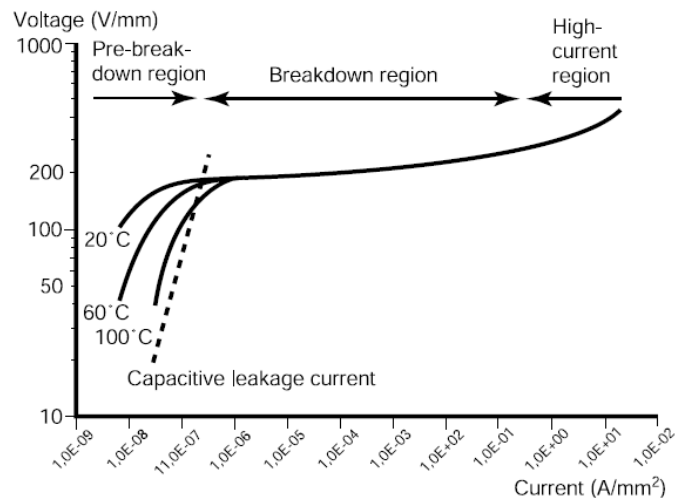
Figure 2.6: The general characteristics of zinc oxide based varistors [36].

The massive migration of ionized donors will reduce the resistance of the intergranular layers and can be explained in the high current region [37]. Each of the varistor's particles is robust and consists of electrically active grain boundaries. With the presence of various active dopant in the ZnO particles have changed the n-type formation of the semiconductor junction which allows their intrinsic properties to

control their non-linear characteristics [9], [34], [38]-[39]. This behaviour allows the microvaristor powder to transfer its electrical properties directly to the composite compound. The microvaristor powder can be mixed with other materials, such as polymer matrices or silicone oil. In general, the electrical properties of zinc oxide microvaristor powder can be tailored according to the formulation of the metal oxide material and the setting of the fabrication parameters such as the sintering process and the microscopic properties of the particle contacts [4], [40]. This tuneable voltage benefits by providing a wide range of switching points in the microvaristor compound, according to the type of powder [8], the size of filler [14], the element composition [40], the fabrication technique [41], the host matrix [9], [33] and the amount of filler [14], [31]. The microvaristor compound exhibits its non-linearity if a sufficient amount of microvaristor is loaded in the matrix which is in agreement to the investigation conducted by Yang et al. [14] who showed that the amount of microvaristor loaded in the polymer matrix has a large influence on the electrical properties of the composite, and these confirm the findings of previous research by Pitha et al. [28].

Figure 2.7 shows the current density profile of microvaristor compound as a function of electric field at different volume (vol. %) of microvaristor content. It is clearly seen that large content of microvaristor materials in the samples would encourage high current density level which directly effect to the lower switching field. However, as the microvaristor loading is reduced to 31 vol. % in the sample, the non-linear of $J - E$ is hardly to obtain.
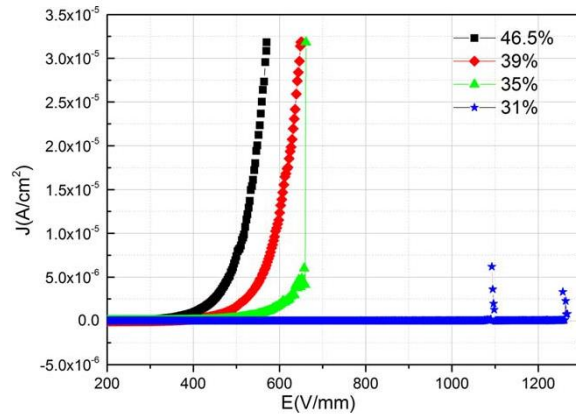
Figure 2.7: Current density as function of electrical field, shown for different amounts of microvaristor loading in particle volume concentrations [14].

Meanwhile Figure 2.8 shows that the field-dependent resistivity of microvaristor compounds are varied according to the selection of host matrix. This behaviour is highly governed from the material properties of the host matrix such as degree of mechanical stress. The resistivity profile are presented; as the microvaristor compounded with silicone oil exhibited higher resistivity compared to the second sample.
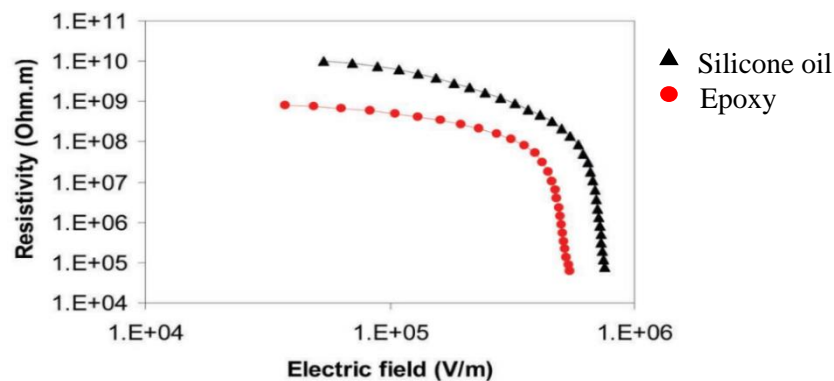
Figure 2.8: The field-dependent resistivity of ZnO microvaristor composites in different types of host matrix [9].

As highlighted, the electrical properties of microvaristor compound can also be adjusted based on the type of microvaristor powder. One of the interesting findings related to this factor is clearly shown in Figure 2.9 which explains that the electrical characteristic of microvaristor powder is governed by its material properties. It is clearly seen that two switching fields were obtained for the two different microvaristor powders.
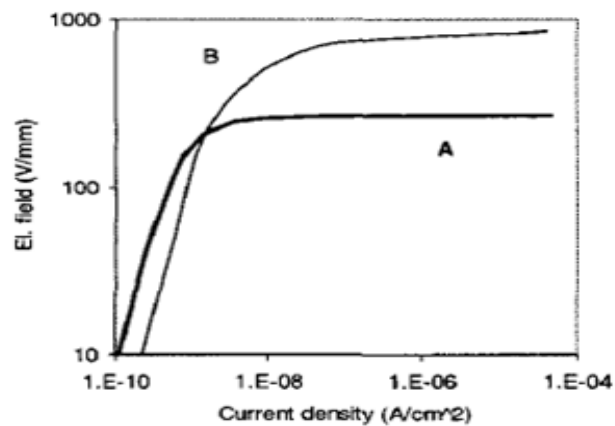
Figure 2.9: Two switching fields that correspond to different types of microvaristor powders [8].

The compounding process between the microvaristors and the polymer matrix is a critical stage, where every aspect has to be considered in order to produce a field grading material with high reliability and excellent electrical performance. The microvaristors and the host matrix have different material properties, which allow agglomeration to occur when the filler is loaded in the polymer. It is a complex process

to obtain compatibility for a compound. Therefore, further investigation was carried out on the polymer selection and on the fabrication technique of field grading material.

2.2.3 HOST MATRIX

A general view of host matrix selection is quite subjective, because the different hosting materials and the amount of filler will directly influence the characteristics of the non-linear resistive composite. A number of investigations have been carried out in the past few years to determine the non-linear behaviour of composites filled with such polymer matrix materials. The technology needed to fabricate the non-linear resistive material based polymer can be greatly expanded, due to the polymer having high flexibility and being lightweight and easy to control. However, there remain some challenges during the compounding process in order to achieve compatibility between the filler and the polymer, due to the polymer matrix being prone to agglomeration and sedimentation, particularly after filler loading. In this subsection, the potential of polymer matrix that has been mixed with non-linear resistive material is discussed.

2.2.3.1 EPOXY RESIN

Epoxy resin is a thermoset polymer that is generally formed by mixing together various components. There are three main component elements to the thermoset system; base resin, hardener and modifiers. Figure 2.10 shows the molecule of epoxy resin which is comprising one oxygen atom and two carbon atoms which is known as an epoxide [42]. Due to its flexibility in molecular structure, the demand for this material is increasing which are widely use in various applications. It offers better mechanical

properties, lower shrinkage and provides excellent electrical insulation at a low cost, which allows the material to be utilised in surface coating and adhesive industries.
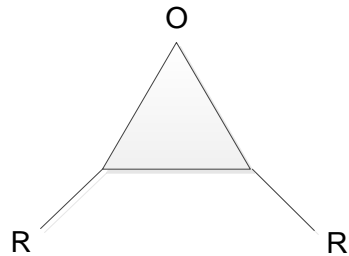
Figure 2.10: The chemical structure of an epoxy group [42].

Meanwhile the performance result of epoxy composite is promising. Using a bonding method, Yang et al. [43] fabricated epoxy resin composites at 20 wt. % of microvaristors concentration, which significantly increased the degree of the nonlinearity between current density and electric field $(J - E)$, α, up to high value of 45.

Ebishi et al. [33] investigated the effect of applying the electrical field force to the epoxy filled with ZnO microvaristor samples. In this research, the microvaristor composites as shown in Figure 2.11 were cured at specific temperature and treated under electrical field of 470 V_{rms}/mm before annealing process to allow the compound create the sufficient current paths. Results showed the samples with high microvaristor contents and treated under electric field exhibited such superior nonlinear voltage-current (V-I) characteristics. In conjunction to these experimental

results, Komesu et al. [44] investigated the movement of varistors in liquid epoxy resin through COMSOL simulation and both experimental and numerical results are compared. The results show in agreement to the both methods. Non-linear material based epoxy resin [16] has been used in high voltage bushings, in order to reduce the electrical field intensity near the end terminals.

However, a number of drawbacks have been highlighted when handling this polymer matrix. Epoxy resin is quite sensitive to high temperature when the base resin is added to the hardener which reduces the pot life of epoxy resin and increases the shrinkage of the material [45]. Because of such matter, the epoxy compounds are fabricated in thin samples [19], [20], [33] as shown in Figure 2.11. However, for industrial applications, bulky microvaristor composite based epoxy resin can be composed with the aid of high technology fabrication process. This material is embedded on to a glass fibre reinforced plastic (GFRP) core, in order to minimise the ageing process caused by partial discharges [46].

Figure 2.11:   A sample of microvaristors composite based epoxy at a thickness of 0.6 mm [33].

2.2.3.2 SILICONE RUBBER
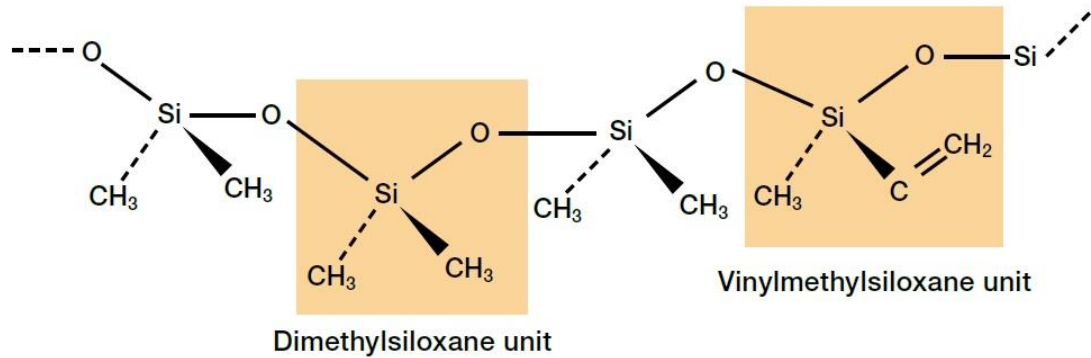
Figure 2.12: Chemical structure of silicone rubber [47].

Silicone rubber is another option for use as the host matrix in the microvaristor compound. The properties of each silicone rubber is different that depending on the organic groups and the chemical structure [47]. In general, the silicone rubber has a structure of polymer chains between the S-O bonds which are attached to methyl groups (CH_3). The diffusion of low molecular weight (LMW) of silicone chains with a combination of methyl groups will be forming a lattice type thin layer on the surface that leading for high hydrophobic properties [32], [47]. Because of such factors, silicone rubber provides good resistance to oxidation and degradation. Moreover, this material may be used for electrical and thermal insulation purposes. This material can also be used in a wide range of temperatures, allowing it to be compounded with other materials. There is a vast number of applications of silicone rubber in non-linear resistive field grading materials, which have been reported in [12], [14], [48]–[54]. Silicone rubber has high elasticity, therefore, it has been used in the investigation of

component properties, thermal conductivity, relative permittivity and electrical conductivity at different filler loadings [1], [55]-[56]. The application of epoxy resin and silicone rubber compounded with microvaristor was discussed in [16] where both of composites minimised the high electrical field, consequently, avoiding the occurrence of partial discharges. Figure 2.13 shows an example of microvaristor filled with silicone rubber sample [11] meanwhile Figure 2.14 presents the application of this compound in outdoor insulators [48].

Figure 2.13: An example of 1 mm microvaristor compound based silicone rubber [11].
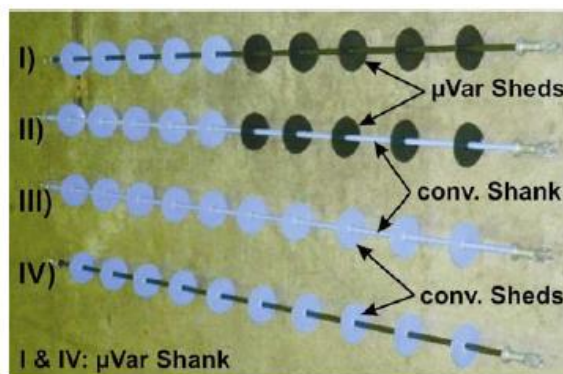
Figure 2.14: The application of microvaristor filled with silicone rubber in long rod insulators with different approaches to implementation. The field grading material is referred to as the green compound [48].

2.3 THE FABRICATION PROCESS OF NON-LINEAR COMPOSITES BASED ON MICROVARISTORS

A general knowledge of silicone rubber is necessary in order to minimise the possibility of agglomeration in the microvaristor compound. Silicone rubber does not solidify when cooled in the absence of hardener. This is due to the low rate of nucleation in solid structure and the possibility of complex polymer chains. However, if solidification occurs, the process will be incomplete [57]. Therefore, a small amount of hardener should be added into the mixture during the fabrication process of polymer composite.

A number of fabrication techniques for compound based polymers were reviewed. This initial study is important in order to understand the fabrication process of compounds, particularly related to the methods of dispersing fillers in the host matrix. Bian et al. [19] explained the impact of agglomeration in the compound caused by the dispersion method, which directly diminishes the performance of the composite.

Agglomeration and sedimentation may occur when dealing with nano-scaled fillers [19], and a large amount of filler loading [58] in the polymer matrix. Therefore, attention will be given to a number of dispersion techniques, and these will be discussed further. The common method of fabricating microvaristor compounds using mixing, moulding and curing was presented by Greuter et al. [7]. Meanwhile in another article [41], the researcher suggested that additional procedures, such as heat treatment and pressure could be applied.

As highlighted in the previous section, the conductivity mechanism of a microvaristor depends on its intrinsic properties and not on the dispersal of particles. However, non-linear conduction is achieved when a sufficient quantity of microvaristor is loaded in a polymer matrix [9], [33], thus encouraging agglomeration to occur between the micro particles and the host matrix. Therefore, it is essential to apply a mixing regime that can minimise agglomeration and distribute the microvaristor powder homogeneously in the host matrix.

Three common methods used to disperse the microvaristor powder in the polymer are mechanical mixing, electrical field application and mixing the polymer matrix with additional substances. Additional procedures such as heat treatment to the polymer are discussed.

2.3.1 MECHANICAL MIXING

Microvaristor particles comprise metallic oxide and do not cohere with the host matrix. Therefore, these particulates will block the movement of particles dislocations that lead to agglomeration. Agglomeration in the compound can be broken by supplying energy to the composite mixture. This can be done by using shear force, such as stirring, ultrasonic or a high shear mixer. The evaluation of applying physical mixing techniques to disperse particles uniformly in the composite have been presented in [59].

Other solutions include adding a small amount of additive that improves bonding between the dispersant and polymer matrix [60] or using a two roll mill technique [8].

Interestingly, the combination of a shear force technique and the use of chemical agents is also reliable, as presented in [14].

2.3.2   ELECTRICAL FIELD APPLICATION

Applying an electrical force to a host matrix filled with microvaristor material is a great method for creating a current path according to electrorheological fluid studies [61], [62]. Due to the properties of the microvaristor that can be polarized under an electrical field, microvaristor chains are encouraged to form.

The experimental works of Ebishi et al. [33] show that, for a small amount of microvaristor loading in an epoxy matrix, the current path of the microvaristor may be created by applying an electrical field during the curing process as shown in Figure 2.15. The measurement of the non-linear electrical characteristics shows encouraging results when the current path were successfully formed at low microvaristor content.
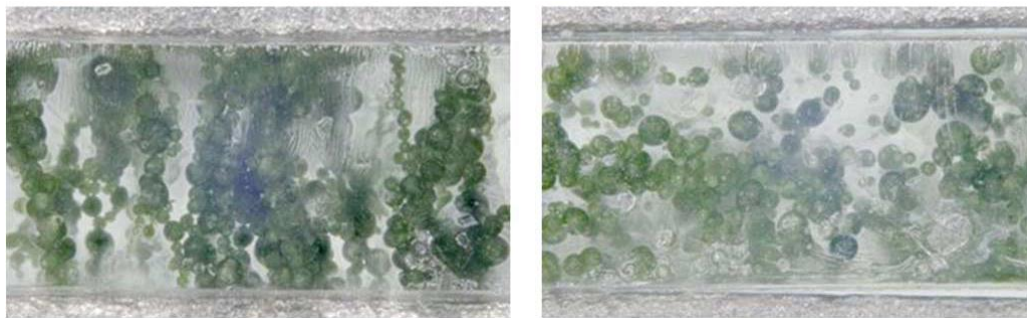
a)   with electrical field application   b) without electrical field application

Figure 2.15: The formation of a microvaristor compound based epoxy resin [33].

2.3.3 CHEMICAL SOLVENT

There is a limitation to applying shear force to the microvaristor mixture. That is breaking up the bulk material into small particulates in order to provide the uniform dispersion of materials will subsequently increase the free energy of the system. However, these particulates are trying to return to their original state, either by reversion, coagulation or coalescence. Therefore, the presence of a material agent is required to modify the surface of the particles. This can be done through chemical additives [19], or by the introduction of additional materials that can enhance the bonding of microvaristor grains and improve the non-linear properties of microvaristor compounds at high microvaristor loading. The application of chemical additives, such as surfactant [63] in nano-composites, greatly improved the dispersion of nano-particles and thus the composite's properties. In contrast to this method, Matsuzaki et al. [58], [64] introduced a semi-conductive whisker to the host matrix, which aided the homogenous dispersion of the microvaristor and significantly improved the electrical contact between the varistors' grains as depicted in Figure 2.16.
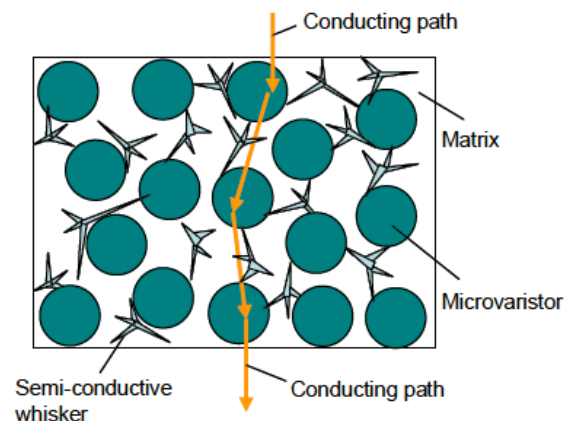
Figure 2.16: A tetrapod of a semi-conductive whisker is added to improve the dispersal of the microvaristor in the matrix [64].

2.3.4   HEAT TREATMENT

The dispersal of microvaristor powder into a silicone rubber matrix is challenging, due to the mismatch of the densities, causing a sedimentation problem between the dispersed particles and the insulating medium. Internal factors such as the viscosity of the materials and the energy barrier of the composite system were investigated.

Heat treatment was applied to the polymer matrix, in order to control the structure and properties of the material. Applying heat treatment will significantly modify the properties of the polymer for example, by reducing the level of crystallites and elastic modulus. An investigation was carried out into the modification of the surface resistance of a polymer, to reduce the moisture in the filler [65] and minimise the viscosity level of polymer [66].

In [65], a number of fillers were pre-heated at certain temperatures to reduce the hydroxyl groups that are normally present in the fillers. The fillers that were still warm were then added to the polymer matrix and made the compounding process easier. The investigation in [66], explained the two different methods that were conducted on the samples at similar temperatures with the introduction of different holding times.   The application of heat treatment to the polymer matrix significantly eliminated the stresses state in the material properties which directly influence the tensile strength behaviour.

2.4 DEGRADATION OF COMPOSITE BASED VARISTORS

2.4.1 DEGRADATION FACTORS

Microvaristor composites that are used for high voltage applications, encounter a range of stresses during service, which lead to degradation and greatly modify the electrical properties of the composite. The following degradations induced by stress are discussed such as operating voltage, partial discharges, current impulses, environmental stresses, and electro-thermal stresses.

2.4.1.1 NORMAL OPERATING VOLTAGE

The composite based varistors that operate under power frequency voltage exhibit an increase in their average power as a function of time. The application of voltage greatly contributes to the degradation, due to the disassociation of ions, migration and changes on the Schottky barrier. Resulting from this, the resistive current is increased and the field stresses that lead to degradation are magnified [67]. In order to maintain the useful life of the material, it is important that controlling the aging issues is solved by improvements in the manufacturing process and by using specially designed equipment, in order to minimise the internal partial discharges [68].

2.4.1.2 IMPULSE ENERGISATION

An investigation [69] has shown that the degradation increases with the number of applied impulses and amplitudes of current impulses until the saturation state is

achieved. In order to exhibit such a reliable result, the impulse needs to be applied less frequently at high amplitude. The degradation of the material can be identified when there is a change in the current – voltage characteristics that allows a high current to flow. The worst scenario occurs when the threshold voltage is reduced significantly below the nominal turn-on voltage. This will accelerate the degradation process and eventually cause thermal runaway in the varistors [70]. An examination of ZnO varistors under high frequency was conducted in [71], wherein the high harmonic content of the voltage signal, which directly influences the power dissipation in ZnO varistors and leakage current, was evaluated.

2.4.1.3 DC VOLTAGE

The electrical and dielectric properties of the material were evaluated to obtain evidence of DC degradation. It was found that the material was easily degraded if subjected to DC current for a certain period [72] and the non-linear coefficient of the varistors were shown to be inversely proportional with time. A laboratory experiment carried out in [73] showed that degradation in the varistors material was caused by the deformation of the Schottky barriers of the metal oxide additives due to ion migration through thermionic and tunnelling mechanisms.

2.4.2   LEAKAGE CURRENT MONITORING

The factors that induce degradation of the sample based on ZnO varistors were highlighted in the previous subsection. Monitoring systems have been developed, specifically to diagnose the leakage current in the continuous operating voltage region,

which could possibly result in deterioration of the microvaristor composite. The monitoring system will evaluate the leakage current response of the microvaristor composite and will predict the occurrence of defects and performance deterioration when the devices are subjected to power system applications. Any occurrence of leakage current that can cause the devices to malfunction and lead, in the worst case, to system failure will be detected. A number of current monitoring methods are listed and discussed below.

2.4.2.1 ON-LINE MONITORING

This technique uses harmonic analysis from the total leakage current I_t in order to obtain 3rd harmonic resistive component [74]. Therefore, scaling is used to obtain the 3rd harmonic of the total current I_t. This technique is less accurate since it introduces errors of almost 40%. In order to deal with the third harmonic content in the voltages, a new technique was introduced in MOV surge arresters using a compensation technique [75]. This technique minimised the errors that depends on the phase relation between the harmonic in the voltage and the harmonic current generated by the arrester.

Meanwhile, Yan et al. [76] studied the characteristics of resistive leakage current of metal oxide surge arrester through numerical method and experimental works. From this investigation, the resistive current characteristic was monitored closely by taking into account the working condition of MOV surge arrester including surface contamination, inner moister, ageing condition and thermal deterioration.

2.4.2.2 MODIFIED SHIFT CURRENT METHOD (MSCM)

This method involves extracting the resistive current component from the total leakage current, I_t of a metal-oxide surge arrester [25]. In this analysis, the voltage signal is not taken into account, due to the difficulty of obtaining a reading of it and the high risks involved in voltage access. Moreover, the voltage signal is exposed to the interference of nearby phases. A comparison between this simulation study and the compensation method is required in order to have good consistency in the current measurements [77]-[78].

2.4.2.3 POINT-ON-WAVE METHOD

The current discrimination technique has been discussed in Haddad and Warne [35] where they consider RC parallel networks for ZnO surge-arrester elements. The significance of this current discrimination analysis is to investigate the resistive current, I_r, that contributes to degradation in the sample. The simplified Point-On-Wave (POW) method does not take into account the harmonic component, nor the presence of odd harmonics without phase shift. Therefore, the I_c and I_r components of the total leakage current, which depend on instantaneous voltage level, are determined.

2.5 ASSESMENT OF THE PERFORMANCE OF FIELD GRADING MATERIALS IN PRACTICAL APPLICATIONS

The results of studies have shown the effectiveness of field grading compounds in high voltage applications. It may be clearly seen that non-uniform field distribution is successfully mitigated, thus, significantly preventing the triggering of discharge activities in the equipment. The assessment of non-linear field grading performance in real applications provides a better understanding of the characteristics of the switching field that correspond to local field enhancement in the equipment. The evaluation of this non-linear material can be obtained through two methods: i) Experimental measurement ii) Numerical analysis.

2.5.1 EXPERIMENTAL MEASUREMENTS FOR FIELD GRADING MATERIALS

Experimental measurement provides accurate results when the electrical device is equipped with field grading material and subjected to high voltage tests. In [8], the prototype of cold shrink with a microvaristor-silicone field grading element is tested under both AC and impulse tests. The experimental results show the relationship between the design concept and real applications.

The use of microvaristor compounds in polymeric insulation is now widely accepted by scientists and researchers. In the research carried out by Rahisham et al. [11], a microvaristor compound was embedded in an 11 kV polymeric insulator, and its

performance was evaluated when subjected to a lightning impulse test (1.2/50). The

experimental results are reproduced in Figure 2.17. The test sample was evaluated

under different conditions; dry − clean and wet − polluted.
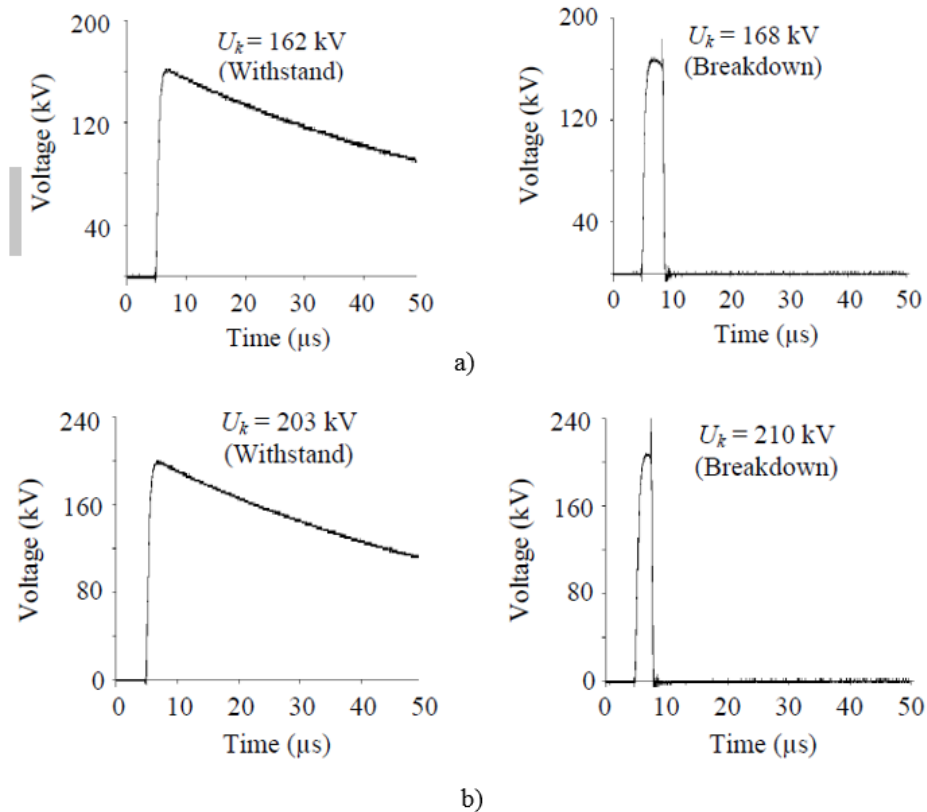
Figure 2.17: The assessment of impulse performance for an insulator a) non-graded, and b) graded with microvaristor compound under dry and clean conditions [11].

The flashover voltage of the compound was increased by up to 21% compared to a

non-graded insulator under dry and clean condition. Meanwhile, a small changes of

breakdown voltage occurred in wet-polluted condition. The results show that the

microvaristor operates in the conduction regime which allows the field intensity to be

minimised on the surface of the insulator under dry and clean conditions. However, it

is necessary to evaluate the test sample under wet and polluted environment. In another publication, Debus et al. [48] evaluated the performance of the composite insulator filled with microvaristor compound under AC voltage in artificial rain conditions. The non-linear material when embedded on a few parts of the insulator structure has shown improvement of field distribution along the insulator surface which minimised the effect of dry band arcing. Meanwhile in [79], the evaluation was conducted on AC end arms wound coils that equipped with three different field grading materials. A comparison performance for all field grading tapes was evaluated as shown in Figure 2.18. The experimental results show the surface potential along the devices were linearized distributed for the different type of grading tapes. This is due to the effect of manufacturing process of grading materials, which directly influence to their electrical performance.
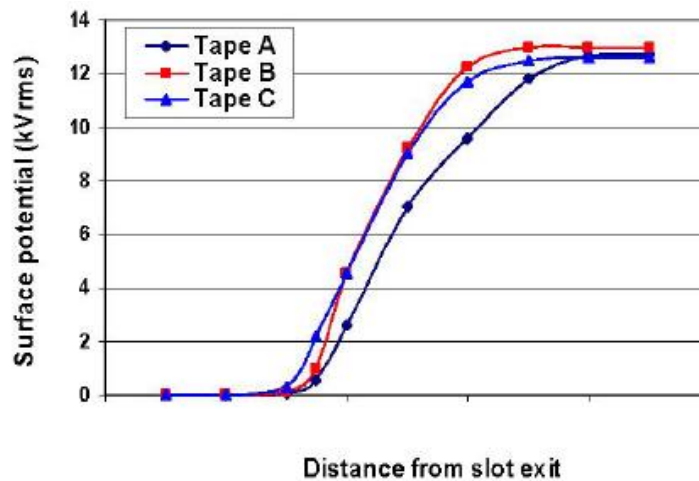
Figure 2.18: The measurement of surface potential after implemented with field grading materials in an AC application [79].

2.5.2 NUMERICAL ANALYSIS

Due to the limitations of laboratory equipment, materials and safety concerns [34], [80], scientists and researchers are shifting their focus to numerical analysis. In a recent article, Kovalev et al. [80] highlighted the importance of the implementation of numerical analysis in high voltage industries, in order to understand the performance of high voltage equipment [81]–[85] and to determine the characteristics of materials [10], [19], [86]-[87]. This alternative method provides faster results at a lower cost. The numerical study is useful for design optimisation and power system application. Dynamic evaluations of field control have been reported in a number of articles [17], [88]–[92] the findings of which are very optimistic about the investigation of field control techniques in order to prevent discharge activities that can lead to flashover. Partial discharges can lead to tracking and erosion which accelerate the aging process of insulation materials. The non-linear properties of field grading material change with the electric field, thus, giving an opportunity to improve the uniformity of field distribution as investigated in [93]. This work evaluated the effect of ZnO stress grading in a composite hollow insulator as highlighted in Figure 2.19. By introducing the field grading material, the voltage distribution along the insulator surface was re-distributed uniformly, which is in agreement to the theory and practical method. It suggests the computation technique is a reliable method to investigate the condition of high voltage equipment with a shorter amount of time.
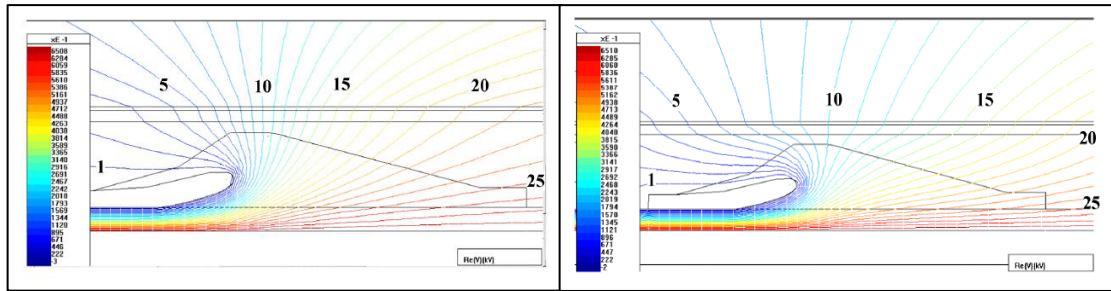
a) With ZnO field grading material   b) Without field grading material

Figure 2.19: The voltage distribution on the composite hollow insulator surface [93].

2.6 SUMMARY

A broad review of field grading materials, particularly microvaristor composite based polymer, has been presented. The important aspects regarding the application of non-linear compounds to the control of electrical fields in high voltage applications are discussed. The fabrication techniques for field grading materials, particularly related to material selection, host matrix and procedures are discussed. In depth investigations of this process will be explained in Chapter 4.

The degradation phenomenon in a ZnO varistors is explained and a number of criteria are considered, relating to the different voltages and frequencies applied, that accelerate ageing. These will be correlated to the high voltage tests procedure in Chapter 3, and experimental results will be explained in Chapter 5. Because the ageing of varistors is governed by the resistive current, a discussion on techniques for

extracting leakage current techniques is presented. A selection of current monitoring techniques are reviewed, and this will be explained in detail in Chapter 3.

The applications of non-linear grading materials are presented, and the evaluation of field grading performance was carried out through experimental or numerical analysis. To address one of these assessment methods, a case study is developed in Chapter 6 that will show the condition of the polymeric insulator before and after the addition of field grading material under different conditions.

CHAPTER 3

LABORATORY SETUP AND CHARACTERISATION TECHNIQUES

3.1 INTRODUCTION

A practical system is essential to investigate the performance of composite materials in dealing with high voltage operations. In a number of publications [4], [12], [13], scientists have highlighted the different approaches of tests to identify the sustainability and capability of varistors based composite to operate under a variety of voltages, frequencies and high temperatures. In order to be accepted in industrial applications, the field grading material should be handled electrically and tested; making it more convenient to use, requiring less maintenance and giving opportunities for flexible design solutions. It may be noticed that the varistors based composite samples may be induced to aging by multiple stresses caused by power frequency voltages, AC, DC and transients. Therefore, the high voltage tests which were conducted on the samples in High Voltage Laboratories, Cardiff University that comply with BS EN 60060-1:2011 and BS EN 60060-2:2011 Standards. The

procedures which were implemented in conducting the laboratory experiments are shown in Figure 3.1.
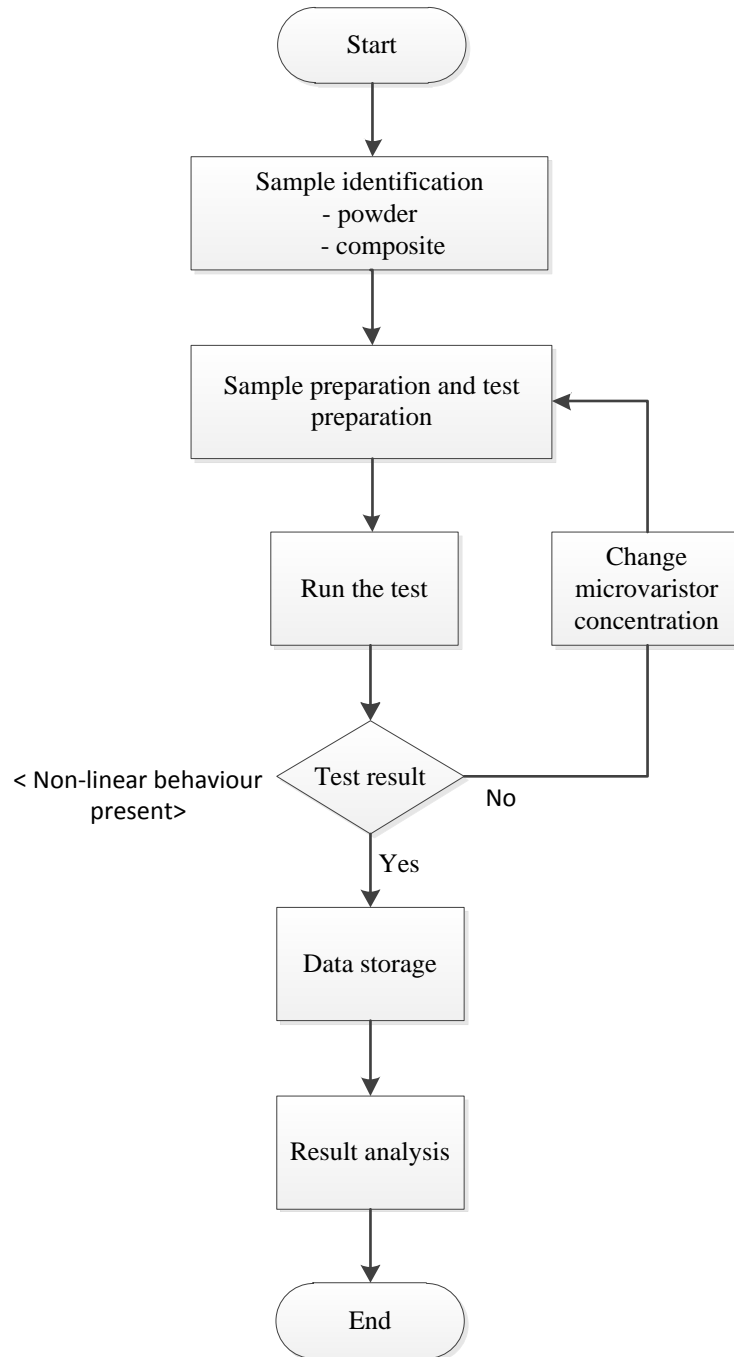
Figure 3.1: Flow chart for laboratory experiments.

The high voltage tests enabled the behaviour of the microvaristor powder and the compounds to be characterised in terms of breakdown, conductivity, resistivity, etc. The samples of powder and compound were subjected to AC test. However, only composite samples were tested under DC and impulse voltages. The microscopic investigation is presented in the last subsection, which will clarify some techniques that may be used to determine the properties of the micro particles, such as grain size and chemical elements. The work findings will identify any effects caused by the material properties of the microvaristor powder on the electrical characteristics of the microvaristor compound, which may assist in understanding the morphology of varistors in powder and composite structures.

3.2   HIGH VOLTAGE AC TEST

This is the most common power frequency test which is conducted on microvaristor filled silicone rubber at normal frequency, i.e. 50 Hz. The test is used to evaluate the inter-contact of the microvaristor grains in the powder and in the silicone rubber matrix, which will determine the nonlinear behaviour of the samples. The electrical properties of the composite will also be determined.

3.2.1 PREPARATION OF TEST SAMPLES

Two types of samples were tested; microvaristor powder and composites compounded from two different microvaristor materials. The samples were assigned as powder **A** and powder **B**. Two test cells were prepared according to the type of test sample.

3.2.1.1. MICROVARISTOR POWDER

This preparatory work was provided by adapting a test cell previously used for another experiment [94] to investigate the nonlinear mechanism in zinc oxide varistors powder as depicted in Figure 3.2. The test cell was equipped with an insulated mounting panel that separated the test electrode and grading system. The cross sectional area for the circular electrode was 100 cm². It was assembled together with a 20 x 20 cm polycarbonate sheet. A weight of 0.2 kg of microvaristor powder was sufficient to fill the test cell while leaving 0.5 cm of adjustable gap between the opposing faces of the electrodes. Uniform pressure was applied to tighten each terminal to ensure that the powder was well compacted in the cell. It was ensured that there were no impurities in the powder, as any impurities could affect the conduction properties of the test sample.
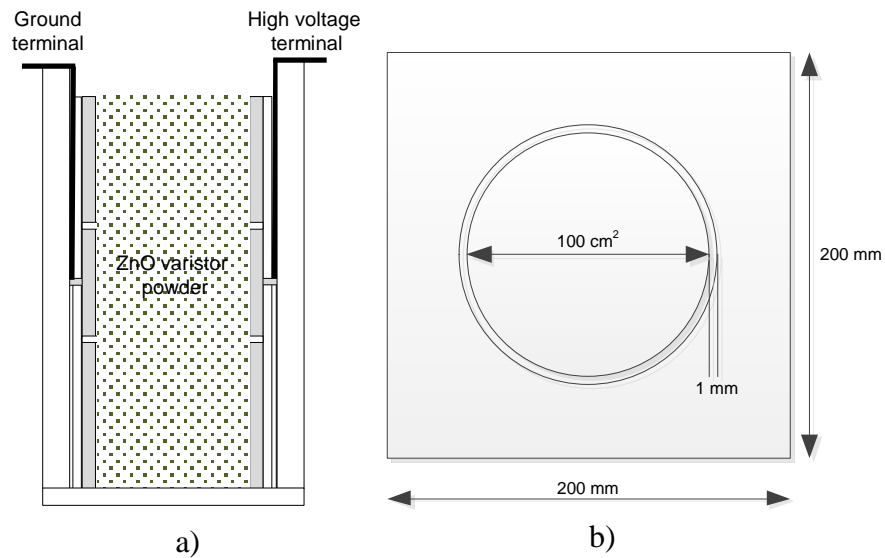
Figure 3.2: Test cell for nonlinear powder a) Test cell b) Electrode.

3.2.1.2.   MICROCOMPOSITE SAMPLES

The test cell for composite samples consisted of two aluminium electrodes that were attached to the supporting insulated structure. Both electrodes had a diameter of 30 mm, with a measured thickness of 10 mm. The guard ground electrode had a circular electrode with a cross sectional area of 0.7855 cm^2. The 1 mm radial space between the two electrodes was filled with structural epoxy material. The edges of both electrodes were profiled to prevent any field enhancement, which might initiate discharge activities. The 5 mm test sample was sandwiched between the electrodes. It was necessary to clean any dirt that appeared on the electrode surfaces by using propanol before and after conducting the tests in order to prevent any distortion of the

experimental measurements due to unintentional additional resistance. The resultant design of the test electrode is depicted in Figure 3.3.
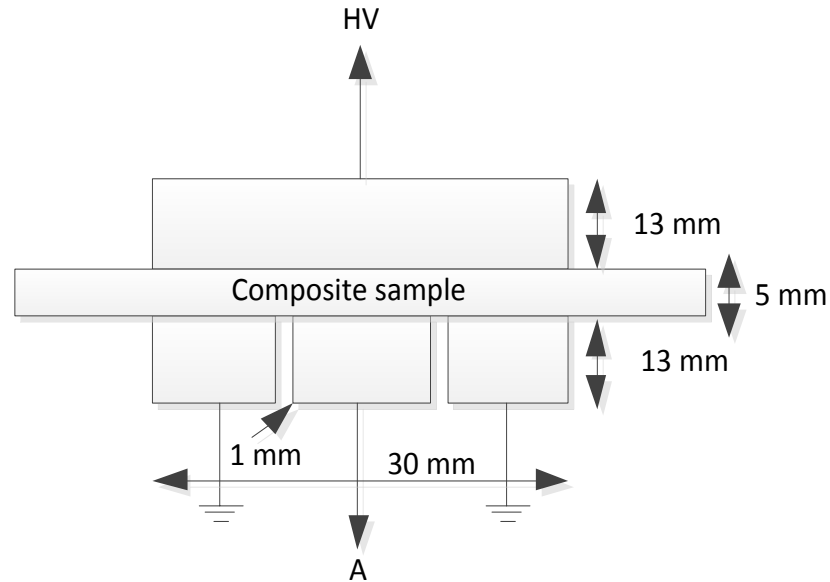
Figure 3.3: Test electrodes for microvaristor composite.

3.2.2   CIRCUIT ARRANGEMENT

The experimental procedures of AC tests including safety requirements and the factors that influenced the measurement system are highlighted. A schematic diagram of the test set up is shown in Figure 3.4. The voltage supply was controlled by a voltage regulator, up to a maximum of 10 kV with the rate of increasing voltage is set to 1 kV for every 30 seconds. A voltage divider with a ratio of 1000:1 was used to measure the actual input voltage across the test sample. A shunt resistor of 1 kΩ was used to measure the instantaneous current during the test. Both the voltage and the current

were displayed simultaneously, using a Lecroy digital storage oscilloscope (DSO). In addition to the DSO, the accumulated data was saved using a computerised data acquisition (DAQ) system, using a purpose developed programme on a LabVIEW platform.
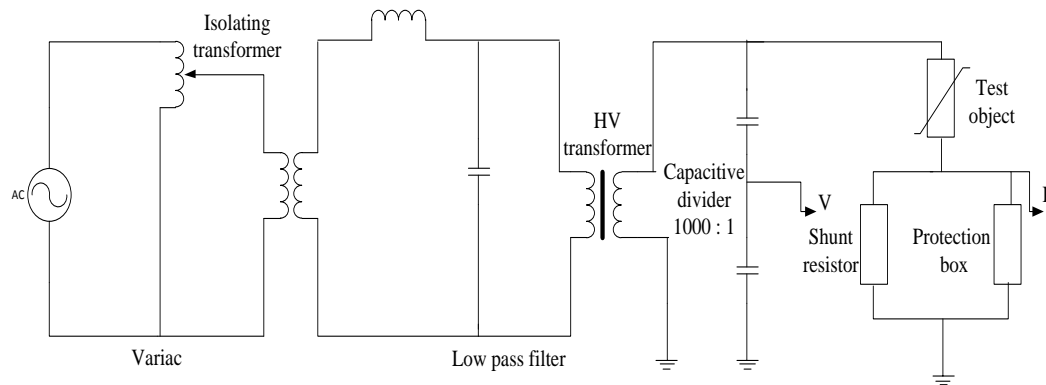
Figure 3.4: Test set up for the AC test.

3.2.3   LABVIEW PROGRAMME

This test was operated under a power frequency of 50 Hz. In data storage system, the computer was installed with a data acquisition board that had physical inter-connection with a SCB-68 connecter block and which was located adjacent to the workstation as shown in Figure 3.5. The LabVIEW based program was designed by following a specification, in order to acquire the data carry out monitoring and save the waveforms of voltages and currents. Important parameters, such as the sampling rate of the data acquisition was set at 10000 samples per second.
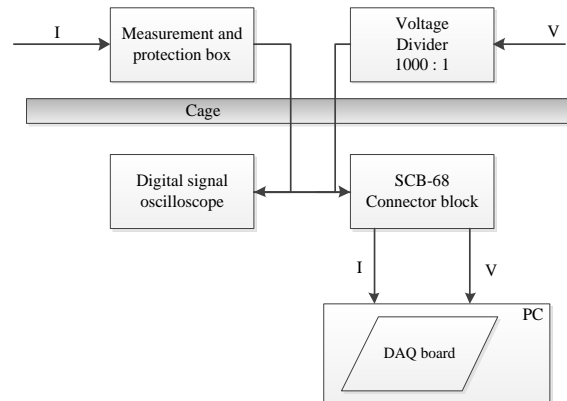
Figure 3.5: Diagram of the data acquisition (DAQ) system.

3.2.4   EXPERIMENTAL ANALYSIS

In order to understand the current conduction mechanism in the samples, the model of ZnO material was presented. In this research, the simplest model consisted of resistance R_g, that represented the ZnO grains in series with the parallel R-C circuit that was implemented. The R-C circuit was used to represent the voltage and frequency dependent resistance and the capacitance of the intergranular layers that are responsible for the non-linear behaviour of samples which ultimately, are governed by the resistance component at high voltages. From this model, the voltage and current (V-I) of the samples were characterised using a series of voltage levels, starting from low voltage, until the samples reached a threshold voltage level in the conduction regime. Moreover, a current monitoring technique to extract current components was

identified to take into account the potential aging caused to the non-linear materials under normal working conditions.

3.2.4.1 POINT-ON-WAVE (POW) METHOD

It is expected that, in the long term, the electrical properties of the material will degrade due to the application of continuous power-frequency voltages. As a result of the stress caused by the system voltage, leakage current in the microampere range will flow through the micro composite material. This leakage current is generally composed of a large capacitive current and a small resistive current. The primary aim of leakage current monitoring is to determine the long-term stability and aging of devices [95].

In this research, the Point on Wave (POW) technique has been applied, as previously discussed in Haddad and Warne [35], by presenting a similar R-C model for ZnO surge arrester monitoring. Since the characteristics of a ZnO microvaristor are similar to those of a ZnO arrester material, there is good argument in favour of using this current analysis application.

The purpose of this current discrimination analysis is to investigate the resistive current, I_r which contributes to degradation of material. The I_c and I_r components of the total leakage current, which depend on instantaneous voltage level, were determined. It is assumed that the V-I characteristics of the microvaristor powder and compound are unique within a voltage cycle, i.e. they are independent of the voltage rate of change. The total current, I_t is calculated using Equation (3.1).

$$I_t(t) = I_c(t) + I_r(t) = C\frac{dV(t)}{dt} + I_r(t) \tag{3.1}$$

I_c is the capacitive current component and I_r is the resistive current component, which together make up to the total leakage current I_t. In this study, the magnitude of the instantaneous leakage current was examined at two different times, t_1 and t_2, which correspond to voltage levels having the same magnitude and polarity. Hence, the calculations can be expressed as:

$$I_t(t_1) = I_c(t_1) + I_r(t_1) = C\frac{dV(t_1)}{dt} + I_r(t_1) \tag{3.2}$$

$$I_t(t_2) = I_c(t_2) + I_r(t_2) = C\frac{dV(t_2)}{dt} + I_r(t_2) \tag{3.3}$$

Since the instantaneous voltage is assumed to have the same magnitude, $V(t_1) = V(t_2)$, the resistive current components can be written as $I_r(t_1) = I_r(t_2)$.

If $\frac{dv}{dt}(t_1) = -\frac{dv}{dt}(t_2)$ the sum of Equation (3.2) and (3.3) gives

$$I_r(t_1) = I_r(t_2) \tag{3.4}$$

Therefore, the above equation can be represented by Equation (3.5).

$$I_r(t_1) = I_r(t_2) = \frac{1}{2}[I_t(t_1) + I_t(t_2)] \tag{3.5}$$

Also, in this case $C = [I_t(t_1) - I_t(t_2)]/2\frac{dv}{dt}(t_1) \tag{3.6}$

Since the data in the LabVIEW program only provides records of voltage and current waveforms, a separate post-processing program was developed by writing Matlab® code for above equations. This programme analyses the conditions of sample materials under different levels of voltage. The original data in "tdms" format is extracted and

converted in Matlab data for quantifying the electrical properties of the samples. The analysis results will be explained in detail in Chapter 5. The results obtained from this test were used as a reference when conducting the DC and impulse tests.

3.3   HIGH VOLTAGE D.C. TEST

The direct current (DC) test is a simple test procedure and provides uncomplicated measurement analysis. This test was conducted following international standards, BS EN 60060-1:2010 to monitor the electrical conditions, such as electrical stress distribution and the charge of samples over an adequate period of time. The DC test is a useful way of measuring insulation resistance, as the charging current for AC is very large, which masks the resistive current. Therefore, a power measurement is necessary to determine the DC resistance compared to that under AC energisation. The resistance profile varies according to the applied voltage, hence, it decreases when the applied voltage is increased. The circuit diagram for the DC test is shown in Figure 3.6.
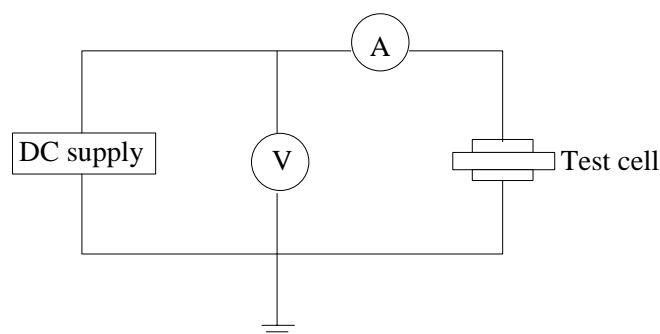
Figure 3.6: The DC test circuit

3.3.1   CIRCUIT ARRANGEMENT

A test cell similar to the one used for the varistors based composite was used for the DC test. A DC power supply, WR series (Glassman), with a maximum voltage of 15 kV, 250 Watts, was connected to the test sample. The voltage measurement was obtained through a capacitive divider having a ratio of 3750:1. Both DC current and voltage measurements were recorded using digital recorders. A few preparatory requirements were undertaken including checking the test samples to ensure that they were dry and clean, setting up the measurement devices and ensuring that the safety procedures for the test were in place. In general, the high voltage test was intended to establish the energy loss in composite insulation. The energy trend depends on the applied voltage, the increase in temperature, the presence or absence of moisture etc. Therefore, a careful monitoring of the voltage profile was done by applying increments of voltage, starting at 300 V. In order to obtain an accurate result, a number of tests were conducted on the microvaristor compound. The test samples were rested for a certain time after each test to minimise the effect of elevated temperatures during the test. The maximum voltage for the test was equal to the threshold voltage that was obtained in the AC test. The test samples displayed non-linear conductivity, enabling them to promote more current flow when they achieved the threshold voltage. The findings of this test will be discussed in Chapter 5.

3.4   IMPULSE TEST

The purpose of this test was to evaluate the behaviour of the micro composite when subjected to transient voltages. Generally, an impulse voltage may cause severe damage to external insulation and promote its degradation as a result of the flow of high current. This relates to the behaviour of negative temperature coefficient for non-linear resistance composites that are associated with high Joule heating and which may cause thermal runaway. Therefore, it is very important to analyse the electrical properties of the micro composite used in this test. Theoretically, disturbances of transient voltages predominantly come from lightning and switching overvoltages. In power networks, the amplitudes of such voltages are extremely high which influences the current flow in the transmission line. Each lightning strike causes travelling waves. However, the amplitude of the impulse will be limited by the maximum insulation strength above which breakdown of the insulation occurs. To replicate real impulse conditions in the laboratory, a test set up with safety features was developed. Two types of impulse voltage tests were introduced; a low voltage impulse test and a high voltage impulse test.

3.4.1   LOW VOLTAGE IMPULSE TEST

3.4.1.1 CIRCUIT ARRANGEMENT

This test was conducted to investigate the response of composite based varistors to low voltage impulses. The set-up is similar to the AC test, except that the device to measure the voltage used a differential voltage probe, at ratio 200:1. This voltage probe was

connected to a Haefely RSG481 recurrent surge generator, which can supply a maximum output voltage of 500 V. The shunt resistor was set at 2 kΩ, and both the current and voltage signals were monitored by a Lecroy digital signal oscilloscope. The sample was placed in the test cell, and the surfaces of the sample and the test electrodes were cleaned before starting the test by using propanol. The results were saved in CSV format. The diagram for the test set up is depicted in Figure 3.7.
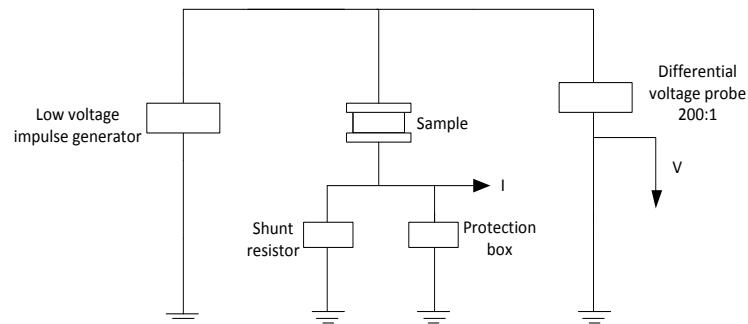
Figure 3.7: Test set up for low voltage impulse test.

3.4.2   HIGH VOLTAGE IMPULSE TEST

3.4.2.1 CIRCUIT ARRANGEMENT

Figure 3.8 shows the test arrangement for the high voltage impulse test. The voltage supply was obtained from a single stage Ferranti impulse generator, with the maximum DC voltage of 55 kV. A commercial current transformer (CT), which has sensitivity of 1.0 V.A^{-1} and a response time of 20 ns, was used. In this test, the conventional voltage measurement was achieved by using a voltage divider with ratio of 2000: 1,

which can be operated up to a maximum voltage of 150 kV DC. The test cell was placed between the voltage divider and the high value front resistor.
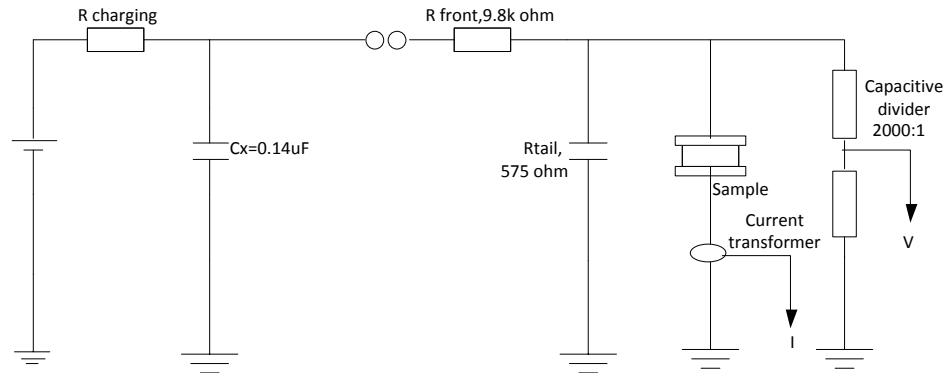
Figure 3.8: Circuit arrangement for the high voltage impulse test.

The voltage and current signals were recorded using a Lecroy Wavejet 314 digital signal oscilloscope with a rise time of 3.5 ns. The recorded signals were in accordance with the bandwidth operation of 100 MHz.

During the conduct of the impulse test, a few important findings were observed. It was noticed that the selection of the voltage divider was important, because there is high risk of distortion in the measurement of fast rising voltages at high frequencies. Further interference and impact on measurements accuracy may be caused by the setup of the test and the nature of the sample being tested.

To minimise any effects caused due to proximity, a suitable distance between the HV devices and any nearby energized or earthed structure was maintained. Such partial

discharge was noted in both voltage and current signals. Therefore, to minimise the presence of this type of interference, the test electrodes and test samples were cleaned before and after the test was conducted. This method was suggested by Kuffel et al. [96] in which they highlighted the fact that the presence of dirt on the electrodes will influence the breakdown voltages.

In this research, the sampling rate was increased in accordance with the charging voltage. In order to make the analysis results more presentable, both voltage and current signals were filtered using the Savitzky-Golay filtering technique. The purpose of this technique was to filter the signals without distorting their original values. The special filter code was created in the Matlab® platform and the signals were filtered in the time domain. Dokur et al. [97] presented this application as one which was feasible to be applied in an impulse test.

3.5 MICROSCOPY EVALUATION

In this research, certain information about microvaristor materials, such as their chemical composition, the size of materials and the microstructure that were responsible for the electrical properties of the microvaristor compound, were still lacking. A number of microscopic analyses of both the microvaristor powder and the compound were used to obtain this information.

The three important elements which are determined under the microscopic investigations are the size of the micro particles, the chemical composition of the powder and the microstructure of both the varistors powder and the composite. Since

the investigation included dealing with a number of matters, different microscopic techniques were applied. These investigations assisted the author to understand the internal properties of the materials themselves that contribute to the electrical performance of the composite based varistors. The specific working procedures are explained in the following section.

3.5.1   SCOPE OF EVALUATIONS

3.5.1.1 MICRO PARTICLE SIZES

A preliminary microscopic analysis of the grain was conducted using a Leica optical microscope. This microscope operates in X and Y measurement mode with a resolution of 1 µm. The measurement scale was set up to 200 µm and the optical images are shown in Figure 3.9.

Further investigations on the grain size of two microvaristor powders, *A* and *B* were conducted under an inverted light microscope, Axio-Imager 2. The purpose of this investigation was to determine the effect of the size of the micro particles on the current path after the dispersal of the microvaristor powder in the silicone rubber. Generally, the size of particles determines the number of particle contacts that lead to non-linear characteristics. With smaller particle sizes, larger current paths are created, which in turn encourage a large current flow. This is due to large surface area-to-volume ratio which will be increasing with decreasing the size of micro particles. This investigation

is important to determine which areas of the microvaristor material are most influential in enhancing the performance of field grading samples.
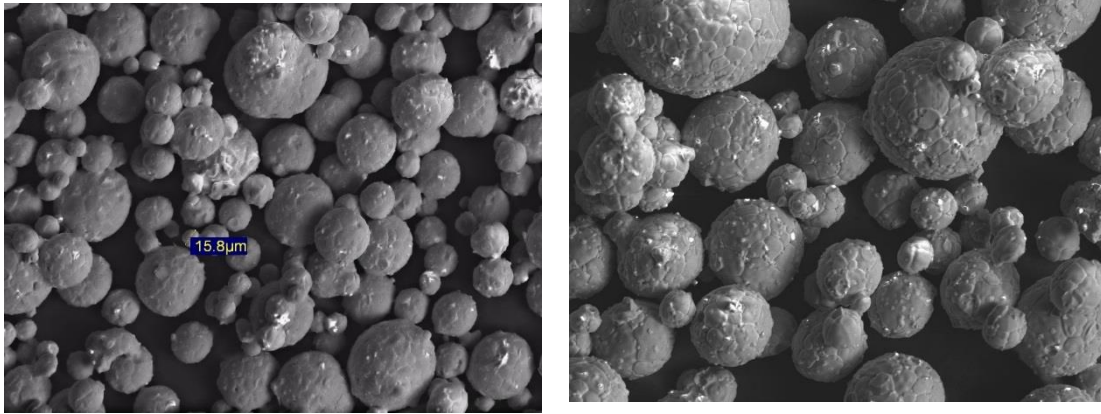
a)The microparticles of microvaristor *A*.   b)The microparticles of microvaristor *B*

Figure 3.9: The optical images for microvaristor particles.

3.5.1.2 ELEMENT STUDIES

Generally, the microvaristor powder consists of approximately 90% zinc oxide together with small amounts of metal oxide additives [3]. The general understanding of electrical properties of ZnO ceramics is resulting from the high resistance of the intergranular layers that are formed between low resistant ZnO grains. The presence of additives in the microvaristor is important and is responsible for the grain development required to increase its nonlinear performance. The uniqueness of the microvaristor powder is dependent upon the morphology condition, the filler modification and the formulation of the microvaristor components.

In this section, attention is given to investigating the formulation of metal oxides for both microvaristor powders, as there is no specific information in relation to the material properties. X-ray Photoelectron Spectroscopy measurement was carried out in a Kratos Axis Ultra – DLP XPS system with a monochromated Al kα [98] to examine the composition of the chemical elements that exist in the microvaristor powder.

3.5.1.3 MICROSTRUCTURE OF ZNO VARISTORS

Investigating the microstructure of microvaristor and their composites has become a major area of interest within the field of varistors technology. It is well known that microvaristor powder and silicone rubber matrices have important properties that are incompatible in the compounding process. Therefore, microstructure analysis is a reasonable approach to understanding the way in which the particles are arranged in the host matrix after the fabrication process. In this work, a TM3030 Scanning Electron Microscopy (SEM) was used. It operates under different accelerating voltages either 5 kV or 15 kV. The image magnification can be adjusted from 15 to 3000X with the maximum specimen size of 70 mm. The detailed images of the dispersed microvaristor in the polymer matrix were clearly visible. This level of detail cannot be obtained using a light microscopy technique. The elemental mapping based of the SEM analysis on the surface examines the chemical elements of the composite after undergoing the fabrication process. An analysis of the dispersal of microvaristor particles was also conducted in order to understand the distribution of micro-particles in specific areas.

3.5.2 PROCEDURES FOR MICROSCOPIC ANALYSIS

3.5.2.1 X-RAY PHOTOELECTRON SPECTROSCOPY

X-Ray Photoelectron Spectroscopy (XPS) is an ultra-high vacuum (HUV) technique for surface analysis in order to determine the elemental composition (atomic %) of elements in the solid sample. The technique operates when an atom absorbs a photon, which has energy greater than the work function of the atom, which allows the electron to be ejected [99]. Generally, the sample will be irradiated with mono-energetic x-rays that causes photoelectrons to be emitted from the sample surface. Because of this reaction, the binding energy and intensity of electron will be displayed through electron energy analyzer. Hence, the composition of elements and chemical state can be identified. Each element has a unique binding energy that originates from electrons in the atomic orbital [98]-[99]. In this analysis, the XPS measurements were taken by Dr Hasliza Bahruji, from the School of Chemistry, Cardiff University.

3.5.2.1.1.   SAMPLE PREPARATION

Approximately 5 g of microvaristor powder from both types of microvaristor powder were prepared for spectroscopic analysis. Dry and clean materials were used in order to avoid possible distortion in the results. Matsuoka et al. [3] explained the general chemical elements that exist in ZnO ceramic, and it was found that some of them are similar to current microvaristor material.

3.5.2.2 AXIO-IMAGER INVERTED MICROSCOPE (Zeiss)

The measurement of grain size was conducted using an Axio-imager inverted microscope made by Zeiss. This microscope offers quality microscopic measurements with time saving for sample preparation and investigation [100]. A small amount of powder was dispersed on a white plate and the dimensions of the distributed particles were checked. The measurement was repeated more than 10 times in order to establish the normal distribution of particle dimensions. The profile of micro particle sizes for both samples were recorded and are reported in Chapter 4.

3.5.2.3 SCANNING ELECTRON MICROSCOPY (SEM)

This technique was used to analyse the micro-magnified image of composite samples which gave information about the surface topography of 'bulk' samples. This apparatus works by focusing repeated electron beams, rather than light, over a given area. Either 5 kV or 15 kV accelerating voltages can be applied to cause the electron beam to make strikes on the samples. When an electron beam 'hits' a sample, it energises the electrons of the material and causes them to be ejected. When the electrons from the material are detected, an image is produced representing the surface and the properties of the material.

3.5.2.3.1   SAMPLE PREPARATION

Solid samples of the material were mounted on an SEM stub before being transferred to the SEM chamber of a Hitachi TM3030. It was essential to keep the samples dry and clean before they were placed in the high vacuum chamber. Conducting double-

sided tape was attached to the sample, which was approximately the size of a five pence coin (estimated diameter 23.4 mm) with thickness 3 mm. The SEM investigation was carried out in the Morgan-Botti Lightning Lab (MBLL), Cardiff University, with support from Dr David Clark and Dr Daniel Mitchard.

3.5.2.4 ENERGY DISPERSIVE X-RAY SPECTROSCOPY (EDX)

The Hitachi TM3030 has dual applications for Scanning Electron Microscopy (SEM) and Energy Dispersive X-Ray Spectroscopy (EDX) built into it. The working mechanism of an EDX is to provide both elemental identification and quantitative compositional information of the samples. The elemental mapping was shown by the EDX spectrum that was obtained when the electron beam hit the sample during the SEM. Each element has a different atomic structure which enables the X-rays to provide particular information for each elemental component of the samples.

3.6   CONCLUSIONS

The preparations for the laboratory tests were discussed, including the procedures required for the high voltage experiments, the set up and the safety requirements. Every test complied with the standard required by BS EN 60060. The purpose of the tests was to investigate the electrical properties of different microvaristor samples when subjected to AC, DC and impulse tests. Such electrical characteristics have been identified and will be presented in Chapter 5.

Meanwhile, microscopic measurements were carried out in order to analyse the material properties of different powders and the composites. These investigations assisted the author to understand the material properties that contribute to the electrical characteristics of the varistors based composite. Some techniques were presented to evaluate the particle size of microvaristor powder, elemental studies and to investigate the microstructure of the compound.

CHAPTER 4

APPROACH FOR THE PREPARATION OF NON-LINEAR FIELD GRADING SAMPLES

4.1 INTRODUCTION

In the modern era, the introduction of micro and nano material filled polymers has been embraced by industry and academia, since this additional material has exhibited extraordinary mechanical, electrical and thermal properties. Previous studies have reported on the advantages of the fillers that form in micro-sized particles [56], [101] and in nano-sized particles [1], [102] specifically in relation to their use in high voltage insulation systems.

Non-linear composite based polymers were produced by dispersing non-linear materials, homogenously, in a host matrix at a certain percentage according to weight (wt. %) or to volume (vol. %). There are three types of polymer that are commonly used as the host matrix. These are thermosets (e.g. epoxy resins), thermoplastics (e.g. polypropylene), and elastomers (e.g. silicone rubber). The idea of combining

properties of non-linear material with polymers has resulted in the fabrication of composites that are light weight and allow for complex design which can be used to replace conventional components.

4.2   PREPARATION OF SAMPLES

Several techniques to fabricate micro or nano - composite samples have been proposed [14], [19]-[20]. However some challenges are inevitable when dealing with these materials, such as heterogeneous filler dispersion, properties incompatibility of the different materials and viscosity effects arising from the polymer matrix. Therefore, it is useful to identify the characteristics of the materials before they are made into a new compound.

4.2.1   MATERIAL SELECTION

4.2.1.1 MICROVARISTOR POWDER

 In this research, zinc oxide microvaristors were used for fabricating new field grading material samples. Two microvaristor powders were obtained from different sources; microvaristor *A* and microvaristor *B*. The materials come in different colours and seem, to the naked eye, to have similar sizes of grain as shown in Figure 4.1. However, with the aid of microscopy instruments, it can be seen that the materials exhibit different properties and characteristics, and these will be discussed in a later section. It is noticeable that the use of non-linear fillers in academic studies and in industry is constantly increasing. Therefore, in order to improve dielectric performance,

considerable investigations have been conducted into the development and fabrication of nano-sized zinc oxide varistors [103]. Taking into account the possibility of agglomeration when dealing with nano-sized powder, the conventional micro-sized zinc oxide varistors is used in such fabrication. It is worthy to note that there are some challenges involved in fabricating micro composite materials due to limitations in the processing technology [43], [104].
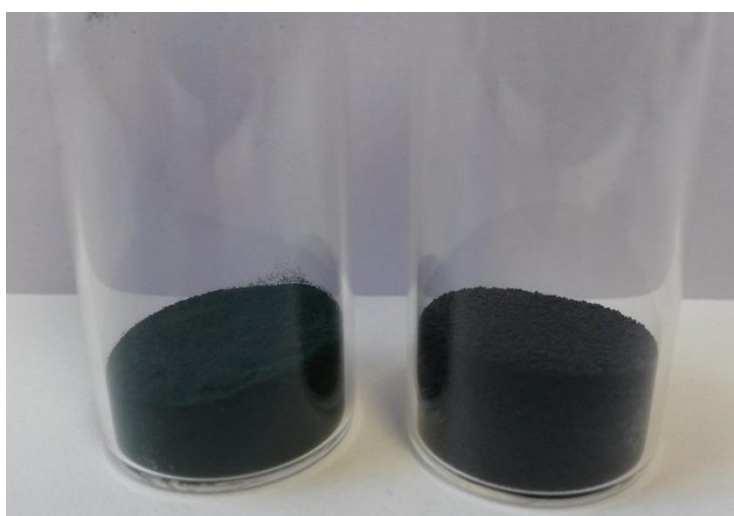
Figure 4.1: Microvaristor powder *A* (left) and *B* (right).

To meet this challenge, a detailed fabrication process is developed in this work, and will be explained in this chapter which will emphasize the advantages and disadvantages of dealing with microvaristor materials.

The sample preparation process was initially developed by trial and error. Therefore, attention was given to every aspect of the process in order to overcome the variable factors that have an influence on the processes and procedures. The thicknesses of the

samples were 1 mm in the initial investigation, but were later increased to 5 mm in order to achieve the objectives of the research. All fabricated samples were tested, and the fabrication process was validated when experimental tests showed satisfactory results.

4.2.1.2 HOST MATRIX

The white-silicone rubber as shown in Figure 4.2 was supplied by Wacker Chemie (Germany). It has shown numerous advantages, such as elasticity, good dielectric properties, and light weight.

The profile of all the materials used in the fabrication process is shown in Table 4.1 and the datasheet of the silicone rubber is presented in Appendix D.
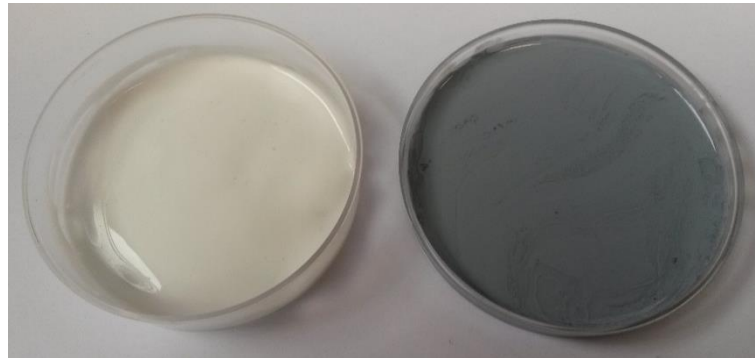
Figure 4.2: The white silicone rubber, Powersil 600-A (host matrix) on the left, and Powersil 600-B (hardener**)** on the right, supplied from Wacker Chemie, Germany.

With reference to Table 4.1, the density of microvaristor **B** was measured through experimental work in this project at Cardiff University. The initial measurement was done for related laboratory apparatus, amount of microvaristor powder and volume of

insoluble liquid; propanol. The amount of microvaristor powder was weighed using a precision digital balance scale, KERN ABJ 320-4 that operates to maximum capacity of 320 g with readability of 0.1 mg. The microvaristor powder **B** was dispersed into propanol and the volume of propanol after dispersion process was taken. The density of powder was calculated by dividing the weight of powder with the discrepancy volume of propanol. A number of tests were carried out in order to achieve good accuracy and repeatable results.

Table 4.1: Material properties of silicone rubber and microvaristor powder.

Materials	Properties	Inspection method	Value
Silicone rubber	Relative permittivity	IEC 60250	2.9
	Density	IEC 1183-1 A	1.13 g/cm^3
	Volume resistivity	IEC 60093	10 x 10^{15} Ω.cm
Microvaristor *A*	Density		5.6 g/cm^3
Microvaristor *B*	Density		[1]Average 5.6 g/cm^3

Microvaristor filled silicone rubber samples were prepared using vacuum-based laboratory procedures. These procedures involved measuring the substances, mixing, degassing and stirring, injection moulding and finally curing. An additional procedure, heat treatment, was introduced in work in order to reduce the viscosity of the host matrix and to eliminate the moisture in the filler. The flow chart of the fabrication

---

[1] Density value was obtained from experimental work at Cardiff University

process is shown in Figure 4.3. The processes were carried out sequentially and carefully observed during the preparation.
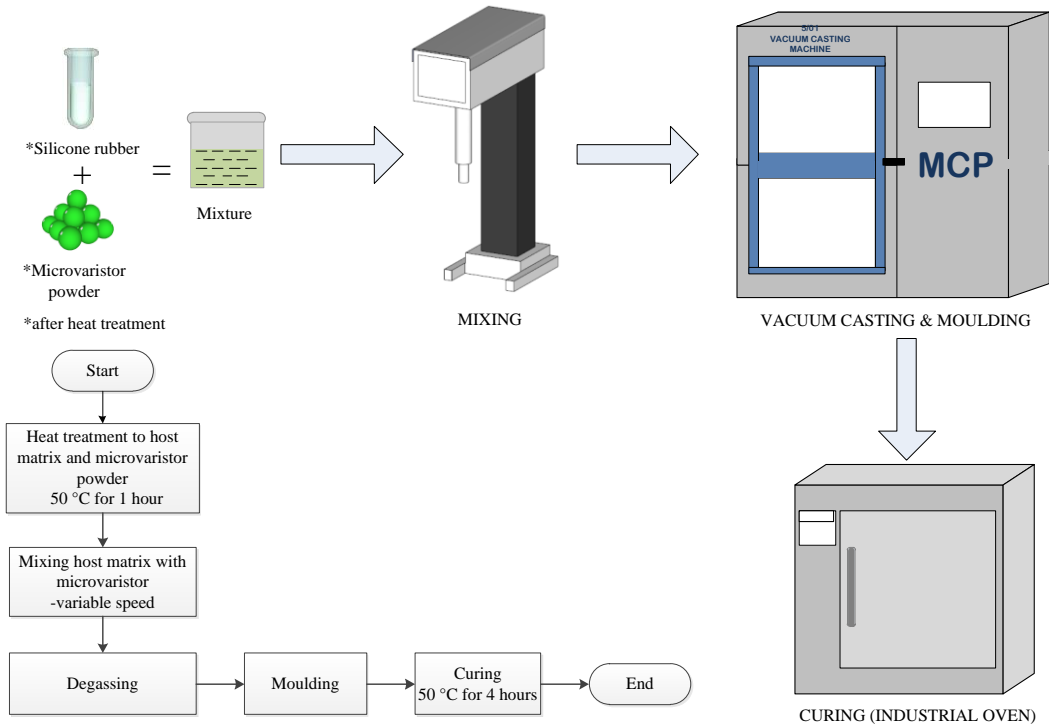
Figure 4.3: The sample preparation process for microvaristor filled with silicone rubber.

4.3 FABRICATION PROCEDURES OF MICROVARISTOR (wt. %)

COMPOSITE SAMPLES

Generally, there are no specific guidelines for handling non-linear fillers compounded with a polymer matrix. It is well known that silicone rubber has high hydrophobic properties, but the characteristics of microvaristor powder need to be investigated.

Therefore, a special test was conducted on the microvaristor powder, as explained in the next section.

4.3.1   IDENTIFICATION OF WETTING PARTICLES

In this test, the microvaristor powder was dispersed in water, as is explained in [105]. The aim of this test was to investigate the wetting characteristics of microvaristor powder. It was observed that the micro particles broke through the surface of the water and sank. Hence, the gravity force on the varistors powder is greater than the surface tension of the particles. This finding is important as it shows that the microvaristor exhibits hydrophilic behaviour, which encourages the formation of moisture in the microvaristor powder.

4.3.2   STAGES OF THE FABRICATION PROCESS

4.3.2.1 MICROVARISTOR COMPOSITION

A number of samples were fabricated with different microvaristor loadings in the silicone rubber matrix. Due to limitation of microvaristor powder, the microvaristor amount was scaled at the following selected percentages, 10 wt. %, 30 wt. %, 60 wt. % and 70 wt. %. Verification of the amount was done when the test result showed a significant response in the electrical characteristics and performance of the composite. As there was a limited supply of microvaristor B, the initial investigation to find the suitable microvaristor loading was conducted on microvaristor A only. It is recommended that the smallest possible volume of polymer is used in order to allow the microvaristor composite exhibits the non-linearity behaviour. It was found that the

introduction of 48 vol. % [33] of microvaristor was sufficient to obtain the non-linear composite, when dispersed into the host matrix.

The amount of microvaristor powder required to produce a reliable compound is somewhat subjective as there are several internal and external factors that need to be taken into account. The type of filler, the grain size, the host matrix used, the dimension of the samples and the fabrication process used, all interact with each other. For instance, as described by Ebishi et al. [33], different microvaristor concentrations of 10 wt.%, 15 wt. % and 20 wt. %, (2.2, 3.5, 4.9 vol. %) were loaded in the epoxy resin in order to fabricate thinner samples. The results were encouraging. The quantity of microvaristor was weighed using a precision digital balance scale (KERN). For this fabrication, the amount of material used was at least 10 times from the size of the eventual sample. This is due to the high viscosity of the mixture which will have an influence during the moulding process.

4.3.2.2 HEAT TREATMENT

The objective of heat treatment is to make it easier to mix the microvaristor powder with the silicone rubber. Both materials were placed in the oven at 50 °C for 1 hour. Adopting this method, the viscosity of silicone rubber can be reduced and the formation of moisture in the microvaristor powder can be minimised. The temperature setting is very important for heat treatment. It would not be possible for the temperature to be set at 100 °C, as this would cause agglomeration to occur during the mixing process when the microvaristor powder dispersed into the silicone rubber matrix.

4.3.2.3 MIXING

Room temperature, vulcanised, RTV-2 silicone rubber Powersil 600-A and Powersil 600-B (hardener), supplied by Wacker Chemie, Germany, was used for the fabrication of the samples. The polymer is light grey and has a viscosity of 10000 mPa.s . The proportion of host matrix to hardener is calculated according to a weight ratio of 9:1, and it is essential that this ratio is adhered to in order to avoid adverse effects on the physical form or the electrical characteristics of the final product being jeopardized. For this study, a mechanical mixer (Ross model HSM-100LSK) was used to disperse the micro composite particles into the silicone rubber matrix. This was done at increasing speeds during the mixing process. The initial speed was 1000 rpm. The benefit of using the machine is that it distributes the microvaristor uniformly in the polymer matrix. Once the microvaristor had wetted into the polymer matrix, the mixer speed was increased slowly to 4000 rpm. The manufacturer recommends that a speed of 6000 rpm is suitable for a high shear laboratory machine when mixing composites [50]. In order to verify the optimum speed for micro particle dispersion, a calculation relating speed to particle diameter was obtained from [19] as shown in Equation (4.1).

$$\text{rpm} = \frac{\text{peripheral velosity (m/sec)} * 60 * 1000}{d(\text{mm}) * \pi} \qquad (4.1)$$

The Ross 100 LSK high-shear mixer has a 16 mm blade diameter, d and a peripheral velocity for its mixing blades of 5 m/s [106], which is sufficient to obtain uniform microvaristor dispersion.

Another aspect of the process which needs to be considered is the duration of mixing. The optimum duration should be set according to the volume of the mixture and the condition of both materials. If the mixing time is too long, it will greatly increase the degradation of the silicone rubber due to heat that is produced during this process.

In an attempt to reduce agglomerate formation, the micro composite should be added to the polymer solution all at once and very quickly, which will allow the wetting of the filler powder before the viscosity of the mixture starts to increase.

4.3.2.4 DEGASSING

Degassing and stirring was carried out simultaneously for at least 5 minutes in the top mixing vacuum chamber in order to remove any trapped air and gas that might have resulted from mixing silicone rubber with a microvaristor. The hardener from another cup was then added to the microvaristor compounded silicone rubber. The degassing process continued until no bubbles remained visible on the surface.

4.3.2.5 MOULDING

The aluminium mould was placed in the lower injection chamber and then connected to the top mixing vacuum through a funnel. A mould made from metal gives the best strength to the casting because more rapid solidification occurs than when plastic is used [107]. A sequential mechanical programme was used to monitor closely the processes taking place in the machine. During the injection moulding, the material started to fill up the cavity of the mould as shown in Figure 4.4 and the operation was stopped when material began to emerge from the venting holes. For this research

programme, the sample was fabricated with dimensions of 50 mm x 50 mm with two

thicknesses, 1 mm for the initial investigation and then 5 mm for the final samples.
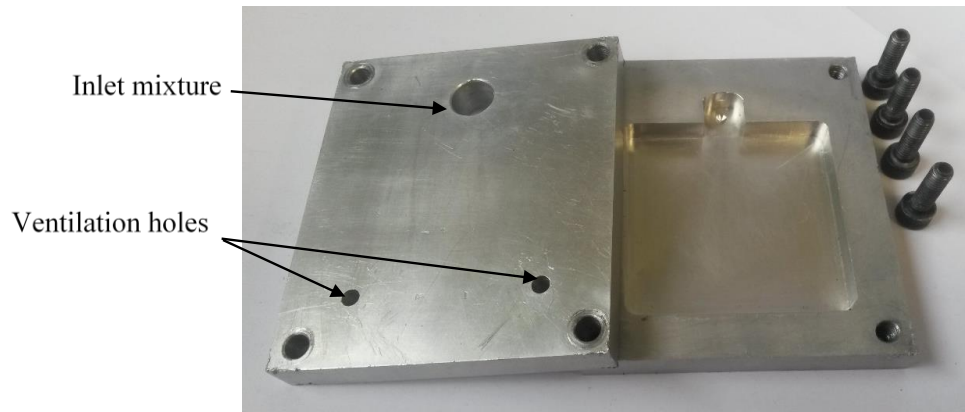
Figure 4.4: Utilised aluminium mould for dimensions of 50 mm x 50 mm x 5 mm.

4.3.2.6 CURING

The mould was then placed in an oven set at 50 °C for 4 hours for curing to take place.

In order to form the cast as finely as possible, the mould was allowed to cool down for

an hour. The sample was then taken out of the mould and an inspection was made to

ensure that no surface voids had formed.

4.4   FABRICATION PROCESS

The focus in this section will be on the fabrication method of microvaristors based

composite, with description of various observations occurring during the fabrication

of the micro composite samples. The key parameters of the fabrication process and the

dimensions of the samples will be highlighted. Afterward, the investigations involved in studying the elements involved, ascertaining the size of the grains and examining the microstructure of the filler in the powder and compound will be introduced.

4.4.1 PARAMETER CONTROL

It has been identified that the mixing regime was the critical process during the fabrication of the micro-composite sample. This is because the dispersal of the micro particles is related to agglomeration. Agglomeration is prone to occur due to the high surface energy of the filler that can cause incompatibility between the filler and the host matrix. A research conducted by Sumita et al. [108] highlighted some factors that contribute to the agglomeration problem, namely the viscosity of the polymer and the size of the micro filler.

As mentioned earlier, the viscosity issue may be handled by applying heat treatment to the silicone rubber before proceeding with the mixing process. The composite that is involved with agglomeration susceptible to reduce the properties of such materials can be described as 'defect'. In order to minimise such problem, the temperature and the material reaction during the fabrication process should be carefully controlled, as discussed in [109]. In order to understand the thermal effect that takes place during the mixing process, a graph of the observations made with different microvaristor compositions and solidification times of the mixture (in minutes) was plotted, as shown in Figure 4.5.
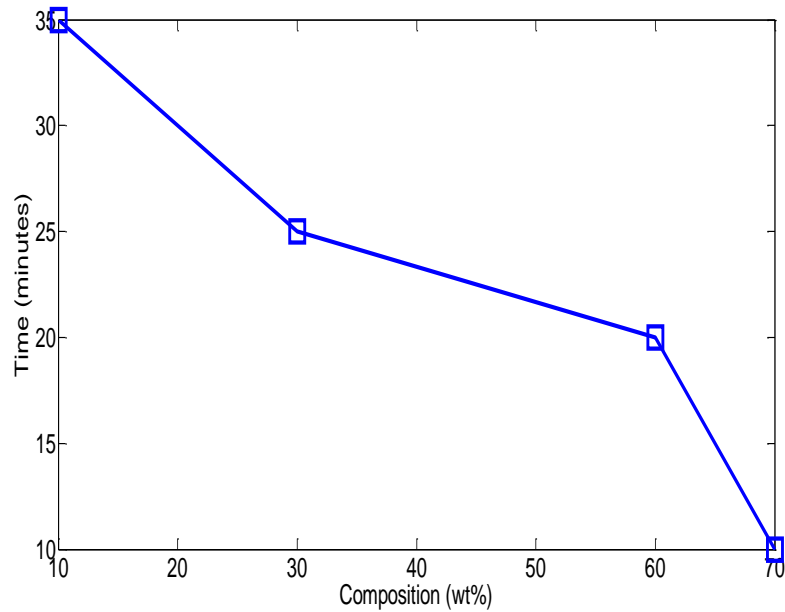
Figure 4.5: The solidification time for different microvaristor concentrations filled with silicone rubber matrices. The measurements were taken during the casting process. The thickness of samples was 5 mm.

The measurements above were taken with the mixing time set at 7 minutes, with the temperature rising to 45 °C for all samples. The time allocation and temperature measurement are important, as it was found from the observations that the moulding process can then be conducted with less risk and without problems occurring. This work confirms the theory that an interaction actively occurs between the microvaristor particles and the silicone rubber at high temperatures, resulting in a lower risk of agglomeration building up. In practice, the initial temperature of the mixture, after heat treatment had taken place, should be 26 °C, which is increased when the mixing process is taking place. Continuous temperature measurements were taken until the

end of the mixing process. Figure 4.6 shows the important parameters to be observed during the mixing process. These parameters need to be monitored closely, in particular, in relation to the increase of temperature which requires the working procedure to be followed. From the observations, if the mixing process takes place beyond the optimum time, the temperature will increase which, in turn, may cause complications to occur during the casting process.
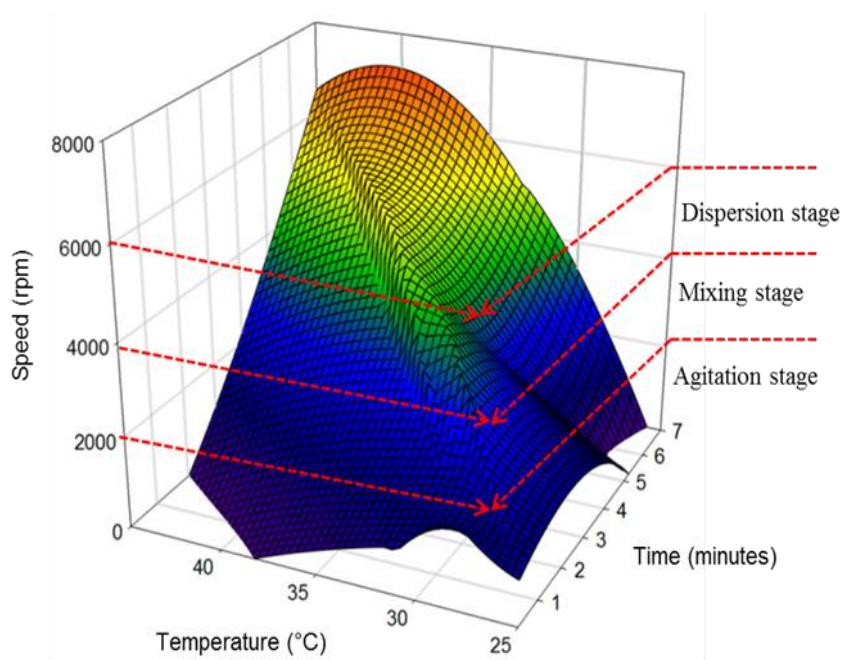
Figure 4.6: The three important parameters to be controlled when using a high shear mixer during the agitation, mixing and dispersion processes.

According to Figure 4.7, agglomeration of a mixture of 70 wt. % microvaristor filled with silicone rubber occurred in the vacuum casting machine. The high temperature that results from the mixing process accelerates the solidification immediately after the hardener is introduced. This is the most important challenge that was dealt with in

order to ensure that the fabrication process meets two essential criteria, which are minimising the material loss while maintaining the quality of the sample.
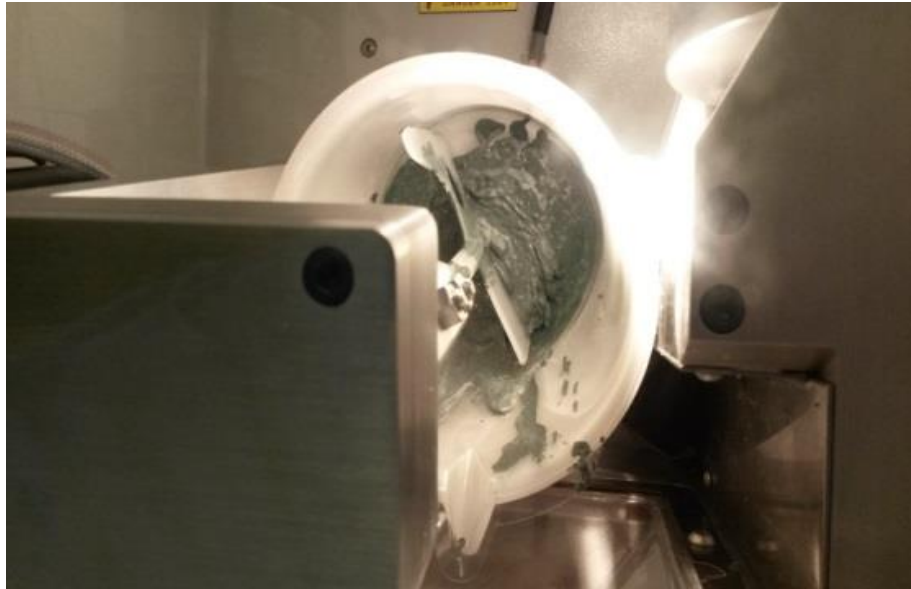
Figure 4.7: Photo showing microvaristor being mixed in the vacuum casting machine. A complication occurs when the duration of mixing is set beyond 7 minutes.

4.4.2 MICROVARISTOR COMPOSITE SAMPLES

As mentioned earlier, there were a number of different compositions of the compounds when different microvaristor loadings (wt. %) were dispersed in the silicone rubber matrix. This study is intended to ascertain the suitable microvaristor concentration in the composite, in order to attain the desired non-linearity characteristics. For this early investigation, only microvaristor *A* was used, due to the limited supply of the second material. A series of fabricated compounds using microvaristor *A* is shown in Figure 4.8 with sample having a thickness of 5 mm. The images show the effect of

microvaristor loading in the samples at different filler loadings. As the amount of microvaristor is increased, a larger volume microvaristor particles filled in the host matrix will contribute to more current path formation.

a) 10 wt%   b) 30 wt%

c) 60 wt%   d) 70wt%
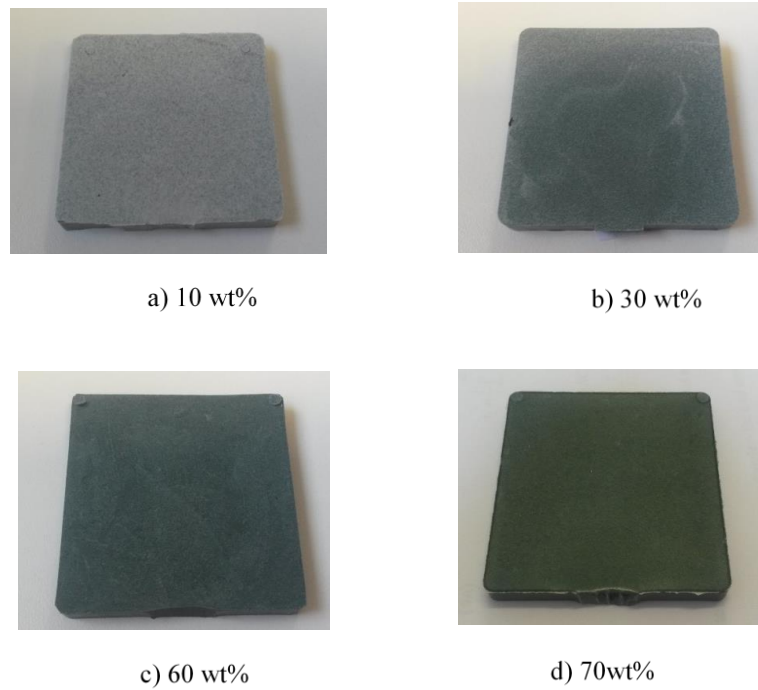
Figure 4.8: 5 mm of microvaristor *A* filled with silicone rubber at different microvaristor loadings.

In this work, it was found that 70 wt. % (32 vol. %) is a suitable microvaristor concentration that allow composite to exhibit the non-linear characteristic. The electrical performance of the fabricated samples will be discussed in Chapter 5.

4.4.3 THICKNESS OF SAMPLES

As discussed earlier in Section 4.3.2.5, the trial and error fabrication process was carried out on the smaller samples, with a thickness of 1 mm, before it was deployed with the 5 mm samples that are depicted in the Figure 4.9. Both samples showed

significant non-linear characteristics that corresponded with the different microvaristor loadings. The sample having the smaller thickness is easier to fabricate compared with the larger sample. Special attention should be given to quantify the amount of mixture which is dependent upon the microvaristor loading in the silicone rubber.

Figure 4.9: The non-linear microvaristor *A* composite samples that were obtained at different microvaristor concentrations and thicknesses. The sample of 1 mm with 60 wt. % (left) and of 5 mm with 70 wt. % (right).

4.5   MICROSCOPY EVALUATION

In Section 3.5, the microscopic techniques and procedures to evaluate the microvaristor powder and compound were discussed. Here, attention will be given to the results of investigations into the elemental composition and micro particle sizes of powders. The morphology of the filler in the silicone rubber will also be discussed. The findings constitute a significant help in understanding the effect of the material properties upon the fabrication process and the electrical performance.

4.5.1   ELEMENTAL STUDIES

The chemical elements of microvaristor powders are described in the following paragraphs. Matsuoka et al. [3] explained the general chemical elements that exist in ZnO ceramic, some of which are similar to current microvaristor materials.

Meanwhile, the classification of microstructural components of ZnO varistors was presented by Gupta et al. [34], explaining the four basic compounds formed in ZnO varistors. Such fundamental compounds are ZnO, spinel, pyrochlore and bismuth (Bi) phases that significantly influence the physical and electrical properties of varistors performance.

The XPS analysis on powder sample A was examined, and a variety of rare - metals were detected, as depicted in Figure 4.10. The presence of oxygen, O 1s and carbon, C 1s, are derived from the presence of carbon and oxygen in the layer that forms on the powder surface. Both peak elements of binding energy (eV) are detected at ~ 529 eV and at ~ 283 eV respectively. The main component, Zn 2p, was evaluated at ~ 1020 eV. It was found that the presence of beryllium, Be 1 s at ~ 101 eV specifically increased the mechanical properties of the sample.

Such additives as Bi 4f were detected at ~ 158 eV, and the formation of Bi_2O_3 in the intergranular layer enhances the stability of ceramics [110] and is used in the production of varistors, as reported in [111]. The ceramic based ZnO- Bi_2O_3 is commonly used in the varistors industry, since its production is quite simple and effective. Other elements such as sodium (Na), fluorine (F) and rubidium (Rb) are apparent at ~ 1061 eV, ~ 679 eV and ~ 300 eV respectively.
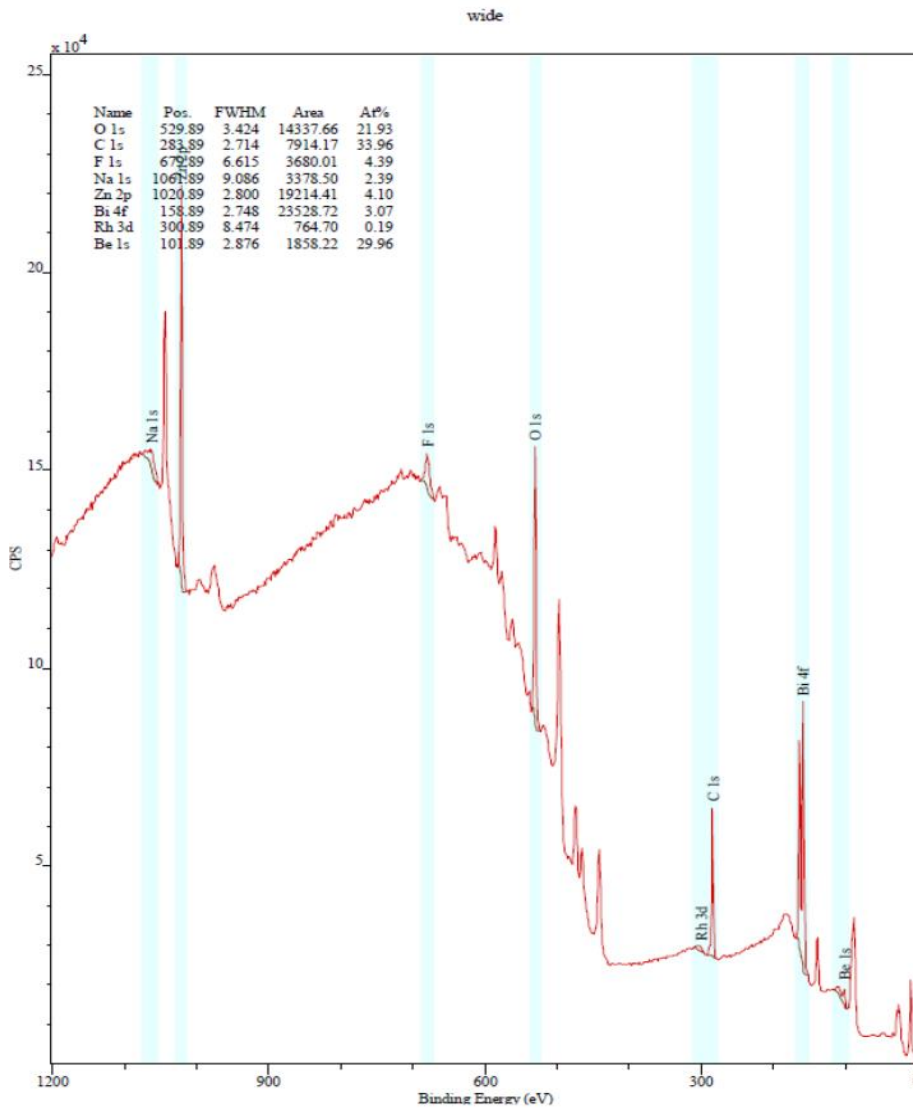
Figure 4.10: The XPS measurement of the chemical elements of microvaristor *A.*

A different chemical composition was detected in Material *B*, as presented in Figure 4.11. The common chemical elements that were observed are zinc, carbon and oxygen. These were traced at ~ 1021 eV, ~ 284 eV and ~ 530 eV respectively. Microvaristor *B* contains 2 additives, bismuth (Bi) and antimony (Sb). The presence of two or more additives in the varistors component will improve the ceramic performance and promote the reliability and durability of the ZnO varistors.

The dopants show binding energies at ~158 eV and ~538 eV. The antimony oxide is particularly helpful in promoting the crystalline growth of ZnO and improves the solubility of the metal in the host matrix [40]. Meanwhile, bismuth oxides improve the stability of ceramic composites. The additives that exist in both samples are summarised in Table 4.2.
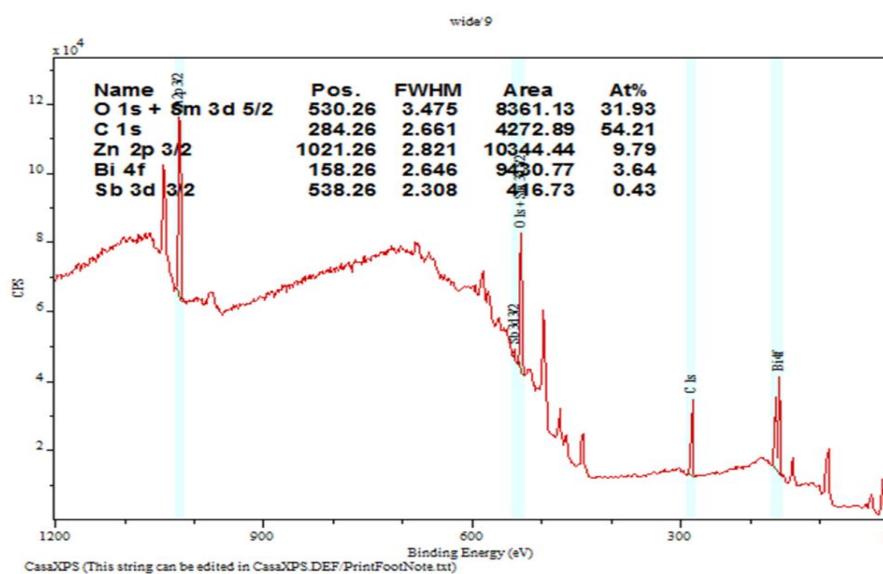
Figure 4.11: The XPS measurement of the chemical elements of microvaristor *B*.

Table 4.2: The summary of additives that exist in both microvaristor powders.

Additives	Roles of additives	Microvaristor
Bi_2O_3	Improve the stability of ceramic	*A* and *B*
Sb_2O_3	Increase the non-linear coefficient of varistor and grain growth retardants	*B*
Na^+	Mitigate the ageing effect at grain boundary	*A*
Be^+	Increase the mechanical properties and grain growth	*A*
F^+	Improve the non-ohmic properties, specifically for the formation of donors	*A*

Generally, the introduction of a variety of metal oxide additives is one of the empirical methods of improving the overall long-term performance and reliability of ZnO varistors. However, obtaining the compatibility of different metal oxides in the composite is quite challenging because it influences the performance of the material, such as in its power dissipation, material stability and current conduction, as has been highlighted by [112].

The presence of different additives may have contributed to the increase in the electrical and mechanical performance of materials. However, there is no effect on the fabrication process during the mixing regime. The powder can be mixed uniformly in the host matrix, and there is no evidence of any complications arising in the micro-composite when heat treatment was applied to the microvaristor powder.

4.5.2 PARTICLE SIZE OF MICROVARISTOR POWDER

In Section 3.5.2.2, the procedures of particle size measurement has been discussed. The profiles of the micro particle sizes for both samples are shown in Figures 4.12 and Figure 4.13. The size distribution trend was obtained for both microvaristor powders, and these clearly show the particle sizes that directly influence the electrical performance of the composite.

Microvaristor sample *A* has a range of particle sizes from 10 μm to 120 μm, which is a lower range compared with that of microvaristor *B,* as is shown in Figure 4.12. The range size of microvaristor *B* was greater, reaching 300 μm, and this influences the current distribution in the composite. Even though the grains are formed in a variety of sizes, the surface area of micro fillers still has a tendency to coagulate easily

compared to nano-sized materials [19]. The mean size of microvaristor *A* and was found to be 37 µm.
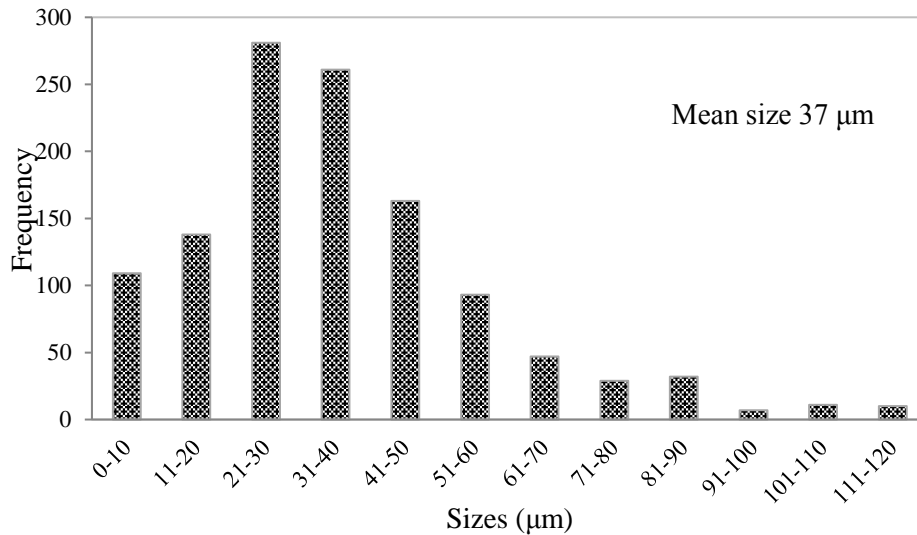
Figure 4.12: The particle size of microvaristor *A*.

With reference to Figure 4.13, there is no particle size in the range 0 to 10 µm exist in microvaristor *B*. However, both powders exhibit the highest frequency of grains in the size range 21 to 30 µm, which may be the fundamental dimension of ZnO ceramic. The mean size of microvaristor *B* was calculated at 71 µm, slightly higher than that of microvaristor *A*. As it has a larger particle size than microvaristor *A*, this second micro particles are expected to distribute a lower amount of current conduction through the powder and compound.
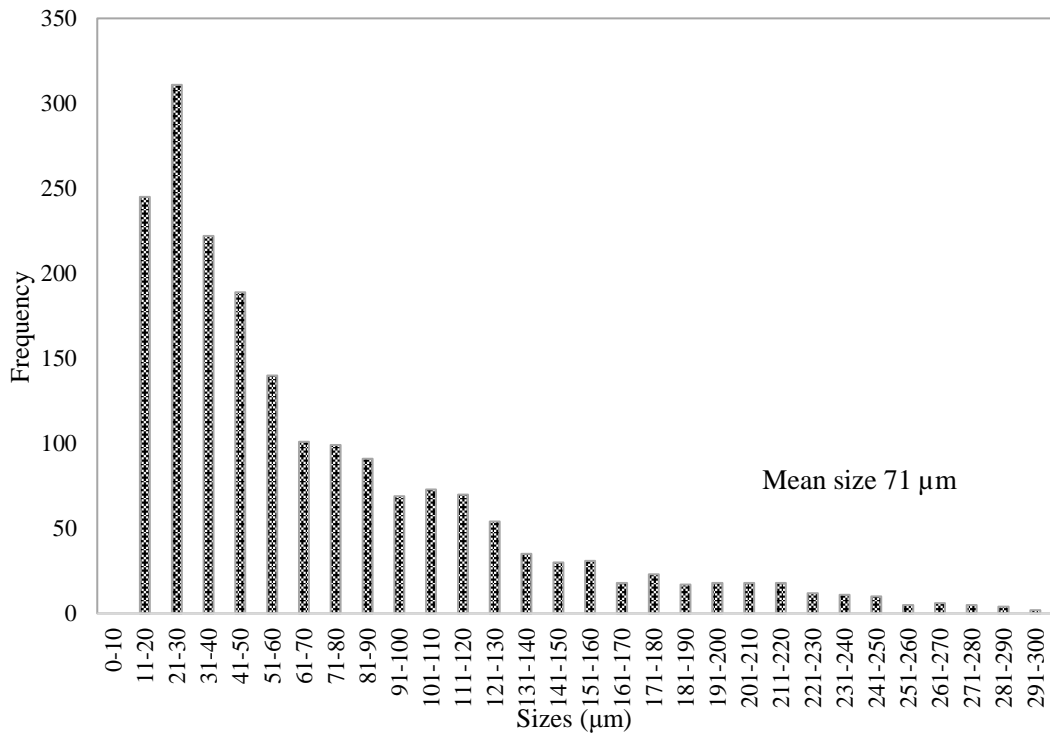
Figure 4.13: The particle size of microvaristor **B**.

Therefore, the electrical properties of composite based varistors can be modified significantly. The profile of current conduction for both microvaristor powders will be discussed in the following chapter. A similar scenario concerning the influence of the particle size on electrical performance was discussed in [111] which emphasized the major dynamic influences on electrical parameters, such as the electrical field, resistivity, conductivity and relative permittivity.

4.5.3 MICROSTRUCTURE AND DISPERSION OF FILLER

Generally, the dispersion of filler in the compound can be done through qualitative or quantitative techniques. Under 40X magnification, the dispersion of microvaristor in the silicone rubber can be clearly seen, as shown in Figures 4.14 a) and b), due to the effect of the grain size in the compound. The smaller size of grains of microvaristor *A* are uniformly dispersed, which helps to build up the large number of particle contacts necessary to allow very large current conduction compared to microvaristor *B* compound.
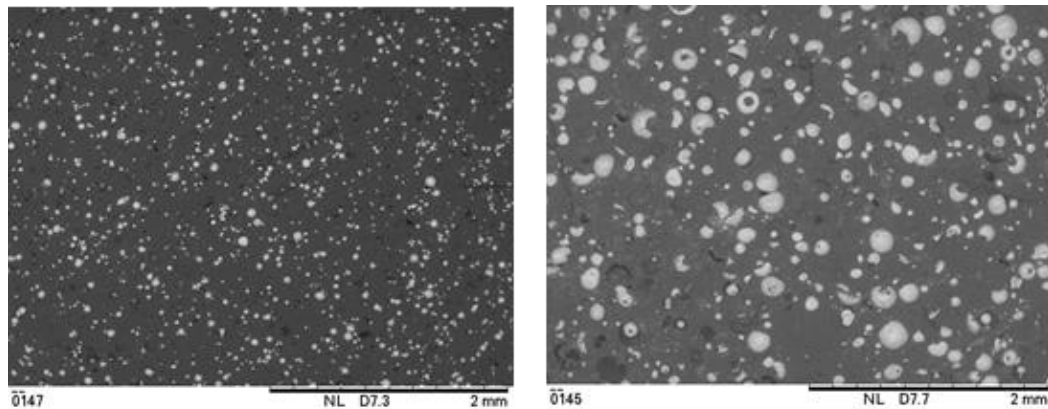
| a) Microvaristor *A* compound | b) Microvaristor *B* compound |

Figure 4.14: The SEM images of the dispersion of microvaristor at 70 wt. % for different microvaristor materials. The microscopy specification was at 40X magnification, 15 kV accelerating voltage.

The dispersion of filler in the compound exhibits a few drawbacks because the evaluation is based on human interpretation and, therefore, judgment can be subjective and dependent upon micrograph images. Therefore, a quantitative assessment was conducted by using light microscopy. This method is different from current practice

as it takes into account the justification for using different materials and the relationship between mathematical analysis and the dispersion of fillers [113].

In order to understand the dispersion conditions, the sample of 70 wt. % microvaristor compounds *A* and *B* were measured along the cross sectional area. In this measurement, the area of 1600 $\mu m^{2,}$ was selected randomly. The multiple focus planes of light microscopy were applied in order to identify the images of micro particles in the silicone rubber matrix as shown in Figure 4.15 and Figure 4.16. The area fraction, A_f was focused to small area of 50 μm^2 in order to obtain a clarity scale of dispersion trend. Figure 4.15 shows the microvaristor *A* powder accumulated in the first (μm^2) region but reduced slightly when the area was expanded.
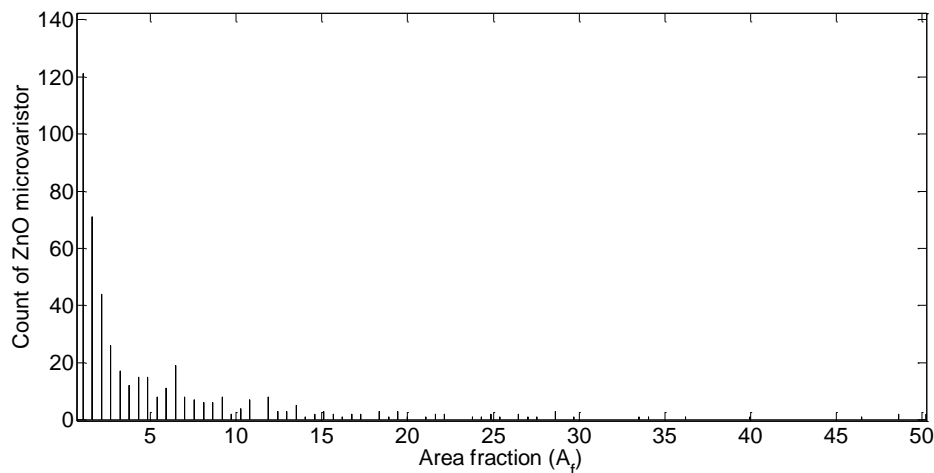
Figure 4.15: The dispersion of microvaristor *A* in the silicone rubber matrix along axis on the cross section.

In contrast, the number of microvaristor *B* particles was a little number which lower than those of microvaristor *A* due to the influence of the grain size as depicted in Figure

4.16. Having a large amount of the non-linear ZnO ceramic in the compound has the benefit of creating a large number of current paths in the composites. The risk of agglomeration is smaller for micro-metre sized fillers, when compared to nano-particles. However, it is still a critical issue when compounding non-linear field grading material. This is because the electrical properties of the compound are derived from the intrinsic properties of the microvaristor. Therefore, obtaining a uniform dispersal of particles in the compound is a priority.
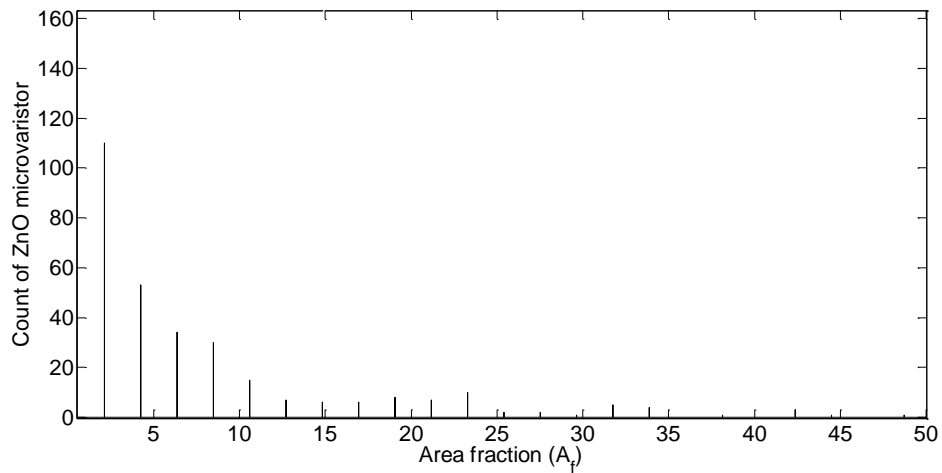
Figure 4.16: The dispersion of microvaristor **B** in the silicone rubber matrix along axis on cross section.

The magnification of the images in Figure 4.14 was then increased to 1800X, in order to reveal the image of the microstructure for both microvaristor materials. The image of the 'soccer ball' of ZnO varistors, with the presence of grain boundaries, is clearly observed as shown in Figure 4.17.

Such varistors' behaviour is controlled by the depletion layer lying within the ZnO grains at the interface of the grains, whereas potential barriers are formed at the grain boundaries.
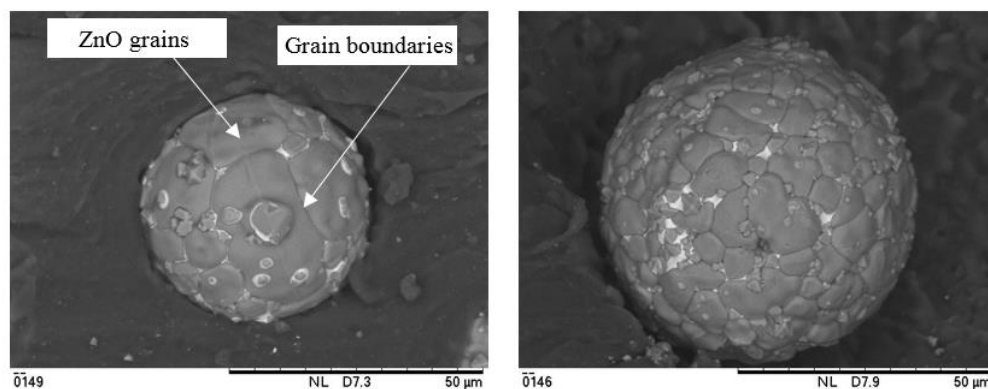
a) microvaristor *A*   b) microvaristor *B*

Figure 4.17: Images of microvaristor particles at 1800X magnification for both microvaristor materials.

In the microstructure of ZnO varistors, the triple points represent the phases between the grains, the intergranular phases and the particles. The whitish areas between ZnO phases at the triple points, known as intergranular material, can be clearly seen. The whitish areas mainly consist of metal additives that partly cover the grain surface of microvaristor *A*. The presence of a large amount of metal additives significantly improved the electrical performance of the composite. In the second image, Figure 4.17 b), it is noticeable that a number of grain boundaries are formed in microvaristor *B,* due to the large size of ZnO grains and the spinel particles. The microstructure of grains generally correspond to its processing, composition and the amount of additives [112].

The mass elements for both composite samples are shown in Figure 4.18. As the EDX is a surface analysis, therefore, it is expected there would be small amount of carbon element appearing in the analysis. The percentage of carbon is also influenced by the organic properties of the silicone rubber. Only four main components were detected in the EDX spectrum; carbon (C), zinc (Zn), silicone (Si) and oxygen (O).
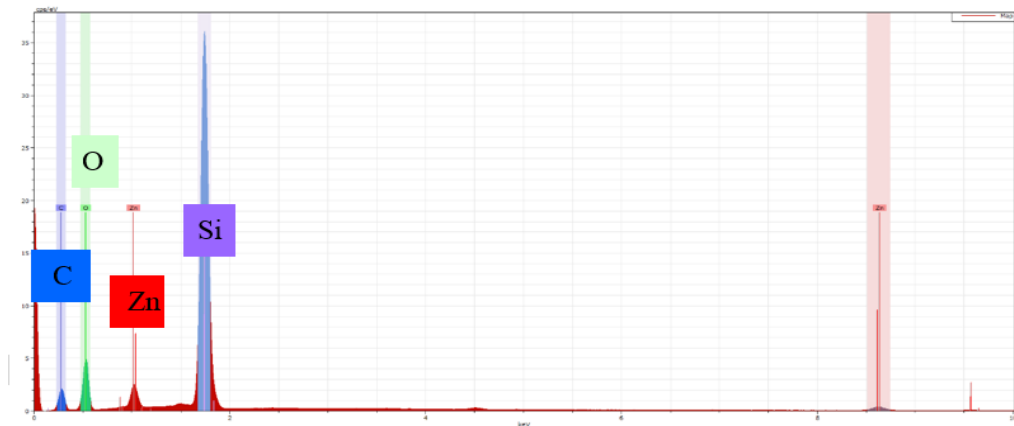
a) Microvaristor *A* compound
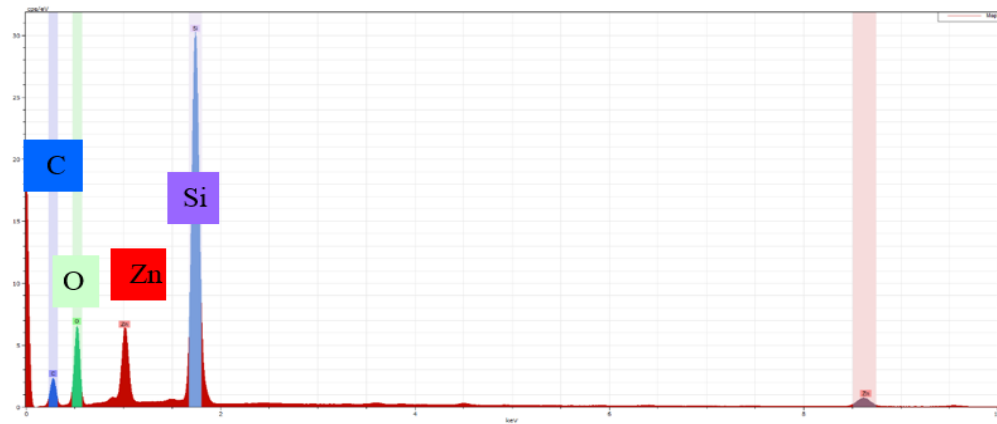
b) Microvaristor *B* compound

Figure 4.18: The EDX mapping and elemental analysis for microvaristor filled with silicone rubber.

The mass percentages of the components of both samples are summarised in Figure 4.19. In this elemental analysis, it was not possible to observe the metal additives that exist in the two microvaristor powders, as previously highlighted in Figure 4.10 and Figure 4.11. This is because of the presence of a small percentage of dopants (not less than 1% and no more than 10%) in the non-linear materials and the fact that some important areas were covered by the silicone rubber matrix. Moreover, the limitations of the microscopy equipment also influence the investigation.
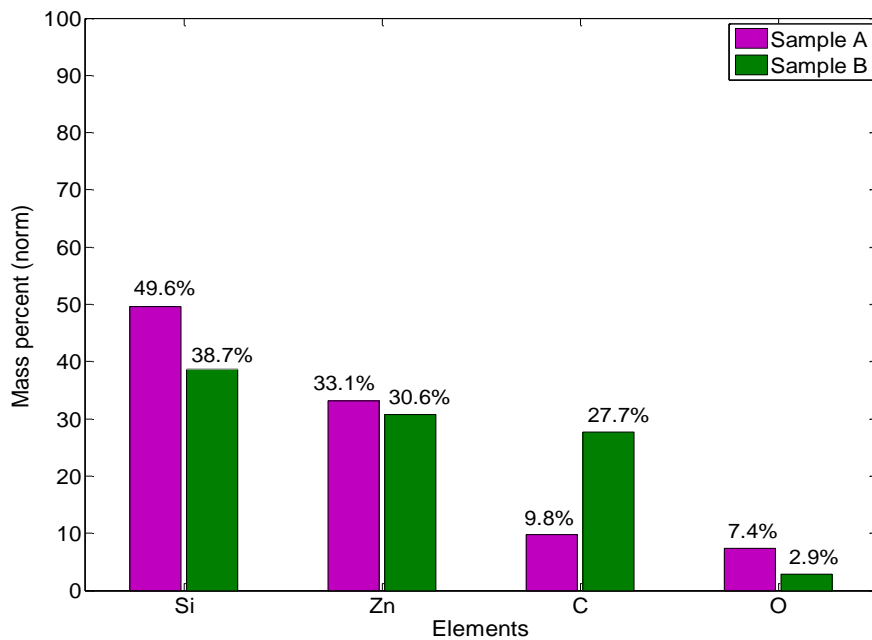
Figure 4.19: The percentage of mass elements obtained from EDX spectrum for both composite samples *A* and *B*.

4.6 CONCLUSIONS

The fabrication process of microvaristor filled with silicone rubber has been clearly explained. The proposed process has been found by trial and error using a number of samples, starting with 1 mm thickness and increasing to the dimension target of 5 mm. It is noticeable that a few factors influence agglomeration, such as the viscosity of the host matrix and the particle size of the microvaristor. In order to minimise agglomeration, heat treatment was applied, in order to control the viscosity of the silicone rubber matrix as well as to reduce the moisture in the microvaristor powder. The different particle sizes of the microvaristor has a slight influence on the mixing process. However, this problem can be controlled. A high shear mixer was used to aid the microvaristors to disperse in the composite without the presence of external chemical agents, which might influence the performance of the micro-composite.

A few critical parameters need to be controlled during the mixing regime, such as the speed of mixing, the duration of the process and the temperature of the mixture. The general processes of fabrication, degassing, moulding and curing were applied for specific durations. This fabrication process is applicable for different thicknesses, from 1 mm to 5 mm samples, and it works well when the concentration of microvaristors is increased. However, the composition of microvaristors loading may be varied to allow the compound to exhibit non-linearity. The experimental results will be discussed in Chapter 5.

The microscopic evaluation of both the powder and the compound was conducted using electron and light microscopy. Elemental studies, particle size and

microstructure were focussed upon, as well as the dispersion of microvaristor in the silicone rubber matrix. The XPS analysis revealed the different chemical compositions of microvaristors *A* and *B* that have a significant influence on the electrical performance. The particle size of microvaristor particles was evaluated. Microvaristor *A* was found to have a mean particle size of 37 μm, while microvaristor *B* had an average size of 71 μm.

SEM was used to investigate the microstructure of the powder and composite. The findings show that the 'soccer balls' of microvaristor powder were well dispersed in the silicone rubber matrix. At higher magnification, the microstructure of microvaristor powder can be clearly observed. The dispersal of the microvaristor in the silicone rubber was evaluated through the qualitative method. Even though the results might be subjective, in that they depend on human interpretation and how the micrographs were viewed, in the work, it was observed that the dispersal of filler is affected by the particle size of the filler and the fabrication technique. Therefore, an assessment of microvaristor dispersion was carried out on a number of random samples. The small size of particle of microvaristor *A* may easily lead to agglomeration. EDX mapping revealed the elemental components that existed in the microvaristor compound. However, the metal additives were not observable. The percentage composition of the elements is discussed. The experimental electrical characterisation results for both microvaristor compounds *A* and *B* will be explained in Chapter 5. In this chapter, the evaluations involve the use of AC, DC and impulse tests. The electrical properties of the microvaristor powder and the compound will be discussed further.

CHAPTER 5

ELECTRICAL CHARACTERISATION OF FABRICATED MICROVARISTOR COMPOUNDS USING AC/DC/IMPULSE ENERGISATIONS

5.1. INTRODUCTION

There is evidence that microvaristors based composite demonstrate an excellent performance in the control of electric field distribution in a high voltage system. Yang et al. [14] indicates that different tuning voltages result according to the composition of the non-linear filler in the polymer matrix when samples are subjected to high voltage tests.

The laboratory set up and procedures for such high voltage tests were introduced in Section 3.2, 3.3 and 3.4. The three high voltage tests were conducted under AC, DC and impulse energisation. Measurements from each test were obtained, and the performance of the test samples was examined. In this chapter, the electrical properties of field grading samples will be characterised according to the method used. The behaviour of microvaristor compounds and powders will be examined based on their

strong relationship with the properties of materials, as described in Chapter 4. A few parameters that affect the fabrication process will be discussed, as the test results will determine the quality of the test samples. By presenting these findings, it is expected that the results of the tests on the in-house field grading samples will promote new knowledge of field grading technology and help to diversify power system specifications.

5.2. HIGH VOLTAGE AC TEST

In this section, the experimental results are analysed by using the Point-On-Wave (POW) technique that was described in Chapter 3. The work findings will discuss the results of the tests to find the non-linear characteristics of microvaristor compounds at 60 wt. % microvaristor concentration with a thickness of 1 mm. The further results are used as benchmark for the further sample of 5 mm thickness and are given in the Appendix A. The electrical performance of the 5 mm composite samples *A* at different microvaristor loadings (10 wt. %, 30 wt. %, 50 wt. % and 60 wt. %) will be reviewed. The mathematical expressions used to derive the electrical properties are presented in Appendix B.

5.2.1 ELECTRICAL PROPERTIES

Two different microvaristor materials in powder form, *A* and *B*, which have been compounded with silicone rubber, will be evaluated. As the non-linear behaviour of microvaristor is predominately derived from their intrinsic properties, this filler can

impart strong electrical properties directly to the polymer matrix. The comparative studies present the non-linear characteristics of the pure microvaristor and with the presence of the polymer matrix in the compound. The waveforms illustrate the condition of different regimes for the non-linear powder and compound.

5.2.2   MICROVARISTOR POWDER

It is well known that the characteristics of microvaristor particles depend on the doping elements in the powder and the processing method. Because of such procedures, the threshold field of this material can be adjusted significantly. Moreover, each of the grain boundaries along the current path contributes to a number of switching levels [114].

A test platform with a gap between the electrodes of 0.5 cm was set up to investigate the electrical properties of powders *A* and *B*. The non-linear characteristics of all samples was seen clearly under the influence of increasing electrical field. The measured total leakage current was analysed using the POW technique to discriminate the resistive and capacitive components of currents. Those components are shown in Figure 5.1 and Figure 5.2.

The transition behaviour of voltage and current waveforms when the voltage levels are increased can be clearly seen. At the beginning, a small voltage was applied to the test samples. This was slowly increased until the samples showed a non-sinusoidal current waveform.
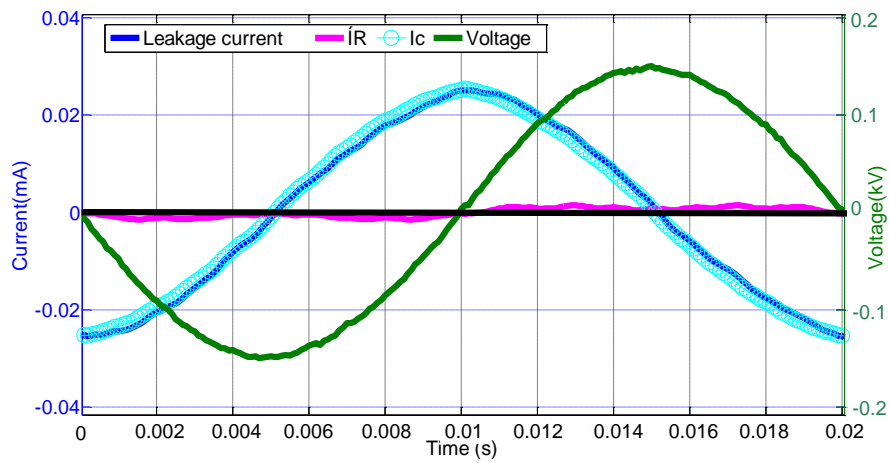
a) at 150 V
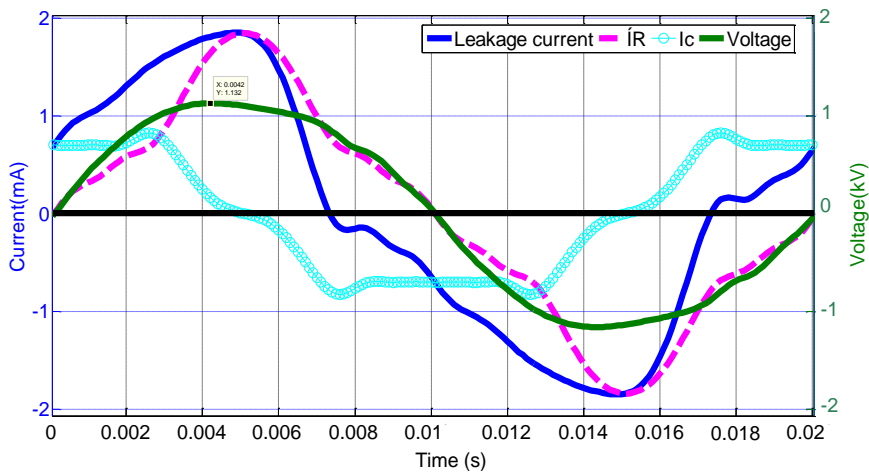
b) at 1.1 kV

Figure 5.1: The voltage and current waveforms of microvaristor powder *A*.
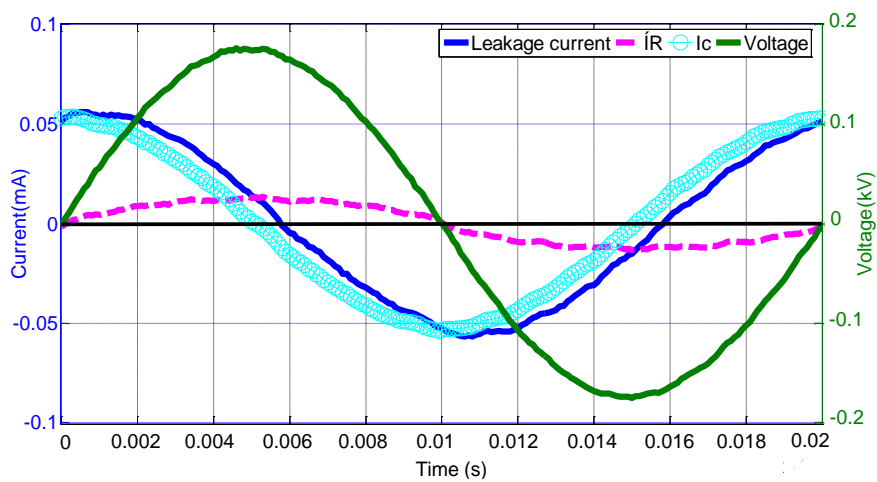
a) at 175 V
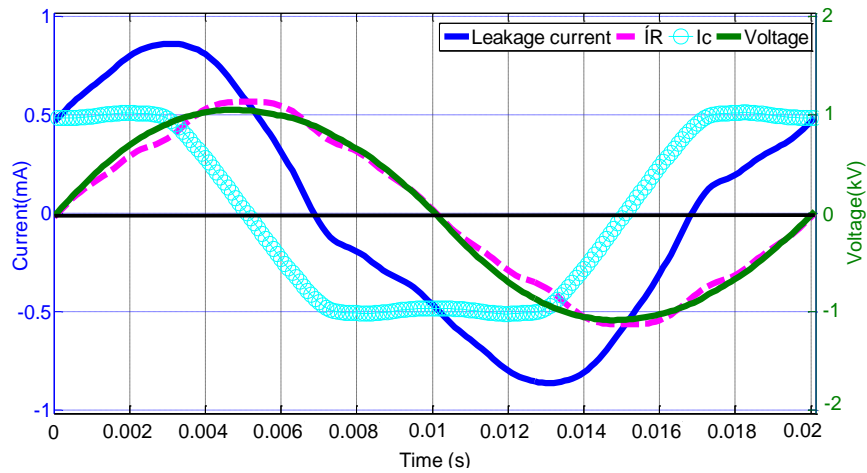
b) at 1.05 kV

Figure 5.2: The voltage and current waveforms of microvaristor powder **B**.

At low voltages, both samples exhibited low current density through the varistors powder. However, when it reached a certain breakdown voltage, V_{BR}, the leakage current rapidly increased, as shown in Figure 5.1 (b) and Figure 5.2 (b). When the voltage approached 1.1 kV, microvaristor **A** started to carry a larger level of current than microvaristor **B**. This is attributed to the grain size of the material. It was difficult to obtain a high resistive current for microvaristor **B**, as any increase in voltage beyond the threshold value will lead to breakdown. During this breakdown regime, a large current flow was expected through the sample. Thus, the test was stopped immediately to prevent damage to the test equipment.

5.2.3   MICROVARISTOR COMPOUND

The assessment of the microvaristor compound was carried out on both microvaristor materials **A** and **B**. Both samples exhibited non-linearity at 70 wt. % of microvaristor loading in the silicone rubber when the samples reached certain threshold voltages. Interestingly, the electrical profiles of both samples were different, and this is

according to the material properties that contribute to the threshold voltages and that allow large resistive current flow through the composite. The various curves in Figure 5.3 and Figure 5.4 correspond to observations made at 3 levels of applied voltage on different 70 wt. % microvaristor composites.

The results shown in Figure 5.3 a) and Figure 5.4 a) are indicative of the pre-breakdown conditions in the ZnO microvaristor conduction regime of composites *A* and *B*, that are characterised by linear voltage-current relationship at low magnitude of 10 µA and 5 µA respectively. Meanwhile Figure 5.3 b) and Figure 5.4 b) show the regime of ZnO conduction near the knee of the breakdown regime, where there is significant change in the leakage current, due to the effect of increasing magnitude of the resistive current. At this level, the voltage increase needs to be controlled carefully, in order to prevent high current flowing through the sample.

As shown in Figure 5.3 c) and Figure 5.4 c), the wave shapes of the resistive current change more significantly around the peak of the waveform. This gives a good indication that the sample is operating in the breakdown regime. In this regime, the electrical properties of the sample change from those of an insulator to those of a conductor. As can be seen from the figure, at this point there is a high resistive current reaching almost 100 µA for sample *B,* whilst this value is doubled for sample *A*.
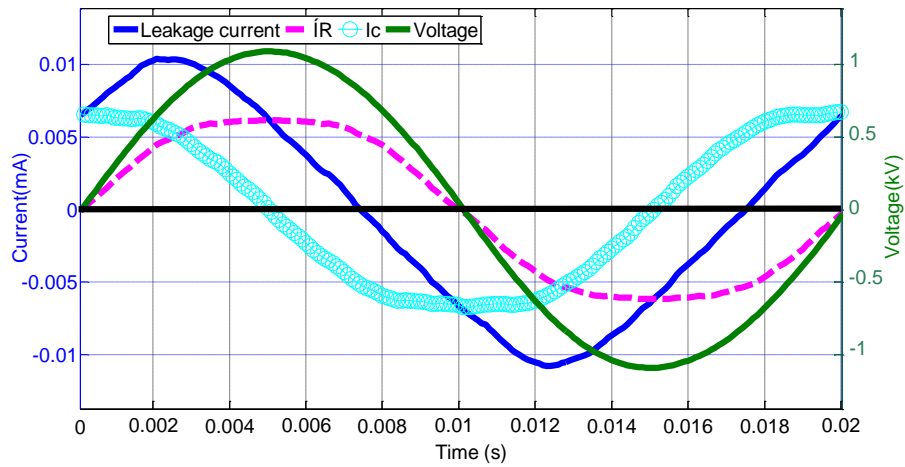
a) at 1.09 kV_{peak}
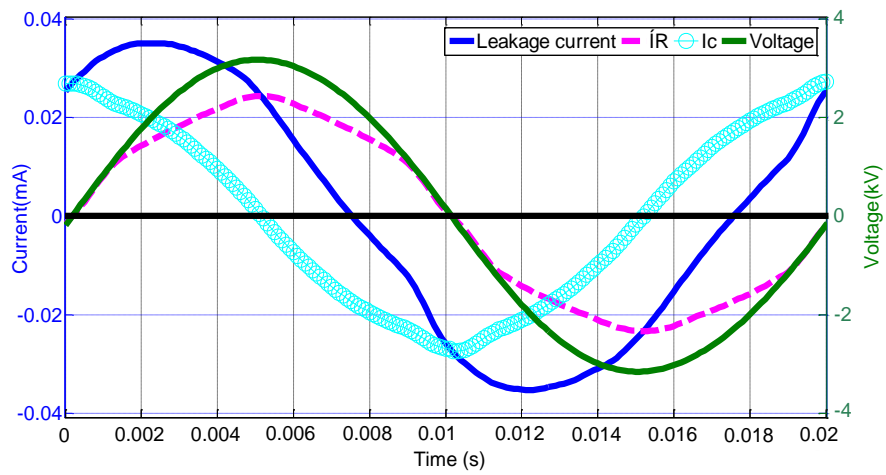
b) at 3.17 kV_{peak}
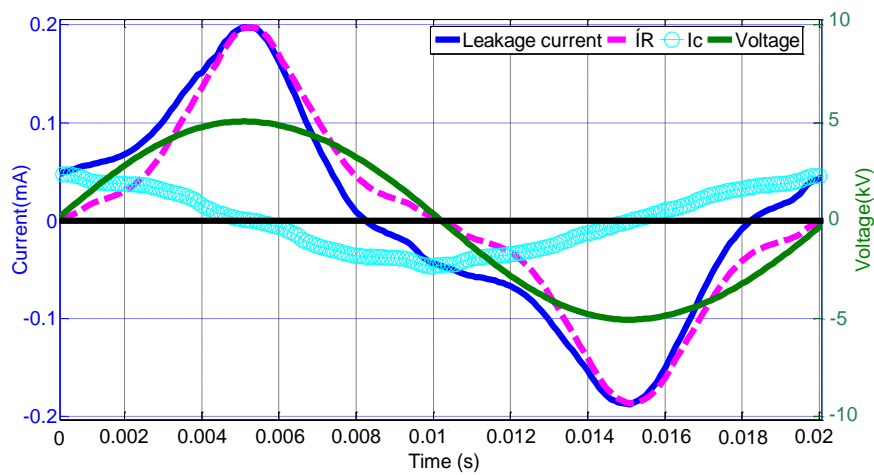
c) at 5.07 kV_{peak}

Figure 5.3: The voltage and current traces of silicone rubber filled with 70 wt. % microvaristor *A* at different voltage levels.
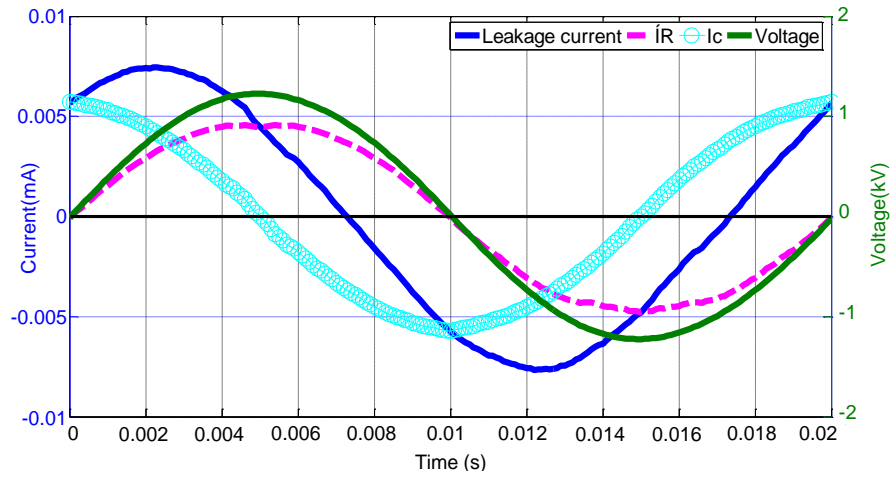
a) at 1.27 kV_{peak}
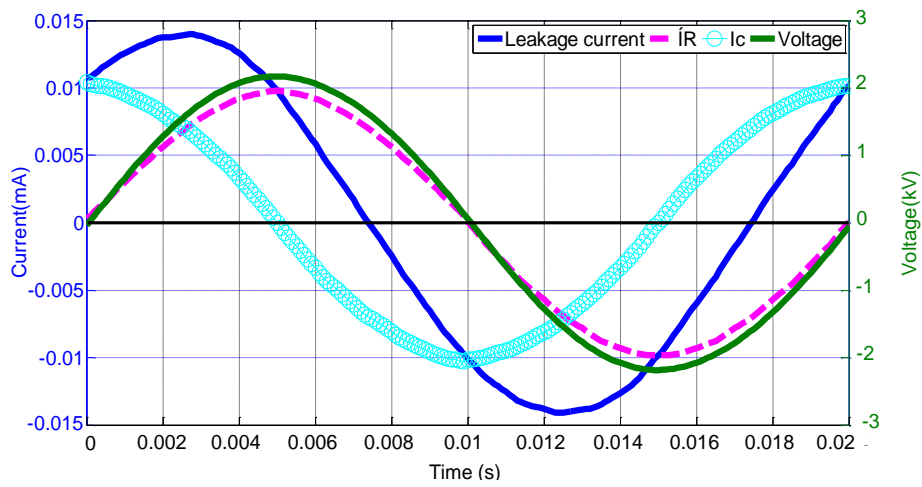
b) at 2.2 kV_{peak}
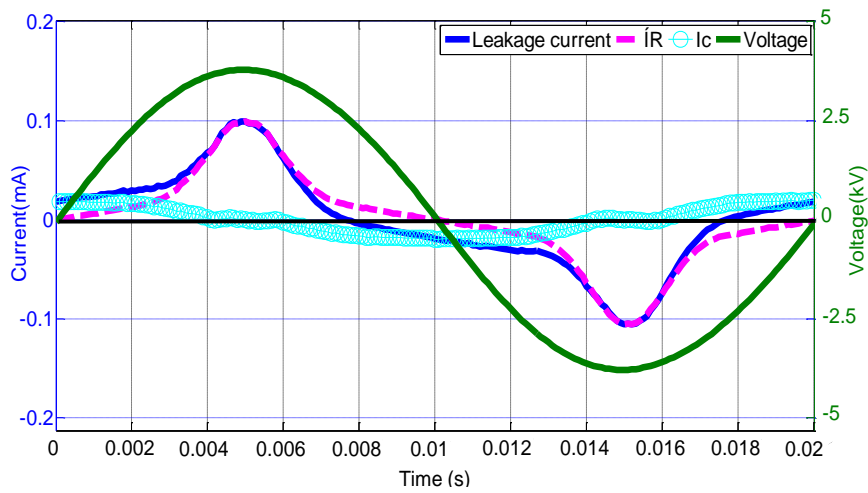
c) at 3.8 kV_{peak}

Figure 5.4: The voltage and current traces of silicone rubber filled with 70 wt. % microvaristor **B** at different voltage levels.

The recorded waveforms of voltage and current are analysed in the next section, in order to present the electrical properties of both samples *A* and *B*, during the breakdown regime in terms of voltage and current (V-I) characteristics, resistivity, conductivity, current density and permittivity.

5.2.4 VOLTAGE CURRENT (V-I) CHARACTERISTICS

For comparison purposes, the voltage-current characteristics have been presented when all the samples entered the breakdown regimes to show the non-linear behaviour of the powder and the compound. The results show the great change in the threshold voltages of the compounds when microvaristor powder is dispersed into silicone rubber matrix, which allows the material to transfer its electrical properties directly.

Figure 5.5 shows the (V-I) characteristics of pure microvaristor powders and composites for types *A* and *B*. The measured values are the peak values for each level of applied voltage. As expected, higher leakage current occurs in both microvaristor powders compared to the mixed compound with the polymer matrix, which possesses good insulating properties. These electrical characteristics are similar to those seen in ZnO surge arrester materials and back-to-back Zener diodes which showed similar voltage and current responses. The current profile is lower in the compound, probably due to presence of the silicone rubber matrix and the dispersal of filler in the compound. Therefore, a large voltage is required to achieve the optimal voltage to drive the compound and exhibit non-linear characteristics.
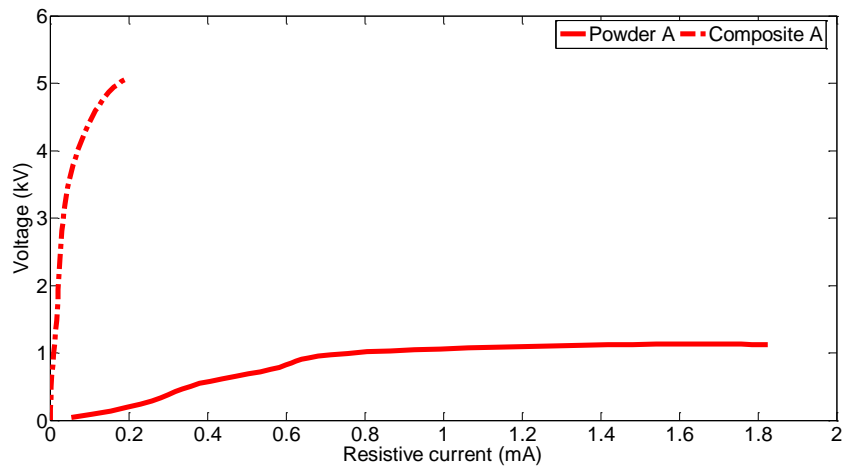
a) microvaristor *A*
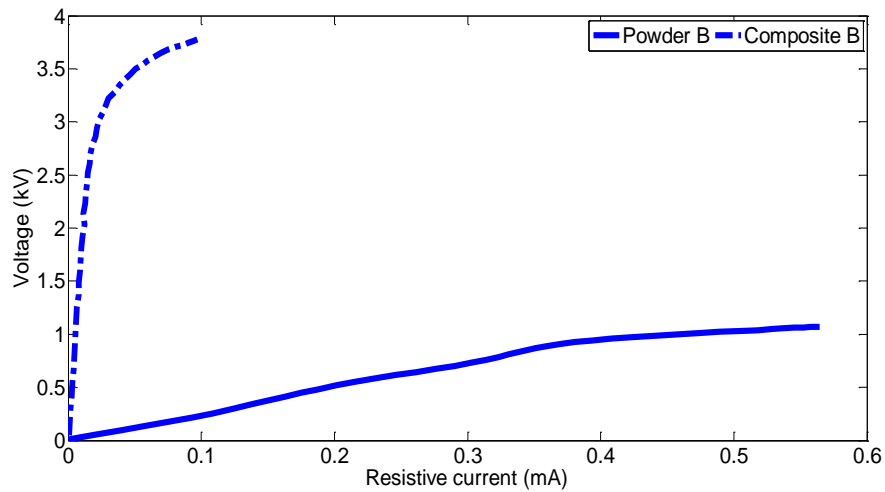
b) microvaristor *B*

Figure 5.5: Measured V-I characteristics for ZnO microvaristor powders *A* and *B* and their compounds in the breakdown regime.

The voltage and resistive current profiles of all samples during breakdown is summarised in Table 5.1. It is clearly seen that microvaristor powder *A* and its compound exhibit higher voltage and current responses than microvaristor *B*. These

interesting findings led to deeper investigation of another electrical properties of microvaristor.

Table 5.1: The voltage and current measurements during the breakdown regime.

Microvaristor	Type of samples	Voltage breakdown, V_{BR} (kV)	I_{BR} (mA)
A	Powder	1.1	1.85
	Composite	5.07	0.18
B	Powder	1.07	0.56
	Composite	3.8	0.09

5.2.5   RESISTIVITY

Using the geometry of the test cells adopted during testing, the voltage-resistive current characteristics data was converted into a resistivity versus electric field profile. As can be seen from Figure 5.6, the resistivity falls sharply, soon after the knee of conduction is reached. Since the silicone rubber host matrix has a resistivity of 10^{15} Ω.m, the resistivity profile of microvaristor materials filled with silicone rubber is higher than that of microvaristor powder.

As expected, the resistivity profile of microvaristor **A** is more dominant compared to the second material. This is due to large current flow in the composite when the voltage level is increased. The calculation of the electrical field is based on the ratio of the voltage applied to the thickness of the samples, which was 0.5 cm in all tests.
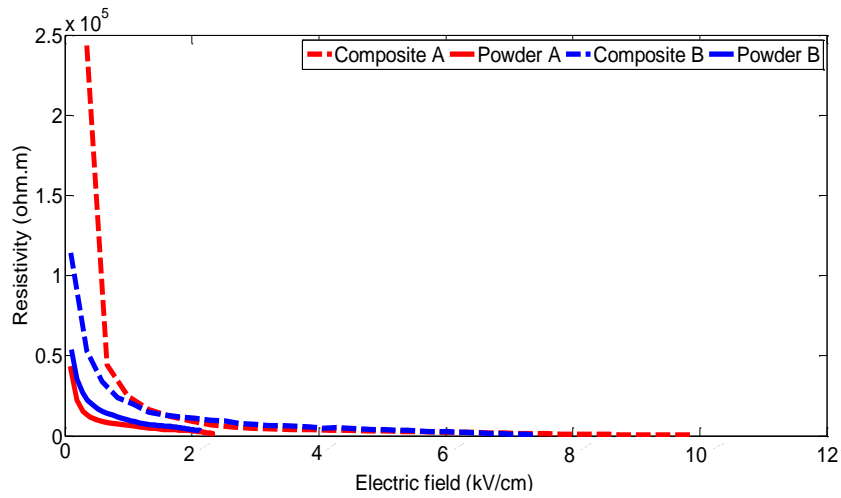
Figure 5.6: The resistivity profile with the function of the electrical field for microvaristor powder and compound.

5.2.6 CONDUCTIVITY

In order to obtain experimental data, which would be useful for numerical field computation when using ZnO microvaristor compounds in high voltage plant, the conductivity dependence on the electrical field was derived from the resistivity data. Figure 5.7 shows the variation of conductivity for both the ZnO microvaristor powder and the grading compound made with silicone rubber. As can be observed, the threshold of conduction for powder *A* occurred just above an applied field of 2.1 kV/cm, whereas a field of 6.5 kV/cm was required before the compound entered the breakdown regime. Meanwhile, a smaller electrical field of approximately 6 kV/cm was required for compound *B* to achieve full conduction. This result is expected from the behaviour of the powder itself that was seen earlier.
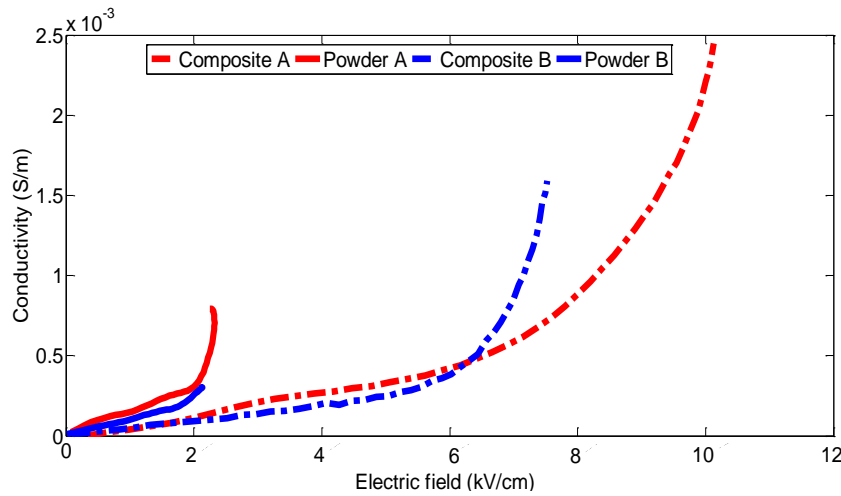
Figure 5.7: Conductivity versus electrical field for microvaristor powder and composite.

5.2.7   RELATIVE PERMITTIVITY

The capacitance values were derived in order to obtain the relative permittivity. Figure 5.8 shows the variations of relative permittivity as a function of the applied electrical field. As can be seen from this figure, the relative permittivity of both test samples was initially high and constant for low applied electrical fields, below the knee of conduction. The values were approximately 110 and 210 respectively for the ZnO microvaristor powder and the compound utilising material *A*. Meanwhile, material *B* demonstrated a permittivity measurement approaching 120 for the powder and 130 for the compound.

The high values of apparent permittivity are thought to be caused by charge accumulation at the boundaries of the ZnO grains and the intergranular layer of the ZnO microvaristor material [115]. Around the knee of conduction, significant changes can be seen in the values of relative permittivity depending upon the type of conduction

mechanism in the ZnO material. Changes of applied field level will cause a sudden increase in the conduction regime, causing a significant fall in capacitance, which affects the relative permittivity of the material.
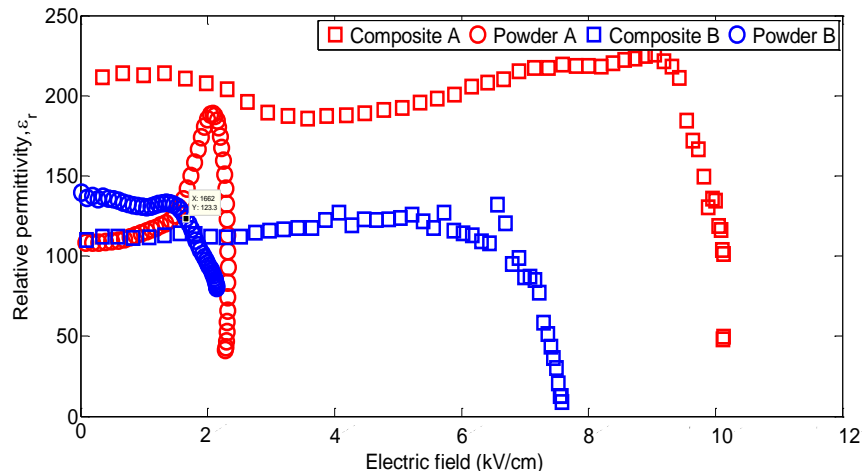
Figure 5.8: Permittivity values as a function of the electrical field for ZnO powder and non-linear compound made of silicone rubber filled with 70 wt. % of ZnO microvaristor.

5.2.8   CURRENT DENSITY

The current density variations in the samples was calculated as shown in the Figure 5.9. By increasing the electrical field, the current density parameter was significantly changed corresponding to the area of 100 cm^2 of powder and 0.7855 cm^2 of composites. Due to the different surface areas and current densities, the much greater resistive current flow in the microvaristor composite compared to the powder can be seen.
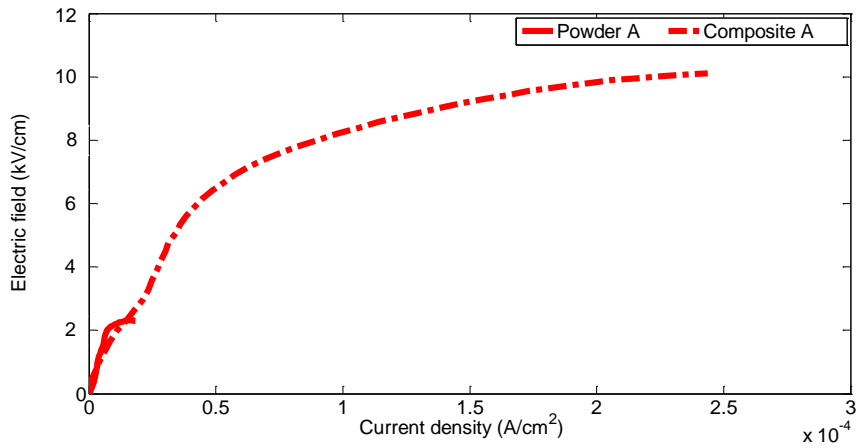
a) microvaristor **A**
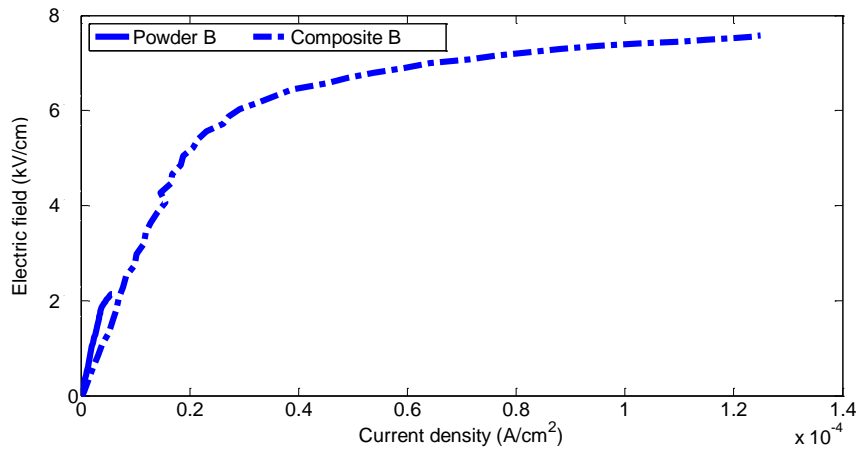
b) microvaristor **B**

Figure 5.9: The current density profile for both the microvaristor powders and the compounds.

A three dimensional assessment explains the relationship between the electrical parameters that contribute to the non-linearity of the compound. In this evaluation, the relative permittivity and conductivity, as functions of electrical fields, are presented. A comparative graph shows the condition of the compound in two stages, pre-breakdown and during the breakdown regime, as illustrated in Figure 5.10 a) and

b). In these three dimensional profiles, the conductivity and permittivity are shown as interdependent non-linear parameters, while the graphs also show the significant effects caused by the increase of applied voltages and the induced changes to the electrical properties of the composites.
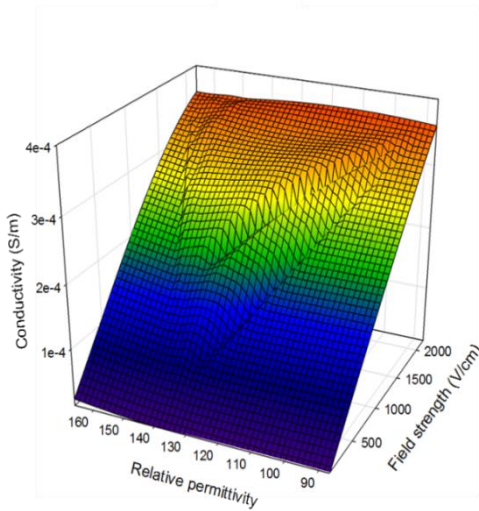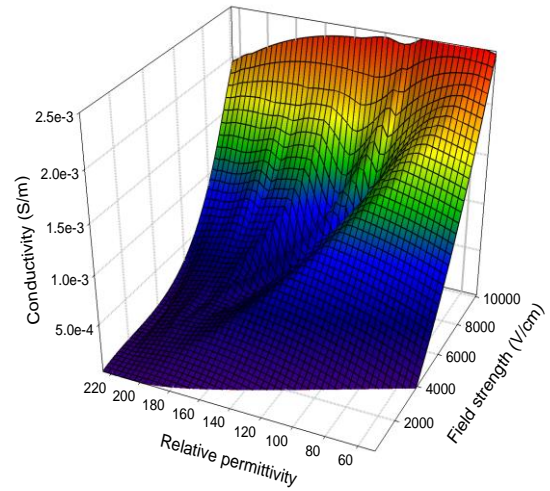
a_1) pre − breakdown region a_2) breakdown region

a)   microvaristor *A* composite
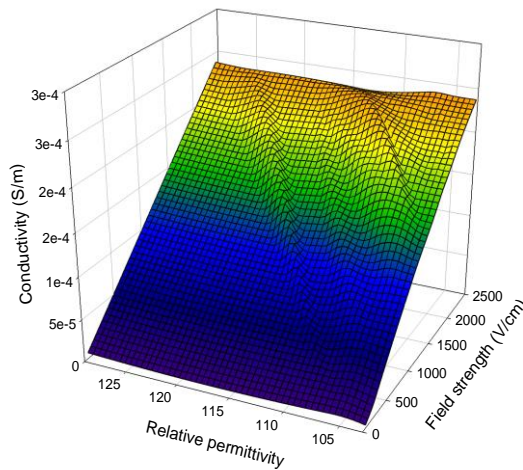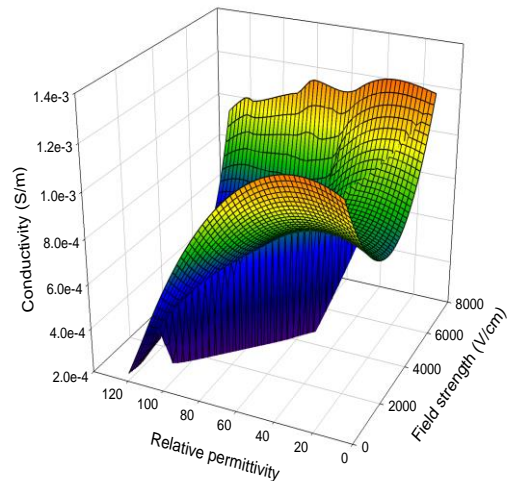
b_1) pre − breakdown region b_2) breakdown region

b)   microvaristor *B* composite

Figure 5.10: The 3D graphs for the electrical properties of microvaristor compounds.

The substantial impact on conductivity and relative permittivity, when the field strength was increased until the samples entered the breakdown regime, can be observed at high applied voltages. On the other hand, the linear response can be clearly seen at low voltage in the pre-breakdown regime. This is seen as sudden rise of leakage current when both compounds reached the on-set of electrical fields between the conduction regimes. In general, the characteristics of the microvaristor compounds are principally influenced by the microvaristor properties, the host matrix and the processing, which has been discussed in [7].

Therefore, a second high voltage test was conducted to investigate the electrical properties of the samples for certain durations under DC voltage. This test identified the V-I response of the samples, which will clarify the accuracy of the electrical profile. The tests were conducted on composite samples only, due to limitations in the supply of microvaristor powder. The voltage used for DC testing must be taken into consideration, in order to minimise the stress level applied to the samples. A threshold voltage from the AC tests was used as a reference for the maximum DC voltage to be applied.

5.3   HIGH VOLTAGE DC TEST

As mentioned earlier, the DC tests were conducted until the threshold voltage was reached. Therefore, the characteristics in the breakdown regions are not shown in this section. Figure 5.11 shows that the current density profile increases in proportion to the applied voltage. The high magnitude of resistive current will degrade the composite

and eventually cause thermal runaway in the varistors. By using Ohm's Law, the resistance values for the compound were measured leading to the resistivity assesment as depicted in Figure 5.12.
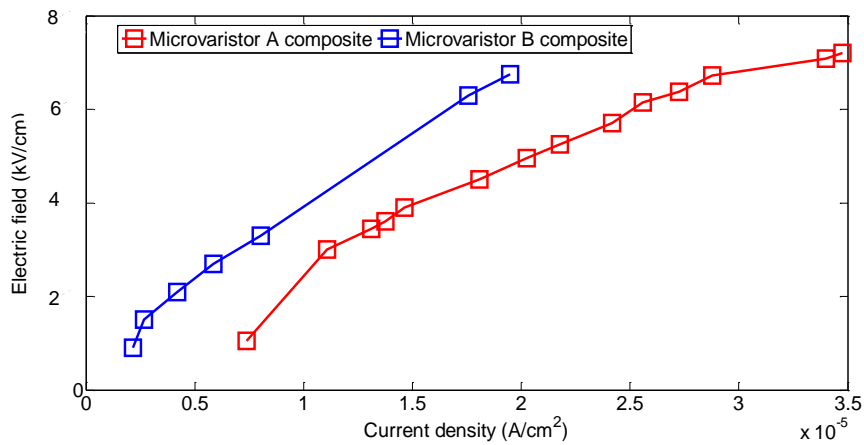
Figure 5.11: The electrical field against the current density.

Figure 5.12 shows the resistivity measurement during the pre-breakdown regime for both samples. It was noticed that microvaristor *A* compound samples exhibited higher resistivity profiles than sample *B* due to the high resistive current flow in the composite.
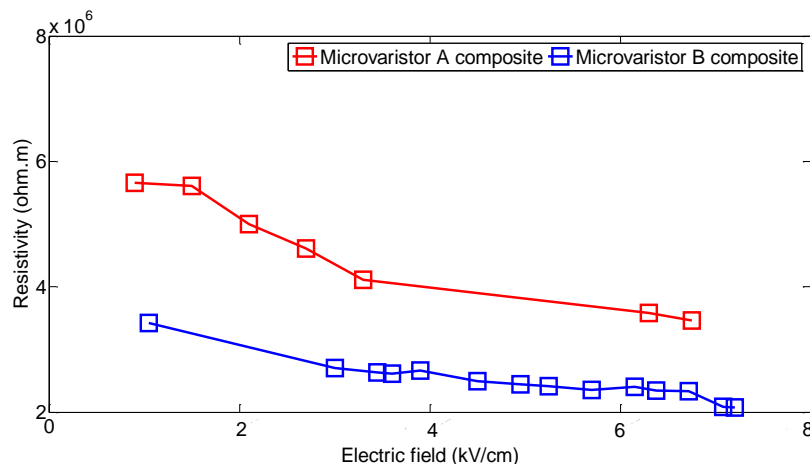
Figure 5.12: The resistivity variations as a function of the electrical field for both microvaristor compounds.

Figure 5.13 shows the results of the average power evaluations for both compounds in the AC and DC tests using various voltages. The voltage values are plotted against RMS applied voltage. As can be seen on the figure, the power consumption of microvaristor *A* composite increased significantly as the microvaristor grains reached the conduction stage and allowed the high resistive current to flow. For the absorbed power under DC voltage, the measurement was made until the knee of conduction threshold voltage was achieved.
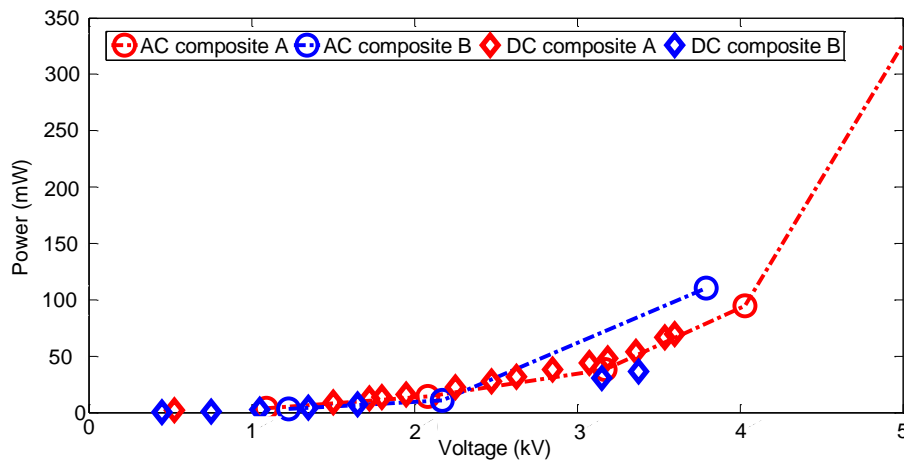
Figure 5.13: The mean power for both compounds measured in the AC and DC tests.

5.4   IMPULSE TESTS

As explained in the outline laboratory procedures in Chapter 3, the impulse voltage test was not conducted on the microvaristor powder in order to prevent damage to the material which could significantly change its electrical properties. In this section, the characteristics of both microvaristor compounds will be discussed further, particularly

in relation to high voltage impulse studies. Meanwhile, the low voltage impulse test records are presented in Appendix C.

5.4.1 IMPULSE SHAPE

The impulse measurements consisted of voltage waveforms that were acquired using a voltage divider and the current waveform from the current transformer. Three residual voltages were evaluated at charging voltages of 6 kV, 8 kV and 10 kV for microvaristor compound A. The charging voltage was set at different levels in order to determine the rise of peak current as a function of voltage. The initial charging voltage was initially set at 6 kV and was increased to 10 kV.

Figure 5.14 shows the levels of voltage and current at low field on V-I characteristic of the material which indicates a peak current, I_p, of 0.1 A and a peak voltage, $V_{p,}$ of 3.43 kV, with the rise time of 2.6 µs. The modification of the circuit parameters, such as a high front resistor (9.8 kΩ) and the selection of the voltage divider [115] produced a rather slower than standard lightning shape of 1.2/50 µs.

There is also the possibility that it may have arisen due to the electrical properties of non-linear test samples. At this applied voltage, the varistors based material consists of a mainly capacitive load that was the main contributor to the capacitive current component. The capacitive current may be measured, as long as the charging voltage is set below the breakdown voltage. By increasing the applied voltage, the peak current moved into the ohmic region, as the resistive current was dominant. The behavior of

microvaristor compound changed significantly at high frequency operation and voltage magnitudes.
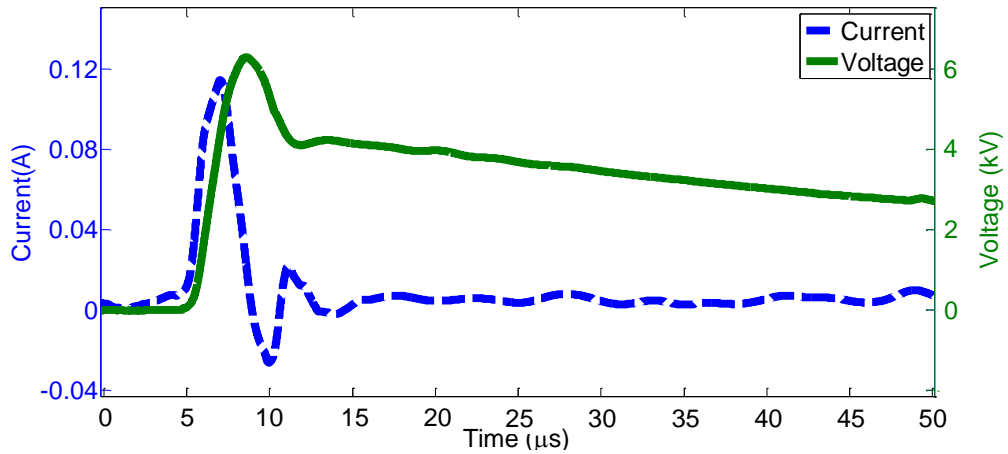
Figure 5.14: Voltage and current records at low field for the microvaristor *A* composite (charging voltage of 6 kV).

Figure 5.15 shows the characteristic of the voltage and current signals when the charging voltage was increased to 8 kV. The peak of the current was gradually increased to 0.47 A, with a minimal presence of capacitive current. The rise of current will significantly increase the peak voltage to 4.83 kV.

After each test, the samples were rested for at least 2 minutes for cooling purposes. The tests were continued with new charging voltage settings, thus influencing the activity of the varistors grains which were driven into a higher field region.
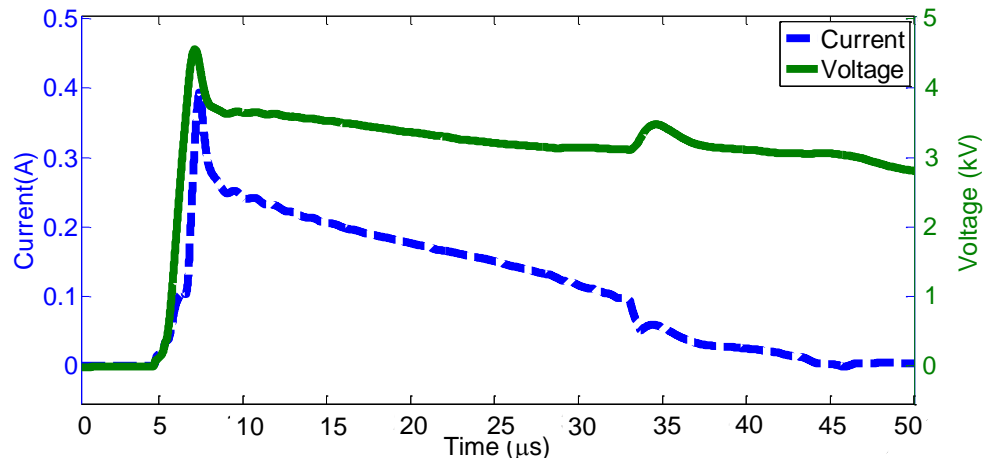
Figure 5.15: Voltage and current records in the ohmic region for the microvaristor *A* composite (charging voltage of 8 kV).

The charging voltage was then stepped up to almost 10 kV, to allow a higher current flow which is clearly seen in Figure 5.16. The electrical current increased significantly to 0.82 A at 5.8 kV (V_p) before falling to close to zero. At this point, the samples exhibited a transition from low to high conductivity. During the conduction regime, the resistive current was dominant and depended on the voltage applied.
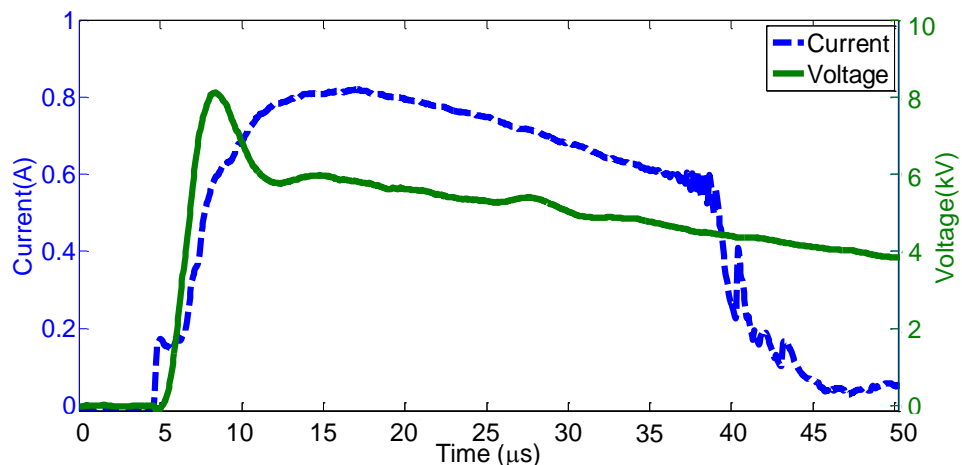
Figure 5.16: Voltage and current at nonlinear conduction for microvaristor *A* composite (charging voltage of 10 kV).

Similar settings of charging voltage were applied to microvaristor **B** composite. In the low field region, the capacitive current was approximately 0.15 A when the charging voltage was set to 6 kV. The rise time was the same at 2.6 μs, with the peak voltage at this current value measured at 4 kV.

The oscillograms depicted in Figure 5.14 and Figure 5.17 show that the capacitive component occurred in the low field region, and this has also been reported in [9]. A comparison of both results indicates that microvaristor **B** composite exhibited a higher capacitive current than microvaristor **A** composite. The capacitive current profile was derived in order to estimate the capacitance and relative permittivity parameters.
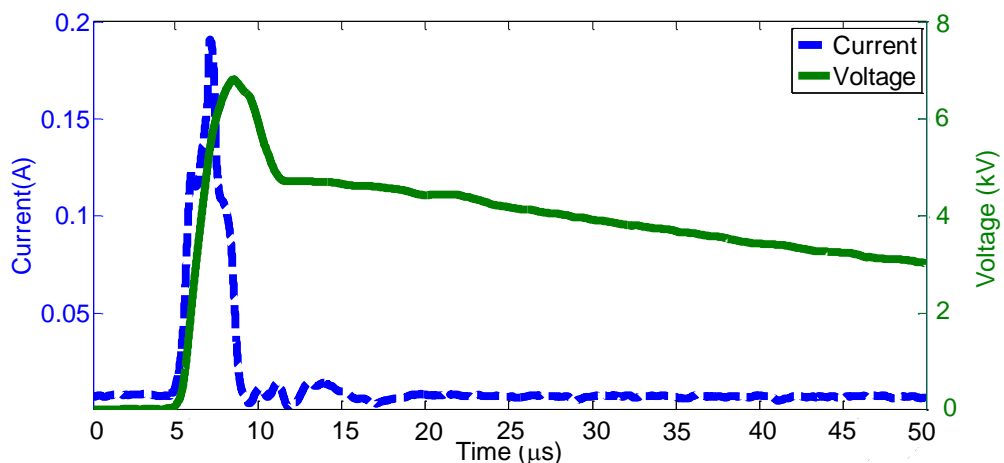
Figure 5.17: The measurement of low voltage of 4 kV contributes to nearly 0.15 A of capacitive current in microvaristor **B** composite (charging voltage 6 kV).

In order to obtain a resistive response, the charging voltage was increased to 8 kV. The current and voltage responses are depicted in Figure 5.18. The current component is dominated by the resistive current which, in turn, varies according to the increase in

116

applied voltage. In this ohmic regime, the measured peak current, $I_{p,}$ is nearly 0.36 A, at a peak voltage of 5.9 kV. The charging voltage was then raised to 10 kV, thus allowing a high resistive current of 0.81 A_{peak} to flow. However, after 15 μs, the current decreased significantly with voltage level. The findings in Figure 5.16 and Figure 5.19 are interesting because microvaristor compounds **A** and **B** exhibit high resistive currents at 0.82 A and 0.81A with peak voltage responses of 5.8 kV and 8.7 kV respectively.
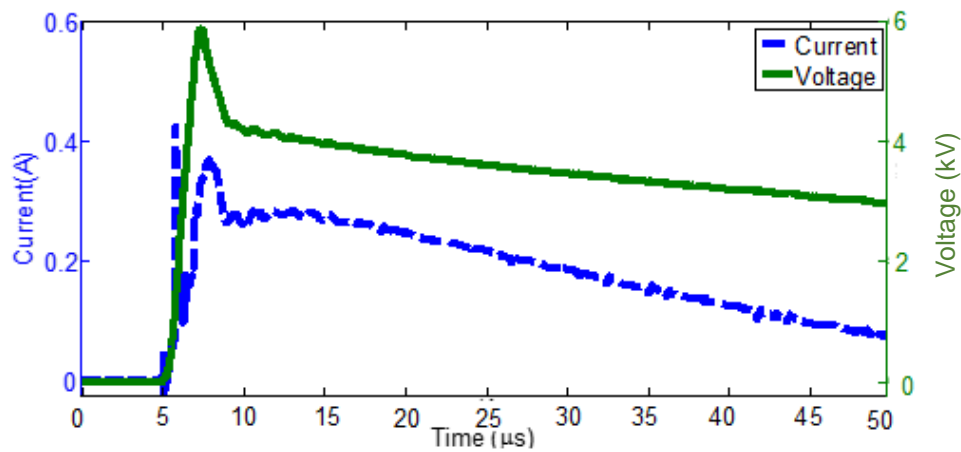
Figure 5.18: Voltage and current shape in the ohmic region for the microvaristor **B** composite (charging voltage of 8 kV).
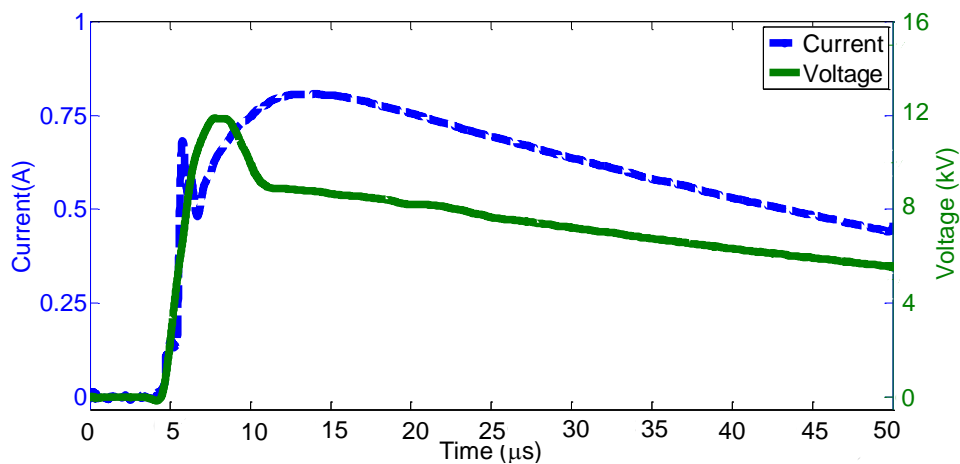
Figure 5.19: Voltage and current at nonlinear conduction for microvaristor **B** composite (charging voltage 10 kV).

5.4.2   VOLTAGE OVERSHOOT

Throughout the observations of applied voltages to the samples, all the voltage signals exhibited overshoot (spike) at either low or high fields. This may be due to inductive effects in the measurements and response of voltage divider. Moreover, this scenario occurs due to the change in the behavior of the composite material, from capacitive to resistive. To understand the voltage overshoot in detail a few publications were considered, and a number of factors that can contribute to overshoot in varistors based material, such as increase in current amplitude [116], presence of additives in the composites [116] and the disturbance of inductance and coupling from test set up [117] were found. In addition, the increase in current amplitude and the temperature caused by a rapid increase in voltage impulses would also influence the voltage spike.

In contrast, Schmidt et al. [118], highlighted that the effect of voltage overshoots that appear in varistors based material can be negligible as they do not determine the overall characteristics of the composites. Taking into account the causes found from experimental set ups, Haddad et al. [119] implemented a new measurement technique in order to eliminate the spike in the voltage signals. In this work, some ideas have been adopted which resulted in some improvement. However, the spike in the voltage waveform still occurs.

As can be seen on Figure 5.20, the voltage - current (V-I) characteristics showed a good relationship as the current increased significantly with the applied voltages. Microvaristor *A* composite showed a peak voltage of 5.8 kV with a much lower peak

current than the microvaristor **B** composite. The rise of current due to large voltage

magnitudes directly influenced the resistivity profile as shown in Figure 5.21.
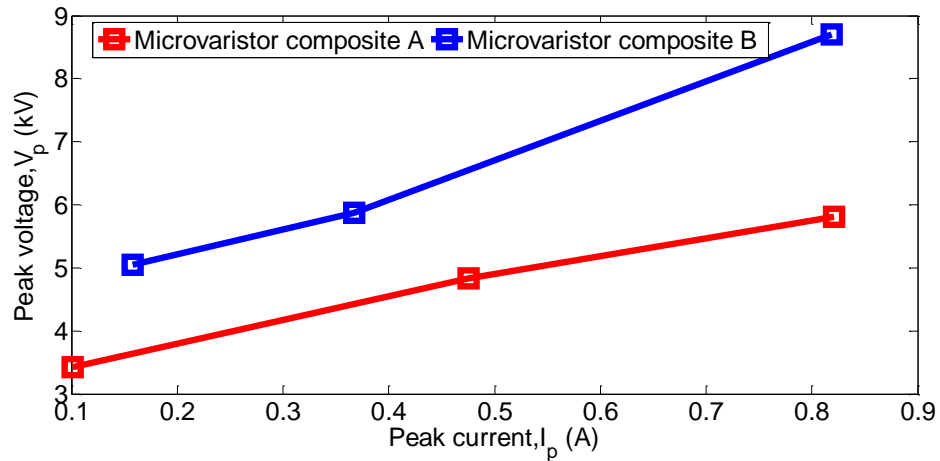
Figure 5.20: Voltage-current (V-I) characteristics of composites under variable applied voltages.
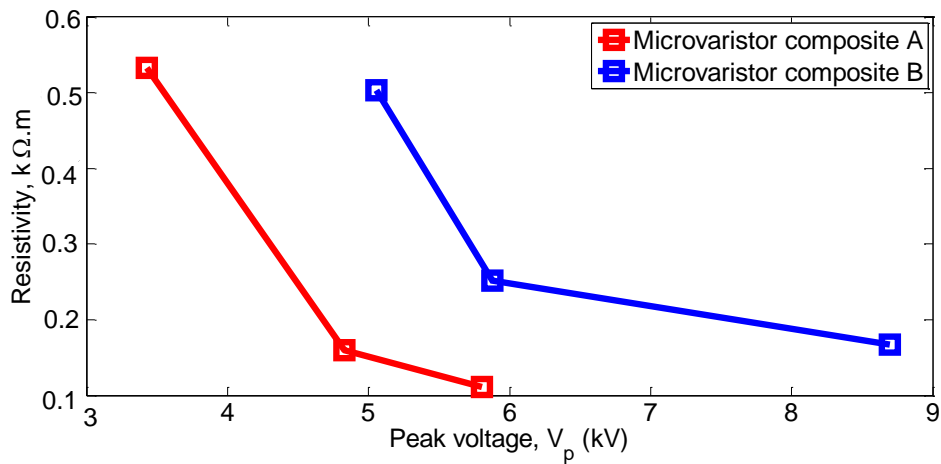
Figure 5.21: The resistivity profiles of both composites as a function of voltage at I_{peak}.

Figure 5.22 explains the conductivity measurements when the samples were subjected to transient voltages. Microvaristor A composite exhibited a higher conductivity value, due to the rise of resistive current, at peak voltage, 5.8 kV compared to the second sample with voltage of 8.7 kV for lower conductivity profile.
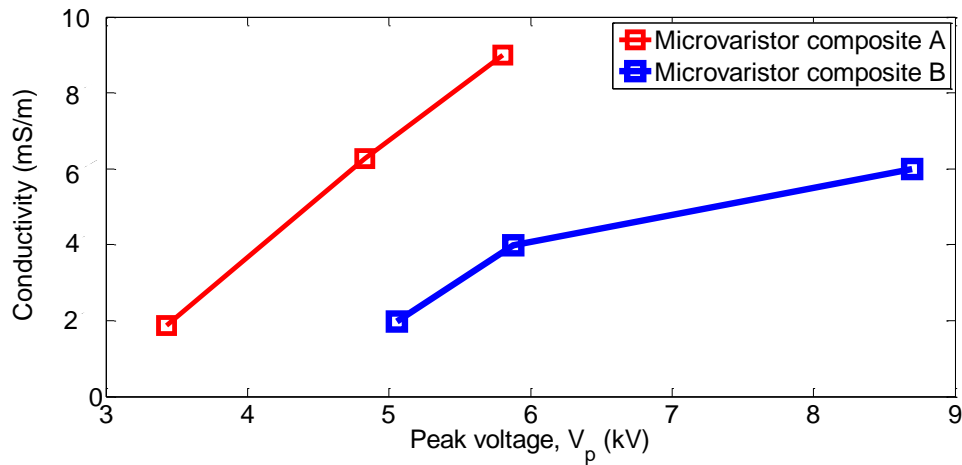
Figure 5.22: Conductivity versus voltage at I_{peak}.

5.4.3 CAPACITANCE

The capacitance and relative permittivity profiles of composite samples were measured under impulse voltage. The capacitance was measured by integration of the current flow until the spike of current occurred [120], according to Equation (5.2)

$$C \frac{dV}{dt} = I \tag{5.1}$$

$$C = \frac{\int_0^t I(t)dt}{V(t)} \tag{5.2}$$

The impulse voltages, V (t), were measured accordingly in the capacitive region, from low to peak voltage at I_{peak}. The capacitance of the composites decreased significantly when the increase in the applied voltage initiated the changing of depletion layers in the microstructure of the ZnO grain-boundary region [115]. The high value of the permittivity value ε_r in transient voltage related to the current response and was slightly higher than in the AC profile as shown in Figure 5.23.
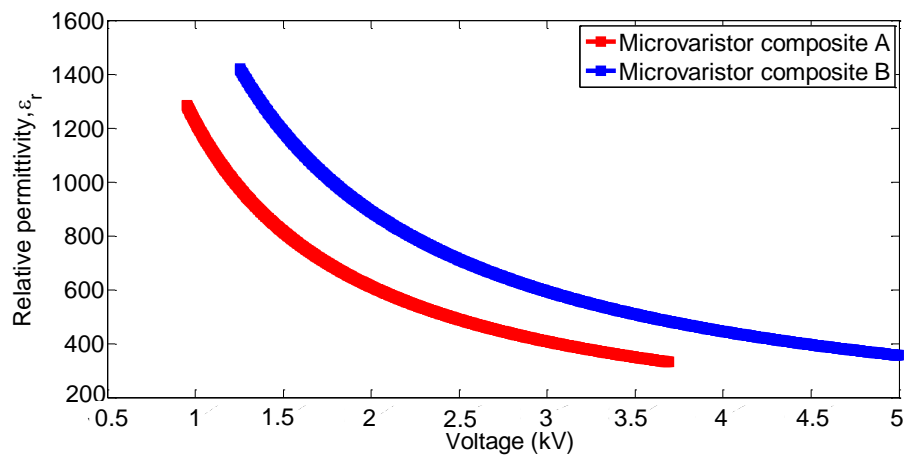
Figure 5.23: The relative permittivity profile for both composites as a function of voltage.

5.4.4   DAMAGE AND RECOVERY

While conducting the test, setting the charging voltage beyond 10 kV caused flashover to occur. Damage, such as punctures, were seen on the test samples due to high current. The increase in the current will cause degradation and eventually cause thermal runaway of the samples.

In this test, it is clearly seen that the samples exhibited excellent self-recovery, when subjected to transient voltages which significantly improved the electrical performance of field grading materials. This scenario also occurred when the compounds were tested under DC and power frequency energizations. An interesting finding showed that both composite samples demonstrated current overshoot when the samples entered into the breakdown regime and had the puncture of the material. This condition occurred due to material composition that affects the characteristics of zinc oxide varistors [116].

5.4.5 COMPARISON OF AC, DC AND IMPULSE PERFORMANCE

Figure 5.24 shows a summary of the current density profiles of composite samples when subjected to high voltage tests. The high resistive current of composite A is much higher than that of the second sample, composite B. Interestingly, both samples were compounded at 70 wt.% microvaristor loading and were fabricated by following similar procedures. These findings led to detailed investigation of the properties of the microvaristor powders themselves. The characteristics of the powders, such as the chemical elements and the size of the micro–powders, were investigated to determine the possible factors that contribute to the non-linear behaviour of the compounds.
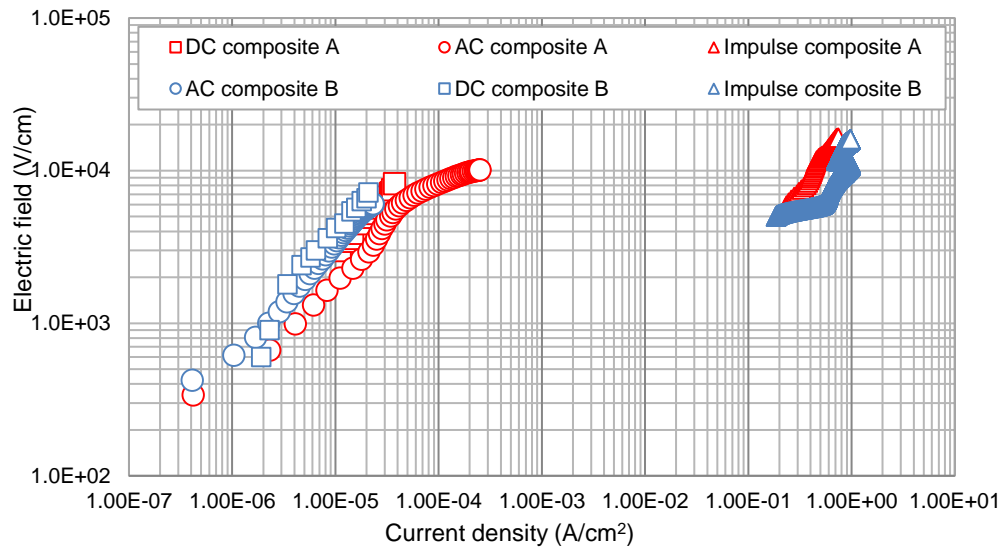
Figure 5.24: A summary of current density profiles for all samples under high voltage AC, DC and impulse tests.

5.5   DISCUSSION

The performance of the test samples was examined. It was noticed that the resistive current directly influenced the joule heating of samples. In [34], a few parameters that contribute to resistive current which prominently come from the effect of material properties, applied voltage, duration of applied voltage and elevated temperature in the material have been highlighted.

The duration of power frequency tests were reviewed. The accumulated time was calculated from the beginning of the test until the sample entered into the breakdown regime. The rate of increasing the voltage level was set at 1 kV/30 s. From the measurement, the duration of the AC test for composite *A* was nearly 3 minutes (at

voltage 5.07 kV) meanwhile, for composite **B**, it was 2 minutes (at voltage 3.8 kV) which corresponds to the applied voltages.

As highlighted earlier, the effect of applying direct current is to increase the temperature of the composite while, at the same time, it influences the dielectric strength of the material. The dielectric strength depends on the rate at which the heat is conducted away. Therefore, the maximum voltage was applied until the sample approached the threshold voltage. The reference value of the threshold voltage was obtained from a power frequency test. If the applied voltage was beyond the threshold point, high current flowed and the composite absorbed the energy which initiated the sample to rupture. The test was conducted several times with an interval of at least 3 minutes to allow the sample to cool, as it was expected that the high temperature was responsible for the initiation of the failure.

A comparison of the power measurements that were obtained from both the AC and the DC tests was then carried out. This verification is important to justify the power consumption during the test. There are few factors which were taken into account during the test, such as the physical condition of the test sample, the electrode design and length of time during which the voltage was applied. These factors contributed to the enhancement of current flow in the sample, by encouraging the sample to enter the breakdown regime and rupture.

In some papers [9], [121], it has been highlighted that the grain size has a great influence on the electrical properties of the powders and compounds. The switching fields can be tailored according to the size of the grains in the polycrystalline particles

and the chemical elements in the powders. With smaller grain sizes, larger grain boundaries are formed which lead to high switching fields.

In order to demonstrate the impact of the above factors, comparative studies of the electrical properties of both materials (powder and compound) were presented. The voltage and current flow through the composites were measured and the correlation between the experimental results and the microstructure of the microvaristor powder was attempted. In this investigation, external factors such as the fabrication procedures were assumed to be practically identical for all samples. In order to obtain a clearer picture, the microscopic results shown in Chapter 4 have been revisited.

5.5.1 GRAIN SIZE EFFECTS

The behaviour of microvaristor compounds depend on the microstructure of the materials and the way they are processed, which has an influence on the size of the material grains. According to the microscopic results in Chapter 4, microvaristor *A* had an average size of 37 µm, while microvaristor *B* had a mean size of 71 µm. With the presence of high volumes of small dimension micro particles in composite *A*, an increase of surface area-to volume ratio was created. Because of this, there are many regions in the polymer structure that encourage the microvaristor to bond strongly with the silicone rubber matrix. When there are major smaller particles, a large number of current paths are obtained, initiating the high on-set electrical fields. As a result, the electrical properties of composites are significantly modified. For example, microvaristor *A* shows a higher threshold voltage than microvaristor *B* in AC tests, due to its smaller grains, which encourage greater current flow.

5.5.2 CHEMICAL COMPOSITION

The presence of B_2O_3 in the chemical composition maybe the cause for current overshoot in both compounds when subjected to impulse voltage [116]. Meanwhile, there is a small quantity of antimony trioxide, Sb_2O_3, in microvaristor powder **B** that significantly contributes to an increase of the non-linear coefficient and to grain growth [112]. However, the lack of small grain sizes in composite **B** has a direct influence on its electrical performance. A further ingredient, such as fluorine, in composite **A,** has been used as an accelerator in order to improve the non-ohmic properties that particularly encourage the formation of ions. The benefits of the different doping elements were discussed in Chapter 4.

5.6 CONCLUSIONS

The high voltage tests, based on BS EN 60060 standard, were successfully conducted on the microvaristor powders and composites. In the preliminary studies, different concentrations of microvaristors filled with silicone rubber (10 wt.%, 30 wt.%, 60 wt.% and 70 wt.%) were proposed and all samples were tested. The experimental results from AC tests showed that the composite samples at 70 wt.% microvaristor concentration exhibited non-linear behaviour when the samples reached certain threshold voltages. The investigation of the non-linear properties of microvaristor powder was carried out under power frequency tests. The voltage and current for all test samples were measured and the electrical properties were derived through a current analysis technique.

The DC test was conducted on all composite samples by following standard procedures. The results were encouraging, and the electrical properties were presented. The measurement of electrical properties of micro composites was succesfully achieved under transient tests. From the experimental works carried out at different applied voltages, the voltage impulse across the test samples showed the overshoot on the voltage waveform. Factors arising from the test set up and the characteristics of the micro composites were found to have an effect on the overshoot. The results showed that the rise time for voltage variations was longer. The impulse currents were evaluated and showed a relationship with the increasing voltages. The electrical properties of the composites were calculated and presented in terms of V-I characteristics, resistance, conductivity, capacitance and permittivity. These characteristics were found to be caused by the reversible changes in the electrical properties in the intergranular phase. From this investigation, it could be seen that pulse voltages and currents can initiate the degradation of the composites, which are dependent on the thermal transport properties of the varistor microstructure as well as the electrical properties of the active intergranular phase.

CHAPTER 6

APPLICATIONS OF FIELD GRADING MATERIAL IN OUTDOOR INSULATION

6.1   INTRODUCTION

In high voltage outdoor insulation, field grading material can minimise the field localisation thus, significantly improving electrical performance. The material is environmentally and design friendly, as it minimises material usage and has a small maintenance cost. Due to its non-linear characteristics, the field grading material allows the electrical field to be controlled on the polymeric insulators, which are susceptible to highly non-uniform field distribution and ageing. Non-uniform voltage distribution along the insulator surface contributes to field enhancement and occurs, in particular, near the metal end electrodes. When the insulators are exposed to polluted conditions, high electric field magnitudes accelerate the formation of dry bands, which may eventually lead to flashover.

Due to the limitation in the supply of the material and difficulties in laboratory procedures, the assessment of in-house field grading material was presented through numerical modelling. A test subject was identified and modelled through the finite element method. A previous study conducted by Rahisham et al. [11] described the implementation of field grading material into an 11 kV polymeric insulator. Taking into account the procedures previously developed, the simulation studies on this insulator were conducted using COMSOL Multiphysics® package. The electrical properties on the polymeric insulator were presented in this model. The electrical field distributions on the polymeric insulator surface under different environments, was examined before a suitable in-house field grading material having appropriate electrical properties was added. The proposed design of the field grading material was reviewed, with the particular aim of suppressing field enhancement along the insulator surface, which was predicted to initiate dry band formation and eventually lead to flashover.

6.2   OVERVIEW OF POLYMERIC INSULATOR PERFORMANCE

There is a growing interest in this subject from engineers and scientists, which shows the importance of polymeric insulators in high voltage insulation systems. A forecast of the application of composite insulators in AC transmission lines was reported in [122] and showed increasing demands year by year. The polymeric insulators show an excellent performance in highly polluted environments, due to low molecular weight (LMW) silicone chains, which diffuse through the pollution layer and permitting the recovery of the hydrophobic properties [123]. LMW has unique properties, as a new

molecule can be rebuilt once it has broken its molecular attachment. As a result, silicone rubber has an excellent life span and may last for more than a decade even if it is exposed to severe climatic conditions.

Hydrophobicity of silicone rubber material is a beneficial property for outdoor insulators, because it prevents the formation of continuous conductive films on the surface of the insulator. In order to understand the degradation phenomena present on a polymeric surface, Starr et al. [32] conducted various experiments and identified that silicone rubber performed better than hydrophilic materials, as it was able to recover its non-wettability within a day. However, this material was still susceptible to failure due to a number of concurrent stresses, as reported in [124], while the main factors that accelerate ageing of composite insulators were emphasized in [122]. Factors such as non-uniform field distribution seem most likely to trigger discharge activities, corona and eventually flashover [125]-[127], and the condition becomes worst when the insulators are exposed to severe climatic conditions [128], [129] with the present of pollution agents [87], [91], [130], [131].

6.2.1 MODELLING OF POLYMERIC INSULATOR

Generally, polymeric insulators comprise three essential components. The end fittings are designed to support heavy load conductors on transmission towers. The fibre reinforced core is attached to both end fittings in order to provide the essential mechanical strength and insulation between the energised terminals. The polymeric weather shed housing is used to protect the fibre core from various environment impacts, and the design is intended to provide good water drainage.

In this research, an 11 kV silicone rubber insulator was used. This insulator is illustrated in Figure 6.1 which shows its main components. The shed diameter is 90 mm and is attached to a 28 mm diameter trunk. The sheds are separated from each other by a 26 mm length of shank and are connected to 16 mm radius metal end fittings. The axial length is 175 mm, while the creepage distance on the insulator surface is 375 mm, calculated from the high voltage terminal to the ground point.
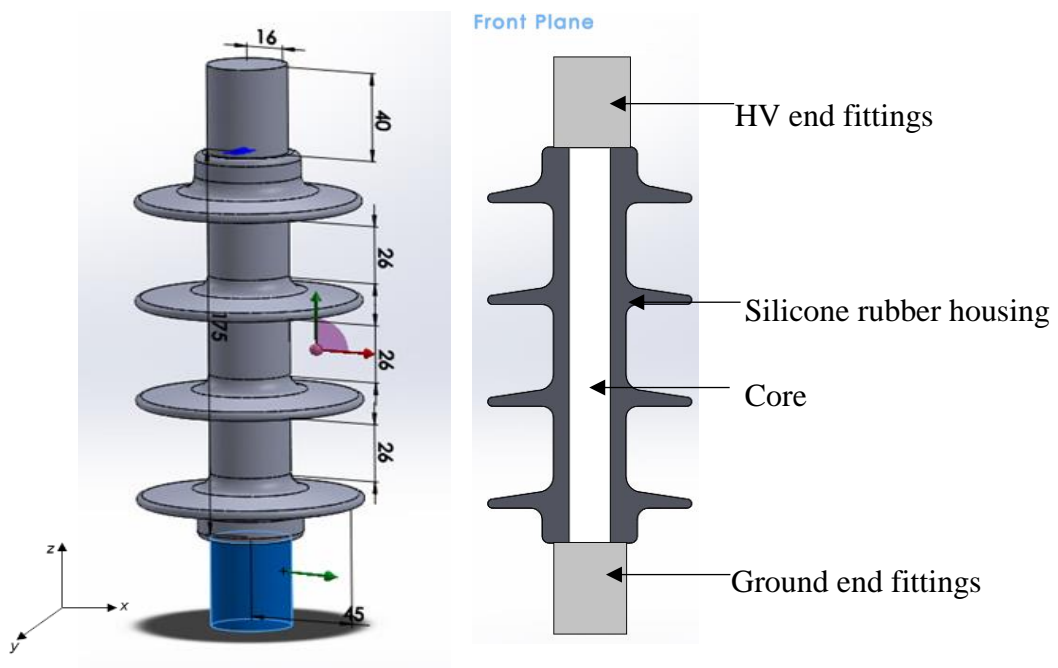
Figure 6.1: A model of an 11 kV silicone rubber insulator.

6.3 NUMERICAL ANALYSIS THROUGH FINITE ELEMENT METHOD (FEM)

The Finite Element Method (FEM) is a numerical approach to solving the partial differential equations (PDE), which represent a physical system. This method is based on mathematical expressions that are generally defined in a built-in software package. In this work, COMSOL Multiphysics ® version 5.0 was used to compute the electrical profiles of polymeric insulators. Three levels of analysis programmes were used for pre-processing, solving and post processing. The levels involve different activities as illustrated in Figure 6.2 [132].
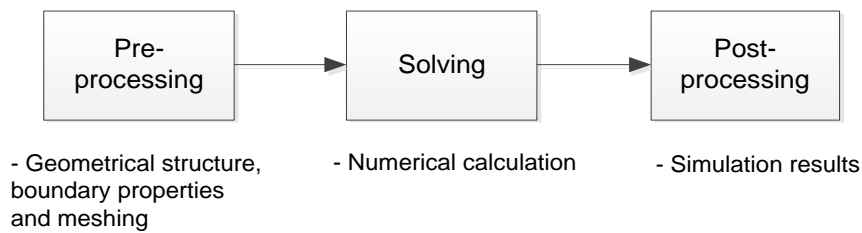
Figure 6.2: Numerical processes via COMSOL Multiphysics ® [132].

The diagram in Figure 6.2 is an illustration of the consecutive stages of pre-processing, numerical solving and post processing. At the pre-processing stage, physical problems such as geometrical structure, material and boundary properties are presented which enables modelling to take place, after which the modelled space is meshed. The meshing of the elements is the starting point for transforming the geometry into small units and simple forms using the finite element method. Numerical solving is particularly dependent on the physical interface and is normally expressed in

differential equations. The final stage is post processing which enables users to generate graphical plots depending on post processing parameters.

6.3.1 PHYSICAL STUDIES

COMSOL® Multiphysics provides a platform for different modelling and simulation programmes, which are linked to selective, advanced, numerical calculations. It is important to undertake an appropriate physical study before carrying out the simulation process. In order to investigate the electrical field distribution along the insulator, the physical platform was set in Electrostatic and stationary studies. This interface is used to investigate the electrical fields in the quasi-static model that operates over long time scales and at low frequency. The quasi-static system provides a precise estimate of 'error' fields in the simulation component before the real application. The numerical equations are used to describe physical properties which can be found in the COMSOL Multiphysics® programme and manual [132].

6.3.2 ELECTRICAL PROPERTIES

The electrical properties of the materials used in this simulation method are shown in Table 6.1. Two environmental studies were investigated, namely dry and clean conditions, and wet and polluted conditions. The polluted environment is represented by a 0.5 mm pollution layer on the insulator surface, with a conductivity of 10^{-6}(S/m) and a relative permittivity of 81. Meanwhile, the selection of the electrical properties of the in-house field grading layer will be discussed in the next sub-section.

Table 6.1: Electrical properties of materials.

Components	Relative permittivity, ε_r	Conductivity, σ (S/m)
Aluminium end fittings	1	2.63×10^7
Silicone rubber housing	2.9	10^{-13}
FRP core	7.1	10^{-13}
Pollution layer	81	10^{-6}
Air	1	10^{-14}

6.4   INSULATOR PERFORMANCE

It is known that a strong and uncontrolled electrical field on a high voltage insulator is liable to cause damage, such as aging and partial discharge. As a result of the insulator design and the different material properties of a non-ceramic insulator, non-uniform electrical fields are generated and encourage coronas, discharge activities and eventually lead to flashover. Polluted particles, such as dust, salt etc., accelerate these dangerous occurrences, which become even worse with the presence of moisture. In order to simulate the actual operation conditions, a computation analysis evaluated the performance of 11 kV silicone rubber insulator in two environments; dry and wet conditions, so that a direct comparison could be made. The evaluation concentrated on the equipotential distributions along the insulator surface, and it was expected that the unfavourable case would occur at the triple point areas. The potential voltage was set at 18 kV at the high voltage terminal and 0 V at the ground point with a nominal power frequency of 50 Hz.

With reference to Figure 6.3, it can be clearly seen that the voltage lines are distributed heterogeneously along the insulator surface under dry and clean conditions. The voltage lines are concentrated near the end fittings which represent three material elements (air-aluminium-silicone rubber) that are known for high emission of electrons in the presence of strong electrical field [8], [17]. Due to this situation, there is a high possibility that flashover would occur, which becomes more likely when the silicone rubber starts to lose its hydrophobic properties.

a) dry and clean   b) wet and polluted
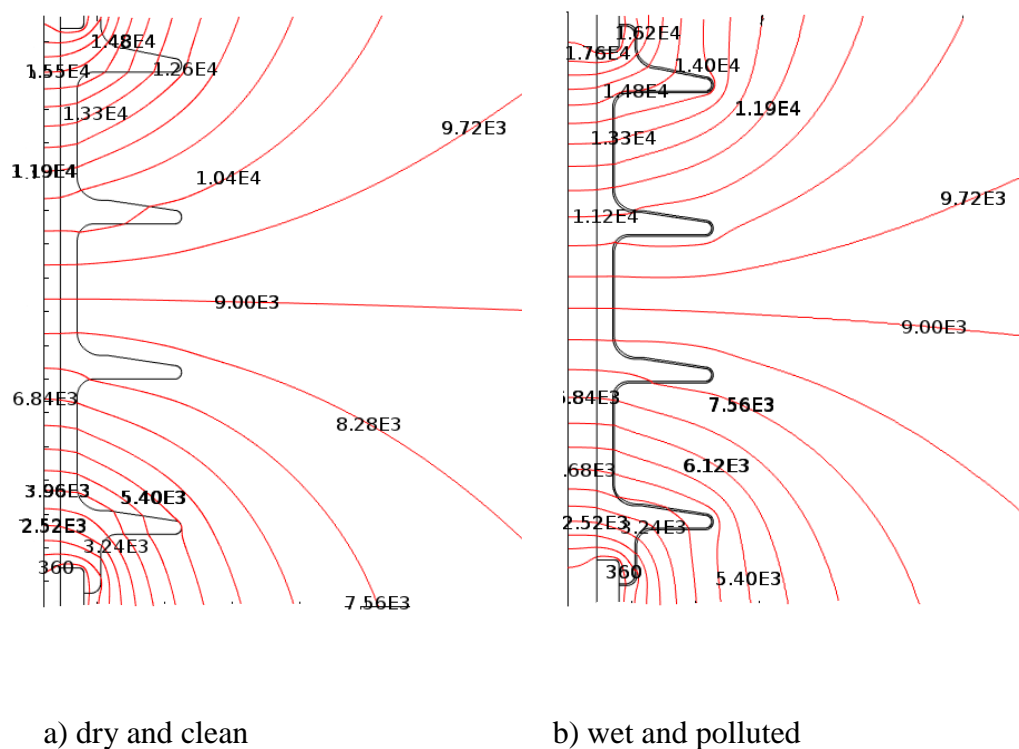
Figure 6.3: The equipotential distribution along the 11 kV silicone rubber insulator under different conditions.

On other hand, it can be seen that the equipotential lines spread uniformly when the insulator surface has been coated with a resistive pollution layer. The higher

conductivity value of the pollution layer allows the potential lines to be redistributed outward to the low field regions with the minimal changes in the potential lines in the middle of the insulator body.

Figure 6.4 shows the potential profile on the insulator surface that relates to the previous discussion of equipotential distributions. The impact of the non-uniform distribution of equipotential lines that occurred at the near end fittings, which contributed to the intensification of electrical field, can be clearly seen.
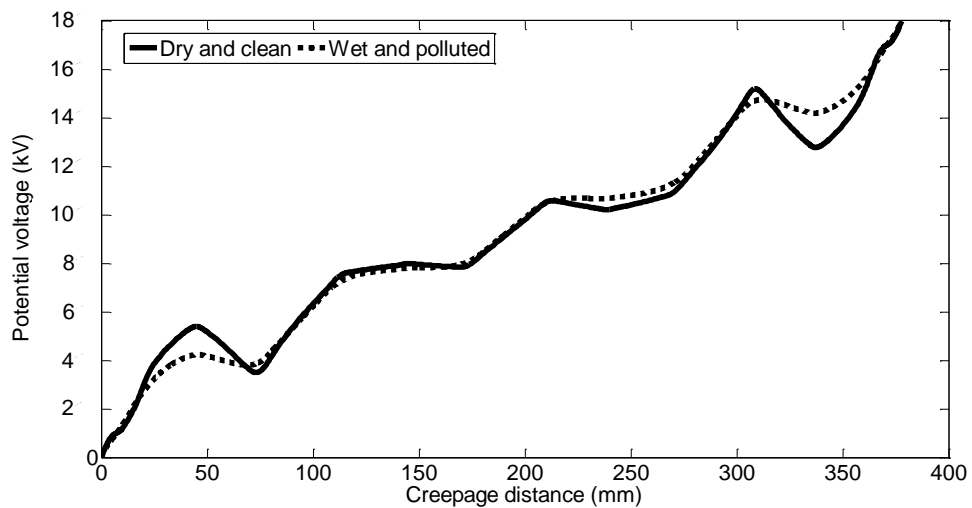
Figure 6.4: The potential profiles on the insulator surface under different conditions.

A comparison of electrical field distributions under different conditions is depicted in Figure 6.5.The following explanation of equipotential distribution is obtained by focussing the tangential electric field distribution along the surface of the insulator. There is a good correlation between the peaks of the tangential electrical field with the equipotential distribution on the insulator surface. The insulator exhibits higher field magnitudes under dry and clean conditions than in wet and polluted conditions. As

discussed in various articles [21], [35], [123] a high electrical field at any point of the insulator surface may cause corona activities if the field value exceeds the threshold level.
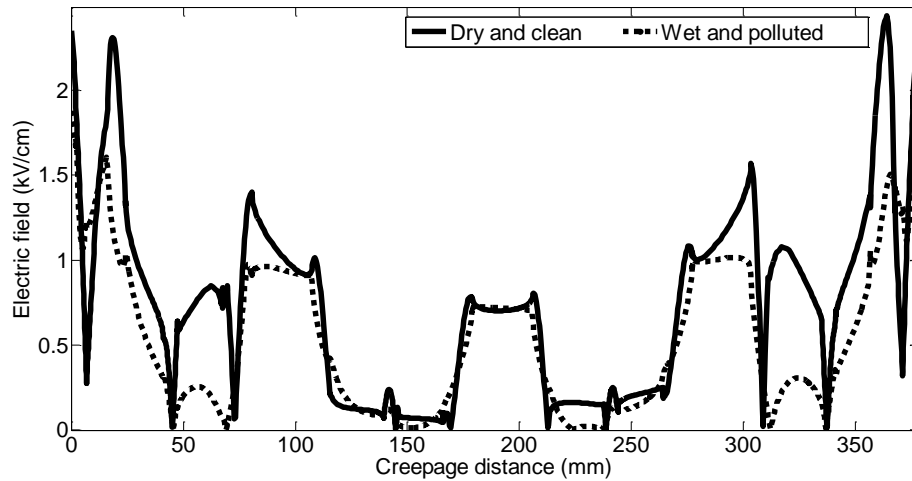
Figure 6.5: The tangential electrical field along the insulator surface under two different conditions.

In contrast, the electrical field under polluted conditions is distributed with lower peaks. With the presence of a conductive pollution layer and when operated under system voltage, the surface resistance of the insulator decreases considerably. The resistive surface leakage current will flow and will dry out part of the pollution layer, due to localized field enhancement and the non-uniform heating effect [11]. The dry bands are formed at certain widths, which may be up to a few centimetres wide, and are energized with the line to earth voltage. After a period of time, air breakdown will occur and this will encourage the interconnection of the dry bands by arcs formed in series with the pollution layer. This process may lead to insulator spark over. If the surface resistance of undried regions is low enough, whilst the dry band discharges

remain active, the process will initiate the elongation of arcs that bridge the dry bands and cause flashover to occur.

Dry band formation is governed by power dissipated on the surface due to ohmic heating. Ohmic heating is the source of the rate of energy dissipation needed for evaporation of moisture from the insulator surface. A calculation of power dissipation is undertaken in a later Section 6.5.2.

When considering the condition of polymeric insulators that are vulnerable to the electrical stress effect, it is important to control the electrical field distribution along the insulator in order to extend the service life of the insulator and increase its performance. There are a few options to manage the field distribution. For example, the use of a grading device will reduce the high electrical field considerably. In addition, improvements in the design of end fittings [133] and corona rings [89] will change the high magnitude and distribution of the electrical field on the surface. However, these conventional field control methods require a complex design and maintenance. Therefore, further control is possible through non-linear resistive field grading material.

As introduced in Chapter 5, a microvaristor filled with silicone rubber is a non-linear resistive field grading material that operates effectively under normal and transient voltages. The non-linear characteristics of microvaristor grains is transferred directly to the compound, allowing the material to control the high electrical field along the insulator surface significantly. The advantages of microvaristors are that they are robust and easy to handle during the fabrication process which makes the material

capable of being reproducible. Two in-house microvaristor compounds were adopted in this simulation in order to investigate the potential of these materials in outdoor insulation.

6.4.1   FIELD GRADING SELECTION

The non-linearity of the microvaristor compound is predominantly influenced by the intrinsic properties of the ZnO varistor grains. The non-linear characteristics of the field grading material is governed by the double Schottky barrier that forms at the grain boundaries of the ZnO varistor grains. Using the idea of percolation, an approach to understanding non-linear conduction in a ZnO varistors is explained in Equation (6.1).

$$\sigma(E) = \sigma_o \exp(\alpha E) \qquad\qquad (6.1)$$

With σ_o representing the initial conductivity and α the non-linearity coefficient for the ZnO grading material.

This equation has been developed to present the conductivity profiles of both of the field grading materials that have been discussed in previous chapters. The conductivity curves correlate with the threshold electrical fields that will exercise control into the high conduction current range. This parameter is an important characteristic in varistors as it determines the transition in the compound from the insulation to conduction. Figure 6.6 shows the conductivity profiles for both in-house field grading materials.

The threshold point, E_o is measured by forming a tangent line from the initial point until it touches the curve of the graph. The above results are interesting, as the two

compounds show different threshold points and operate differently in the high
conduction region, even though the microvaristors loadings of the compounds are the
same. As discussed in Chapter 4, it is the grain properties of the varistors that govern
the amount of current flow. Two electrical parameters for each compound,
conductivity, σ (S/m), and relative permittivity, ε_r, at the threshold point, were adopted
into the simulation models. The electrical field distribution is well controlled when the
switching properties of the compounds were effectively operated under the insulator
specifications and conditions.
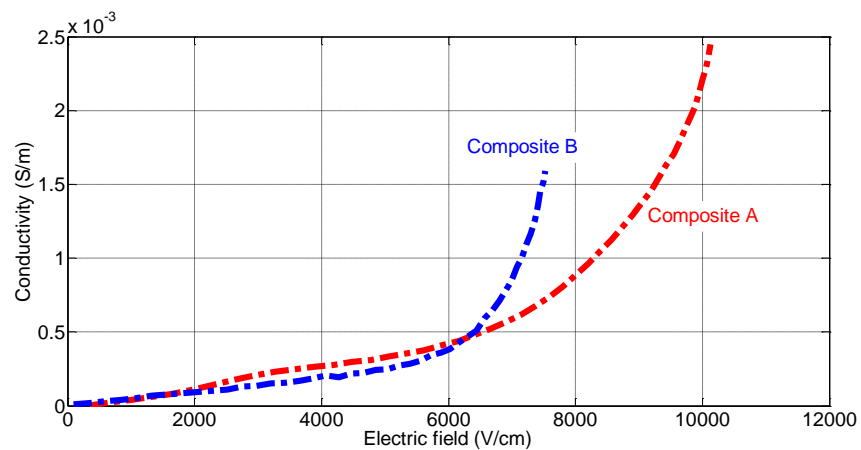
Figure 6.6: The conductivity profiles of both field grading materials at 70 wt. %
microvaristor concentration. The threshold point, E_o for composite A = 6.5 kV/cm and
for composite B = 6.0 kV/cm

6.4.2 INSULATOR SWITCHING FIELD THRESHOLD

It is essential to determine the field switching profile of the insulator before starting
the implementation process of the field grading material. In previous research [11], the
computation of field switching threshold was conducted at the interface between the
core and the insulator surface, by embedding field grading material in a cone-shape

near end fittings and this showed promising results. A comparison with another integration of field grading layer, at the exterior of the insulator housing and along the rod, was carried out in [134].

This implementation of field grading layer along the rod showed some drawbacks, such as continuous leakage current, that led to insulation failure. It is an opportunity to investigate a similar design of field grading material [11], by looking at some improvements in field distribution.

The electrical field is calculated from the high voltage terminal to the grounding end fitting which is between the interface of the core and insulating material. This measurement concept has been highlighted in [11] which emphasize the electrical field profile at the designated area before inserting field grading material into the insulator as depicted in Figure 6.7. As can be seen on the figure, the highest field was found at both end fittings; ground terminal (5.9 kV/cm) and high voltage terminal (6.0 kV/cm). It is important to reduce the high magnitude of electric field at these regions in order to maintain the excellent electrical performance of polymeric insulators. Therefore, a field grading compound with suitable field threshold as shown in Figure 6.6 is determined.
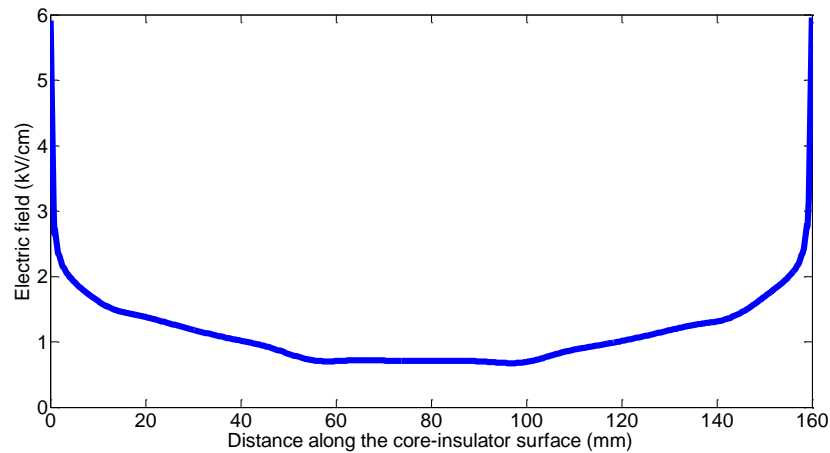
Figure 6.7: Normalized field distribution appears in the middle between the core and the insulator surface [11].

6.4.3 FIELD GRADING LAYER DESIGN

This section sets out the important criteria that contribute to minimising the electrical field on the insulator surface. A number of design proposals were presented such as the implementation of cylindrical shape at both end fittings and the introduction of conical shape at one or both terminals with different dimensions of field grading materials. The benefits and drawbacks of all design proposals were discovered and the author found out the conical field grading material was successfully reduced the high electrical field along the insulator surface which also highlighted in [11]. However, this design caused high field levels around the middle surface area the core of insulator. This condition corresponds to the re-distribution of the equipotential lines, which are associated with the high voltage and ground terminals, along the length of the microvaristors compound.

A solution is proposed in this work to solve this problem by introducing the field grading structure in the middle of the insulator body. This design concept is addressed by investigating the region of formation of the high electrical field and dry band on the insulator body, through computational analysis [135] and experimental work [136]. The design is presented in Figure 6.8. The cylindrical structure is placed at the starting point of the middle shed with a gap of 2 mm from the core. It is noticeable that the thickness of the field grading material is very important to ensure that the field is distributed homogenously with lower peaks and that there is minimal heat generation from the surface.

In this research, 2.5 mm of cylindrical field grading material was used following consideration of some additional factors that affect insulator performance, such as the insulator structure and housing. From the computation results, the field enhancement around the middle of insulator shank was investigated and the optimum field strength was obtained.

To evaluate the performance of outdoor insulators with graded material, the electrical properties of microvaristor compound *B*, with a threshold field 6.0 kV/cm, were identified as being excellent to suppress the high field located near the end fittings. The material is designed to trigger non-linear conduction directly, as the local field magnitudes reach the threshold field, thus, improving electrical stress control. The performance of in-house grading material is evaluated under two main environmental conditions; a) dry and clean and b) wet and polluted. In both cases, the investigation

is conducted under the nominal power frequency of 50 Hz and under impulse energisations.
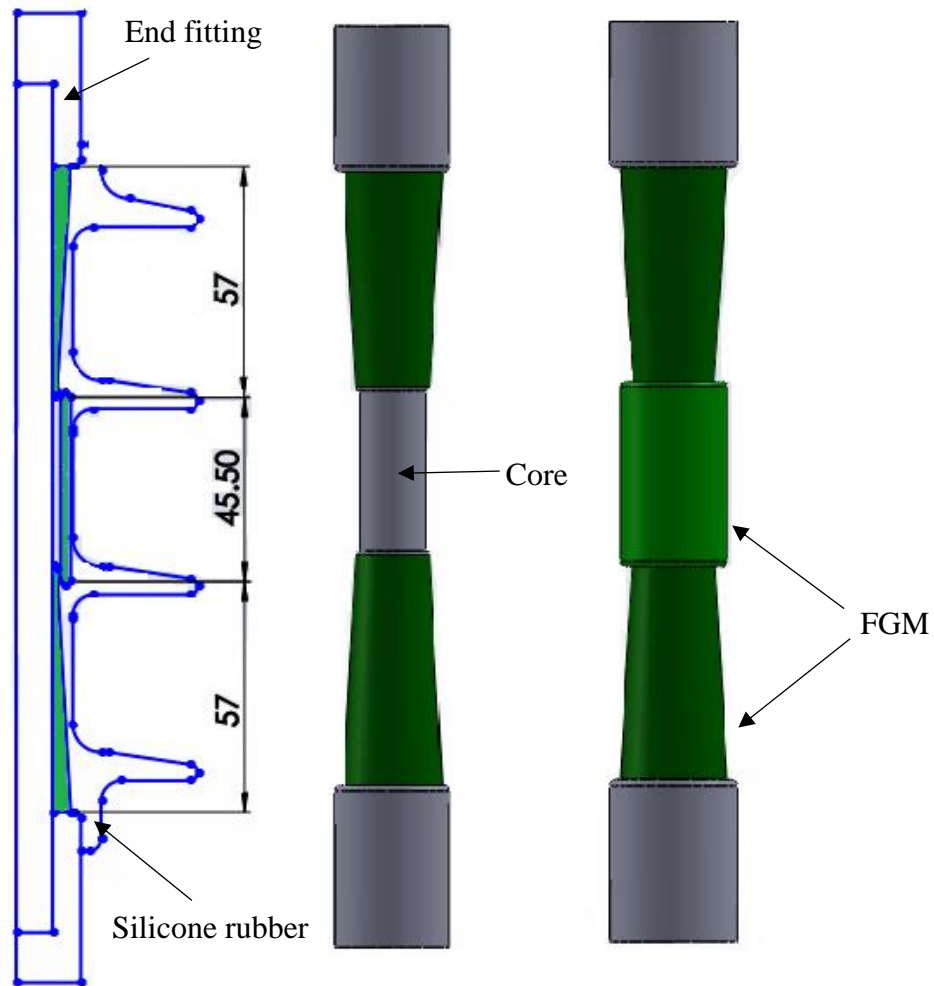
a) the physical layout of development   b) inserting a conical shape of FGM at both end fittings   c) installing a 2.5 mm cylinder of FGM in the middle of insulator shank

Figure 6.8: Structure of field grading material (FGM) that was deployed into a core of 11 kV silicone rubber insulator.

6.5 INSULATOR PERFORMANCE OF FILLED WITH FIELD GRADING MATERIAL

6.5.1 POTENTIAL AND FIELD DISTRIBUTION

A comparison of equipotential distribution, under different environments, at nominal frequency, is shown in Figure 6.9 and Figure 6.10. As the field strength is associated with the voltage distribution, the equipotential lines under dry and clean conditions are spread further apart starting from the terminals, which significantly minimised the field enhancement.

The potential lines are distributed uniformly along the insulator surface, after the installation of field grading material into the insulator housing. The high magnitudes of electrical field at both end fittings are effectively transferred to the adjacent areas, while the field distribution at the middle shank shows a very small change, which allows the field magnitudes to distribute to the optimum levels . This particular field profile can be compared to the insulator without the presence of field grading material.

Meanwhile, the potential lines under wet and polluted conditions spread much wider than those of dry and clean surfaces, due to the effect of the resistive pollution layer. The electrical field profiles for both conditions are shown in Figure 6.11 and Figure 6.12.

a) without field grading material **B**   b) embedded with field grading material **B**
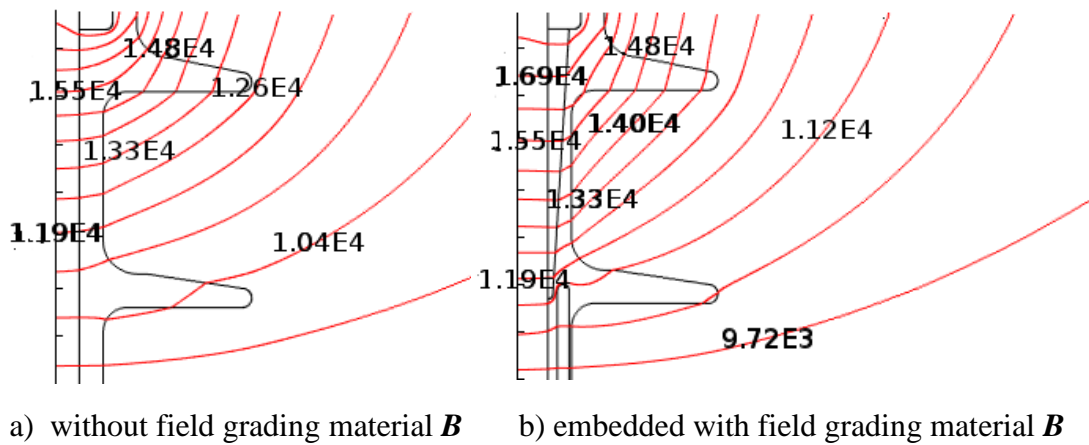
Figure 6.9: The equipotential distribution along the insulator surface under dry and clean conditions.

a) without field grading material **B**   b) embedded with fieldgrading material **B**
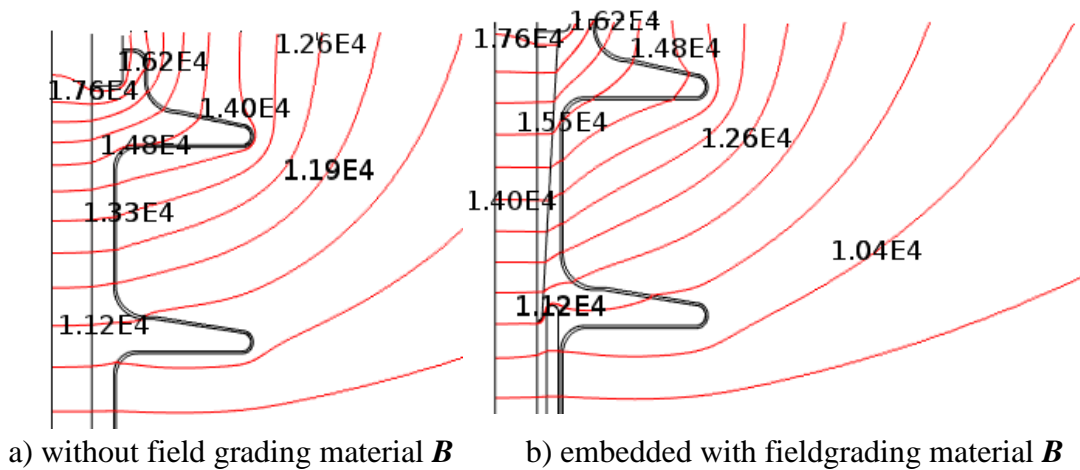
Figure 6.10: The equipotential distribution along the insulator surface under wet and polluted conditions.

Figure 6.11 shows the maximum tangential electrical field was successfully reduced from 2.37 kV/cm to 2.1 kV/cm at the high voltage terminal, and from 2.35 kV/cm to 2.0 kV/cm at the ground terminal, after the integration of the field grading material into the insulator body. The electrical field at the end fittings was directly transferred to the adjacent shanks which increased the field in the vicinity.

However, the field enhancement only made a small difference to the field distribution at the middle shank (Shank 2), due to introduction of field grading material in this area.
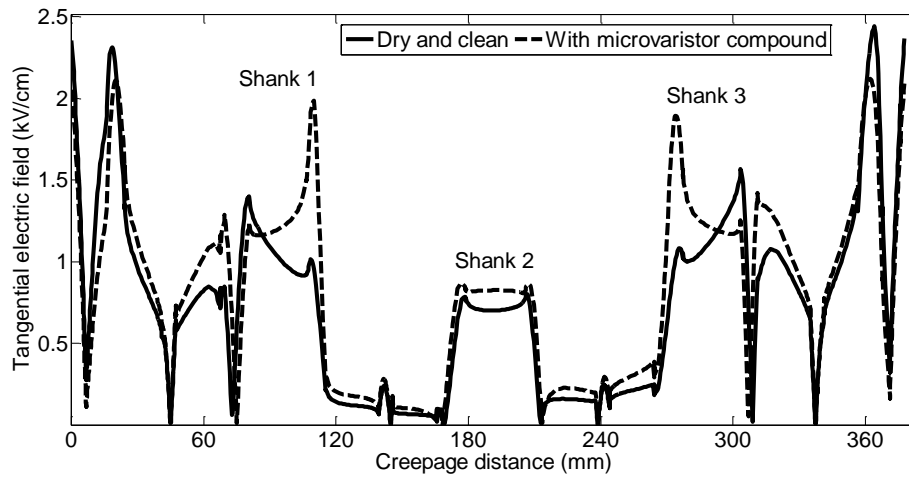
Figure 6.11: The electrical field profile under dry and clean conditions with and without field grading material **B**.

As expected, the insulator showed a field profile with lower magnitudes, when subjected to wet and polluted conditions, due to the presence of the resistive layer. The reduction in the field was clearly observed when the potential lines were modified after passing through the graded material and going through to the insulator surface.
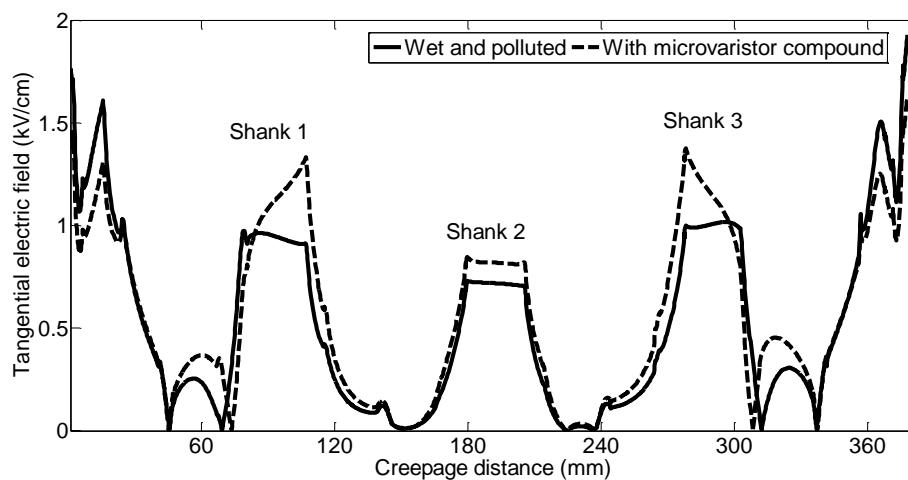
Figure 6.12: The electrical field profile under wet and polluted conditions with and without field grading material **B**.

These distribution improvements are summarised in Table 6.2, which shows an assessment of the field peak at different insulator regions. According to the field profile, the high electrical field obtained under dry and clean, and wet and polluted surface conditions was reduced, which would reduce failure and degradation of the silicone rubber material due to corona and surface discharges [135].

Table 6.2: The magnitude of tangential fields at different insulator regions.

Region areas	Dry and clean (kV/cm)		Wet and polluted (kV/cm)	
	Without FGM	With FGM	Without FGM	With FGM
HV end fitting	2.37	2.1	1.89	1.63
Shank 1	1.38	1.9	0.97	1.31
Shank 2	0.79	0.85	0.72	0.82
Shank 3	1.57	1.9	1	1.37
Ground end fitting	2.35	2	1.87	1.56

6.5.2 POWER DISSIPATION

When the insulator was wet and polluted, there was still the possibility of dry band formation, which is governed by power dissipated on the surface due to ohmic heating. Ohmic heating is the source of the rate of energy dissipation needed for evaporation on the insulator surface. It can be expressed as follows:

$$P_{area} = \sigma E^2 t_p \tag{6.4}$$

P_{area} is power per square meter (W/m^2), t_p is the uniform thickness of pollution layer = 0.5 mm and $\sigma = 6x10^{-7}$ represents the conductivity of the pollution layer.

Meanwhile, power dissipation per unit volume is measured by following Equation (6.5). As can be seen in Figure 6.13 and Figure 6.14, there is a large difference in power dissipation with and without the insulator being modified with non-linear resistive material. The evaluation of both dissipated power profiles shows promising results, as the graded material allows an amount of power to dissipate, either through the surface or through the volume of the material.

$$P_{volume} = E^2 \sigma \ (W/m^3) \qquad\qquad (6.5)$$
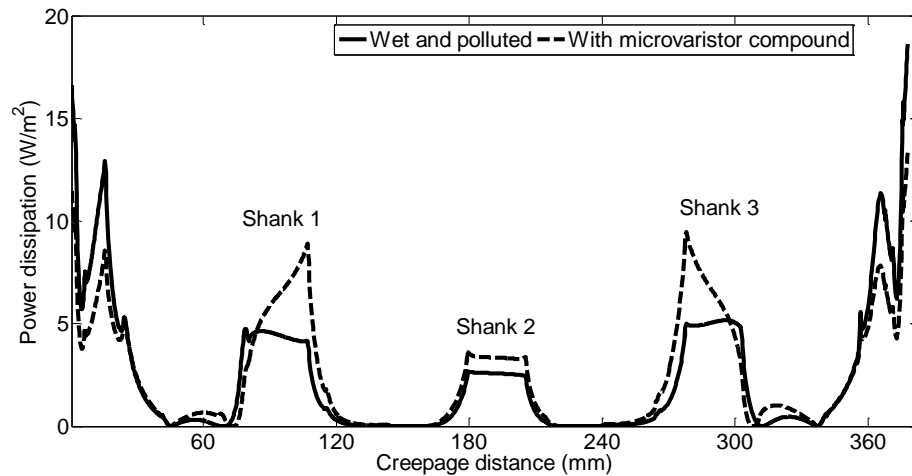
Figure 6.13: The measurement of power dissipation per unit area along the insulator surface.
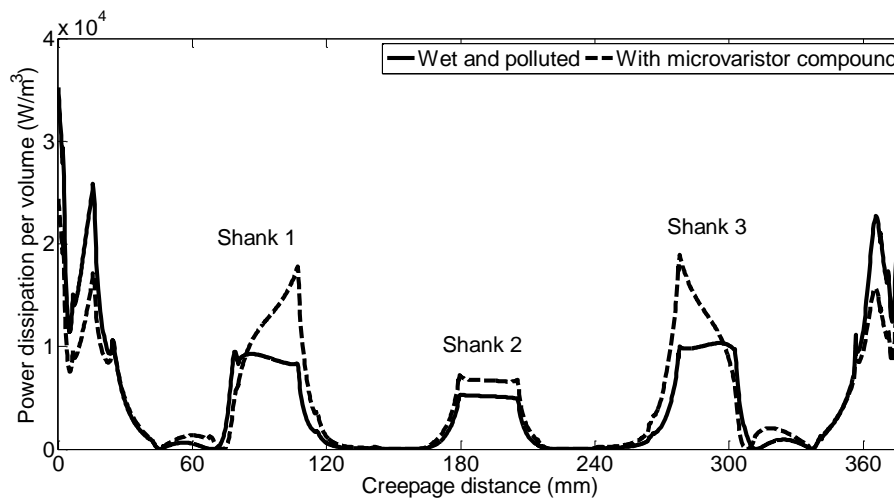
Figure 6.14: Power dissipation per unit volume occurring along the insulator surface.

The measurement of power dissipation is summarised in Table 6.3. There was large improvement on power dissipation on the insulator surface and volume when using the insulator embedded with field grading material *B*. Almost 35% of power generation was reduced which affected all insulator areas.

Table 6.3: The profile of power dissipation corresponding to surface and volume.

Region areas	Surface power dissipation (W/m^2)		Volume power dissipation (kW/m^3)	
	Without FGM	With FGM	Without FGM	With FGM
HV end fitting	17.95	13.32	37.26	26.64
Shank 1	8.89	4.73	17.79	9.27
Shank 2	3.37	2.59	6.76	5.21
Shank 3	9.48	5.09	18.72	10.26
Ground end fitting	17.63	12.18	35.27	24.36

6.5.3 IMPULSE PERFORMANCE

A further investigation of the field response of the microvaristor compound was carried out by simulating the insulator when energized with an impulse voltage. This computational simulation evaluated the behaviour of the non-linear grading material, which had a great influence on the insulator flashover performance. The applied impulse consisted of a 1.2/50 μs lightning surge, with energisation voltages of 160 kV and 110 kV, which were adopted from experimental studies [11] under dry and clean, and wet and polluted conditions. The Equation (6.6) represents the impulse voltage that adopted from [137];

$$V = V_o[\exp(-\alpha t) - exp(-\beta t)] \tag{6.6}$$

where α and β are constants of microsecond values.

Figure 6.15 and Figure 6.16 show the potential profile under dry and clean, and wet and polluted conditions along the insulator surface were calculated for three different time periods; before it reached the rise time (at 150 ns), during rise time (at 1.2 μs) and after the peak voltage fell to half value (at 50 μs). It can be clearly seen that the potential profile along the insulator surface changed significantly when the insulator was embedded with field grading material. The voltage increased to nearly 160 kV at 1.2 μs and decreased slowly to almost 80 kV at 50 μs, which is in accordance with theoretical expectations [137].

The maximum voltages during the different time periods showed small changes before and after the insulators were modified with field grading material. In contrast, the voltage profiles were modified when the test samples were energised at 110 kV under wet and polluted conditions as shown in Figure 6.16.

The maximum voltage increased significantly when the insulator was equipped with field grading material, compared to the insulator which was not equipped with grading, at 1.2 μs. A similar condition occurred at different times, being originally influenced by the pollution properties.

As the voltage rose with time, the electrical field increased according to the conduction stage of the field grading material $\boldsymbol{B}$ under different conditions as shown in Figure 6.15 and Figure 6.16. The observation was done at two time instants, when the peak voltage was evaluated at a low voltage level of 150 ns and when it was evaluated at a maximum voltage of 1.2 μs. In both graphs, the new instantaneous time was set to 650 ns, in order

to analyse fully the operation of the field grading material at the optimal field switching

threshold.
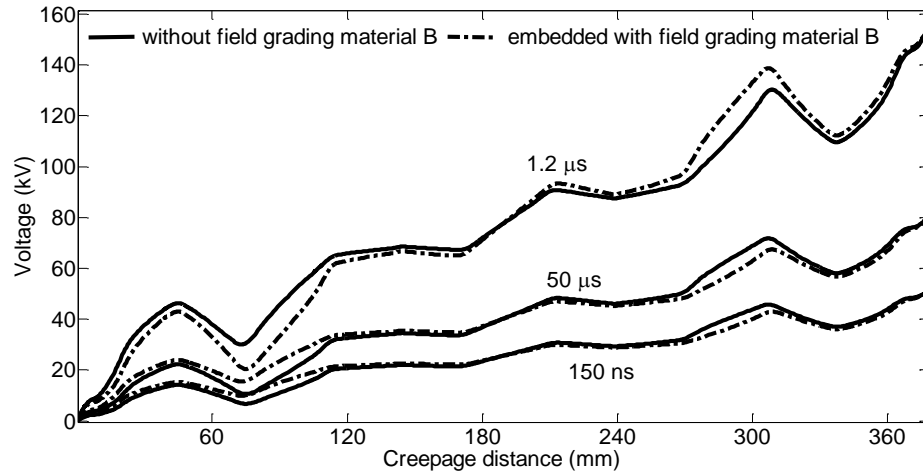
Figure 6.15: The profile of potential along the insulator surface under dry and clean conditions. Applied voltage 160 kV.
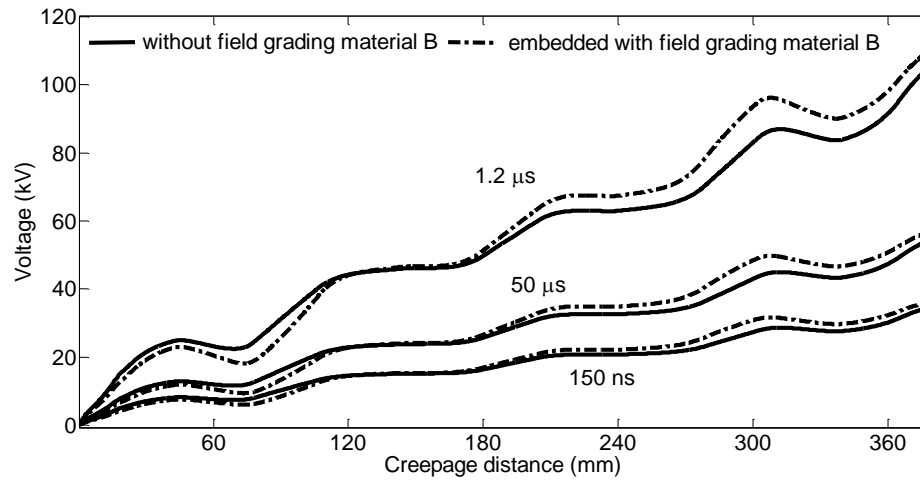
Figure 6.16: The profile of potential voltages along the insulator surface under wet and polluted conditions. Applied voltage 110 kV

According to the Figure 6.17 and Figure 6.18, the operation time at which field grading materials reached the threshold field under dry and clean, and wet and polluted conditions were different according to the energised voltage and environments. At 150 ns, in dry and clean conditions, the field grading material operated perfectly in the conduction regime that allowed the material to change its behaviour, from insulator to conductor. In contrast, the transition behaviour of field grading material *B* occurred at 650 ns when the insulator operated under wet and polluted conditions.

Meanwhile, the maximum voltage at 1.2 μs, for dry and clean conditions was 17.9 kV/cm at the high voltage terminal and 17.6 kV/cm at the ground terminal. The peak voltage was computed as 9.6 kV/cm at the high voltage terminal and 9.2 kV/cm at ground terminal, under wet and polluted conditions.
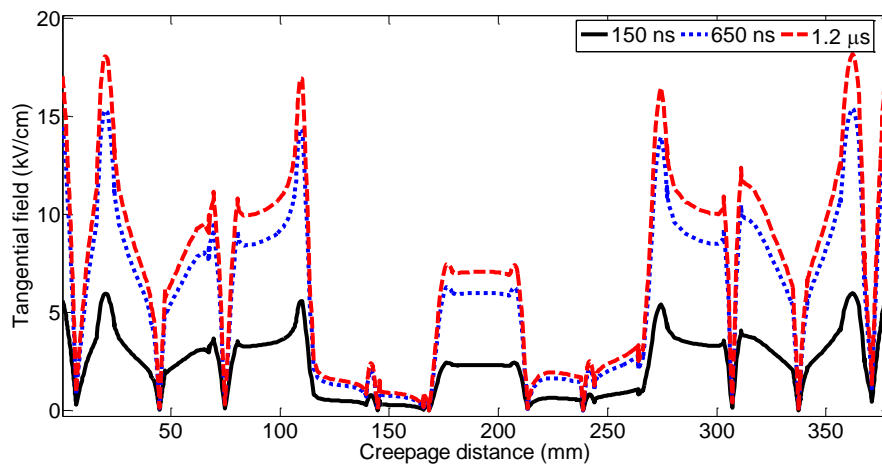
Figure 6.17: The tangential field of impulse response for microvaristor *B*-graded insulators with variable time instants under dry and clean.
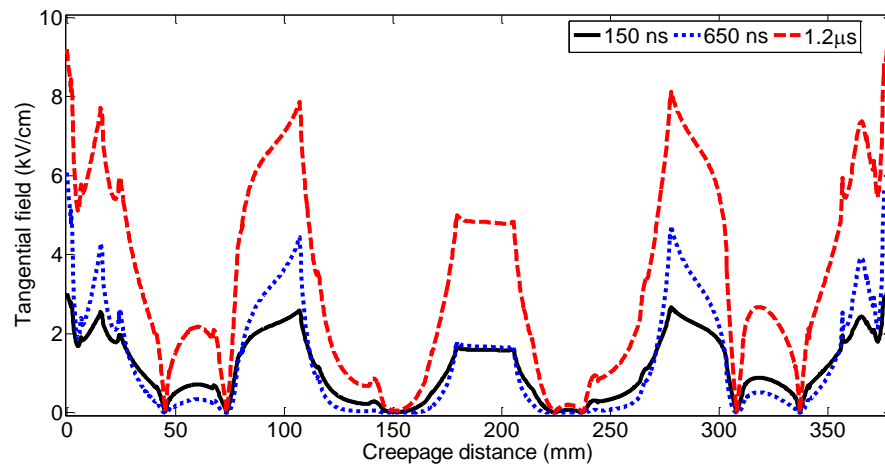
Figure 6.18: The tangential fields of impulse responses for microvaristor **B**-graded insulators with variable time instants under wet and polluted conditions.

A comparison of power dissipation profile for outdoor insulators when subjected to impulse voltage is depicted in Figure 6.19 and Figure 6.20. Table 6.4 shows the summary of the power measurement profile at different regions. The computations were taken for the cases with and without field grading material **B**. In this study, the time operation was set at 650 ns when the field grading material **B** was fully operated from an insulator to a conductor.

It is clearly seen the power was dissipated at high impulse voltage compared with the voltage levels at power frequency. This is due to high magnitude of electric field which acts on the microvaristors, affecting its non-linear operation. With the presence of field grading material, the power dissipation magnitudes particularly near the end fitting were successfully reduced.
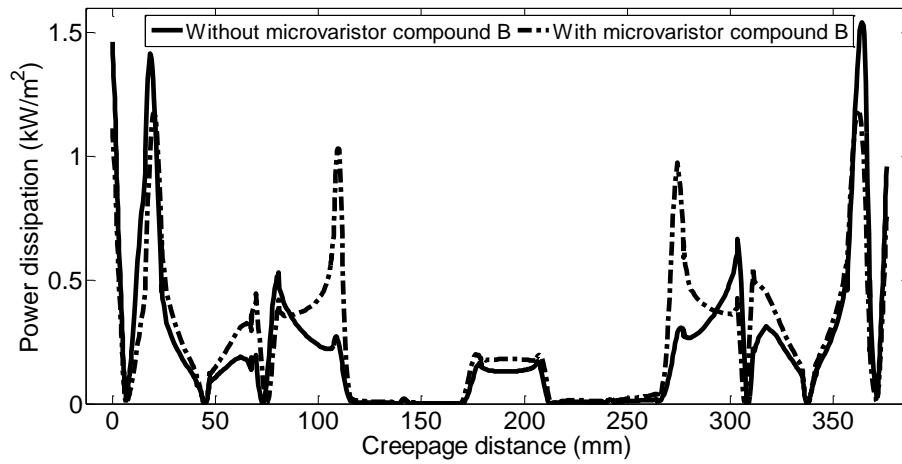
Figure 6.19: The measurement of power dissipation per unit area along the insulator surface under impulse energisations.
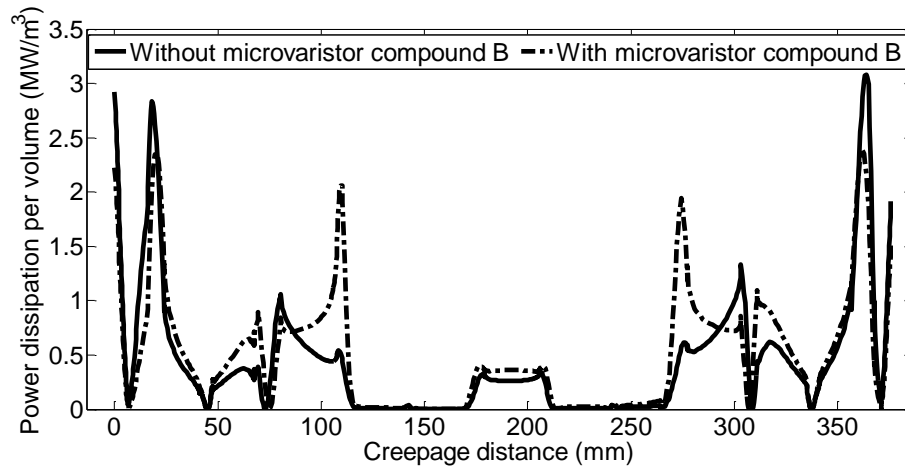
Figure 6.20: Power dissipation per unit volume occurring along the insulator surface under impulse energisation.

Table 6.4: The profile of power dissipation corresponding to surface and volume under impulse energisation.

Region areas	Surface power dissipation (kW/m^2)		Volume power dissipation (MW/m^3)	
	Without FGM	With FGM	Without FGM	With FGM
HV end fitting	1.46	1.11	2.92	2.23
Shank 1	0.53	1.03	1.06	2.06
Shank 2	0.17	0.19	0.36	0.37
Shank 3	0.67	0.97	1.33	1.95
Ground end fitting	0.96	0.76	1.92	1.53

It is important to note that there are additional effects that take place due to the introduction of field grading material. The power dissipation level from the end terminals were transferred to the adjacent shanks, thus would increase the power dissipation magnitudes at Shank 1, 2 and 3 correspondingly. Interestingly, there were minimal rise of power levels at middle shank (Shank 2) due to the introduction of a field grading material at middle shank compared to previous design concept [11].

6.6   CONCLUSIONS

The investigation of the performance of in-house field grading material was successfully performed using the finite element method by COMSOL Multiphysics ®. The 11 kV polymeric insulator was modelled by presenting its dimensions and material properties, and it was examined under different environmental conditions. The potential distribution along the insulator surface was measured and the tangential field was calculated accordingly. It was noticeable that a high field occurred at the triple regions in the area near to the end fittings.

In order to obtain a homogenous field distribution, a novel method was introduced of embedding the insulator with microvaristor compounds. The non-linear characteristics of compounds have been discussed in a previous chapter. The assessment of the field profile of the insulator led to the identification of the suitable electrical properties of the field grading material. The design of the field grading material has been presented. A combination of conical and cylindrical structures of field grading materials was

proposed for insertion in the FRP core. This design aims to improve upon the previous design and provide better field distribution along the insulator surface.

The effect of the implementation of field grading material has been investigated through comparative studies namely, with and without field grading material and when the insulator was subjected to dry and clean, wet and polluted under transient conditions. The results were promising, because the high field intensity near the terminals was greatly reduced, which is predicted to reduce the dry banding and discharge activities of composite insulators.

The heating performance along the polluted insulator was analysed. The calculation of power dissipations was presented. The high dissipated power, particularly near the end fittings, was reduced after the integration of field grading material, thus reducing the possibility of dry band formation.

Under transient systems, the field grading material successfully minimised the field enhancement within a short time and allowed the material to operate in the conduction regime. The material operated in the time scale of $150 - 650$ ns, at which time the grading material reached the conduction thresholds, corresponding to dry and clean and wet and polluted conditions. The results demonstrated that the electric field magnitudes were redistributed accordingly, when the voltage and time were increased significantly.

CHAPTER 7

GENERAL CONCLUSIONS AND RECOMMENDATIONS FOR FUTURE WORK

This thesis is aimed at obtaining a better understanding of field grading material based on ZnO microvaristors, specifically when used for controlling the field distribution in power system applications. The fabrication procedures of microvaristor filled with silicone rubber have been presented. The in-house field grading samples exhibit non–linear material properties during experimental tests. The results from the experimental investigations were used in computation modelling, in order to evaluate the effect of field grading material in real applications. An overview of the research work findings, the major conclusions which have been drawn and the suggested future research work is presented in the following sections.

7.1 GENERAL CONCLUSIONS

An extensive review of field grading material and the material composition has been presented. The review highlighted the importance of employing field grading material in high voltage equipment, particularly for controlling field distribution. Examples of field grading material have been presented, demonstrating their benefits and shortfalls. Field grading materials based on microvaristors exhibit excellent properties due to ZnO material being superior to non-linear voltage-current characteristics. A number of sub-topics have been covered, including the challenges of fabrication processes of field grading materials, degradation mechanisms on varistors based composite and modelling considerations.

The laboratory high voltage tests were conducted in accordance with BS EN 60060-1:2011 and BS EN 60060-2. Two different test cells to accommodate the test samples were specifically designed and fabricated in order to facilitate the testing of microvaristor powder and the grading compounds. Characterisation of the performance of field grading materials was established using AC, DC and impulse tests. New test techniques were proposed to achieve full characteristic of these highly non-linear materials. General procedures regarding safety requirements and test procedures were recommended.

A new fabrication procedure for field grading materials was developed independently in this work, which highlighted a number of critical processes that

need adopting such as heat treatment, mixing regimes, degassing, moulding and curing. More importantly, no chemical solvent was used in this proposed fabrication process. This fabrication techniques offers an alternative method to control the particle agglomeration in the compound which directly influences the electrical properties of the resulting field grading materials. The homogeneity of microvaristor particle distribution within the compound was achieved and had been verified through microscopic investigations.

A number of microscopic assessments were conducted on the microvaristor powders and compounds and these included a) Scanning Electron Microscopy (SEM), which was particularly used for microstructure analysis, b) X-ray Photoelectron Spectroscopy (XPS) which was used for elemental studies, and c) the Axio-Imager 2, which was used to obtain grain size distributions. The findings highlighted the different material properties obtained from two types of microvaristor powders; *A* and *B*. These results were exploited when investigating the influence of material properties on the electrical characteristics of compounds.

The current discrimination based Point-On-Wave (POW) technique was adopted in the AC tests. A similar R-C model was applied to represent the voltage and frequency dependent resistance and the capacitance of the intergranular layers which are responsible for the non-linear characteristics. This current discrimination analysis will extract the resistive current from the total leakage current. The behaviour of resistive current, I_r is worthy of note because it contributes to

degradation of material which will determine the long-term stability and aging of materials. Such approach allowed the detailed quantification of resistance values which will interpret the profile of resistivity, conductivity, and current density while the capacitance measurement will distinguish the relative permittivity in the tested samples.

By using this current characterisation technique, it has been found that the field grading compounds exhibited such non-linear behaviours at different applied voltages when 70 wt. % of microvaristors mixed with silicone rubber for sample size of 50 mm x 50 mm x 5 mm. This is the suitable filler concentration which allow the build-up of sufficient current paths in the compounds. On the other hand, the electrical properties of compounds at different thickness and microvaristor loading were attached in Appendix A.

The direct current (DC) was conducted in order to investigate the resistance profile of field grading materials as the charging current in AC analysis is masked by the resistive component. A DC power supply, WR series (Glassman) with a maximum voltage of 15 kV was used and connected to the test samples. The samples were subjected to a number of DC voltage levels until they reached the maximum voltage which was equal to the threshold voltage in the AC test. Any increment voltage beyond the threshold value will promote large resistive current to flow in the samples.

For high voltage impulse characterisation, three set of charging voltages were used, namely 6 kV, 8 kV and 10 kV. The impulse voltage source was obtained from single stage Ferranti impulse generator, with the maximum DC voltage of 55 kV. The non-linear behaviour of field grading materials were clearly seen at the different charging voltages. In this test, the capacitive effect was observed on the test samples when the charging voltage was set at a low level voltage of 6 kV. Meanwhile at 8 kV, both samples exhibited such voltage and current shape that operated in the ohmic region. On the other hand, a charging voltage level of 10 kV led to the initiation of puncture, which eventually caused damage to the test samples.

The application of in-house fabricated microvaristor composites in outdoor insulators was demonstrated through finite element modelling using COMSOL Multiphysics®. In this investigation, a case study was carried out on an 11 kV polymeric insulator. It was demonstrated that the polymeric insulator was susceptible to surface discharge due to non-uniform field distribution for both clean and polluted surface conditions. The comparative performance of the insulator was established under two main conditions; dry-clean and wet-polluted for the cases of standard insulator design and insulator with field grading material. In this computation analysis, it has been found that the highest normalized field at both end fittings were 5.9 kV/cm at ground terminal and 6.0 kV/cm at high voltage

terminal. Therefore, a field grading material with suitable field threshold is required to reduce the high magnitude of electric fields at the susceptible areas.

The field grading material, microvaristor *B* compound with the threshold point, $E_o = 6.0 \text{ kV/cm}$ was integrated into the insulator housing in the proposed design. The results were promising when the high magnitude of the electric field particularly near the end fittings were reduced with minimal heat effects at the middle shank. In dry condition, the magnitude of tangential field was improved from 2.37 kV/cm to 2.1 kV/cm at high voltage end fitting, and from 2.35 kV to 2.0 kV/cm at ground end fitting. Under wet and polluted condition, the tangential field was reduced significantly from 1.89 kV/cm to 1.63 kV/cm at high voltage end fitting, and from 1.87 kV/cm to 1.56 kV/cm at ground end fitting.

The power dissipation profile have shown a decrease of up to 35 % when using the field grading material. This result was encouraging in order to maintain the excellent electrical performance of polymeric insulators when subjected to wet and polluted environment.

7.2 FUTURE WORK

Based on the investigations in this field work, some further improvements have been identified:

a) It is necessary to examine the performance of the field grading materials under varying temperature conditions which will clearly define the non-linear characteristics of microvaristor compounds. The test cell should be redesigned and equipped with an additional controlled temperature facility.

b) The fabrication of large samples, made according to the proposed fabricated procedure, is necessary, in order to examine the performance of the insulator, after being embedded with field grading material. The insulator should be tested under pollution and transient conditions.

c) The investigation of the field grading material would be more interesting if both microvaristor compounds were deployed in different high voltage equipment according to the requirements of their electrical properties.

d) Modelling of the non-linear characteristics of the microvaristor compounds is a potential research area, which may enhance the performance of field grading materials. Comparative measurements need to be conducted and compared with the current experimental results.

e) The numerical modelling could become more realistic and can provide more information about insulator performance, by the development of 3D finite element modelling and by simulating the actual geometry of an 11 kV overhead line configuration.

REFERENCES

[1]   G. Momen and M. Farzaneh, "Survey of micro/nano filler use to improve silicone rubber for outdoor insulators", in Reviews on Advanced Materials Science, vol. 27, pp. 1–13, 2011.

[2]   B. Sonerud and K. Furuheim, "Field grading layer", US Patent App. 14/132, 351, 2013.

[3]   M. Matsuoka, "Nonohmic properties of zinc oxide ceramics", Japanese Journal of Applied Physics, vol. 736, 1971.

[4]   M. Hoidis, F. Greuter, L. Donzel and R. Kessler, "Microvaristor Based Overvoltage Protection", US Patent. Appl. 0045907 A1, 2009.

[5]   D. Weida, C. Richter and M. Clemens, "Design of cable accessories using ZnO microvaristor material based on FEM simulations", in IEEE International Power Modulator and High Voltage Conforence, Atlanta GA, pp. 94–97, 2010.

[6]   D. Weida, J. Nevoigt, H. Ye, M. Clemens, D. Stefanini and J. Seifert, "Effects of microvaristor material on the occurrence of partial discharges upon insulators in rain test", in IEEE International Power Modulator and High Voltage Conference, Atlanta, GA, pp. 497–500, 2010.

[7]   F. Greuter, M. Siegrist, P. Kluge-Weiss, R. Kessler, L. Donzel, R. Loitzl and H. J. Gramespacher, "Microvaristors: Functional Fillers for Novel Electroceramic Composites", in Journal of Electroceramics, vol. 13, no. 1–3, pp. 739–744, July 2004.

[8]   L. Donzel, T. Christen, R. Kessler, F. Greater and H. Gramespacher, "Silicone composites for HV applications based on microvaristors", in IEEE International Conference on Solid Dielectrics (ICSD), Toulouse, France, vol. 1, pp. 403–406, 2004.

[9]   L. Donzel, F. Greuter and T. Christen, "Nonlinear resistive electric field grading Part 2: Materials and applications", in Electrical Insulation Magazine, vol.27, no.2, pp.18-29, 2011.

[10]   E. Mårtensson, "Modelling electrical properties of composite materials",

Ph.D dissertation, Department of Electrical Engineering, Kungl Tekniska Högskolan, Stockholm, Sweden, 2003.

[11]   R. A. Rahman, "Investigations of ZnO Microvaristors For Stress Control on Polymeric Outdoor Insulators", Ph.D dissertation, School of Engineering, Cardiff University, United Kingdom, 2012.

[12]   J. Schulte-Fischedick, F. Lehretz, H. Denndorfer, J. Seifert, H. Ye, M. Clemens, J. Debus, V. Hinrichsen and M. Bornowski, "Electric field grading using insulators with microvaristor filled silicon rubber", in IEEE International Conference on Solid Dielectrics (ICSD), pp. 226–229, 2013.

[13]   L. Donzel, F. Greuter, and T. Christen, "Nonlinear resistive electric field grading Part 1: Theory and simulations", in Electrical Insulation Magazine, vol.26, no.6, pp.47-59, 2011.

[14]   X. Yang, J. He and J. Hu, "Tailoring the nonlinear conducting behavior of silicone composites by ZnO microvaristor fillers", in Journal Appied. Polymer. Science, vol. 132, no. 40, pp. 1–6, 2015.

[15]   J. Stolz, B.Gutheil and P.Weiß, "Microvaristor filled silicone elastomers − Advantages and restraints of principal adaptability", in 16th International Symposium on High Voltage Engineering, Innes House, Johannesburg, pp 1-6, 2009.

[16]   H. Ye, "Application of Non-Linear Microvaristor-Filled Materials in High Voltage Devices and Algorithmic Optimization of High-Voltage Simulations Based on Surrogate Models", Ph.D dissertation, Bergische Universitat Wuppertal, 2015.

[17]   N. M. Jordan, Y. Y. Lau, D. M. French, R. M. Gilgenbach and P. Pengvanich, "Electron emission near a triple point", in IEEE International Power Modulators and High Voltage Conference, Las Vegas, NE, pp. 311, May 2008.

[18]   E. A. Cherney, "50 Years in the Development of Polymer Suspension-Type Insulators", in IEEE Electrical Insulation Magazine, vol.29, issue.3, pp.18-26, 2013.

[19]   S. Bian, "A Study of the Material Properties of Silicone Nanocomposites Developed by Electrospinning", Ph.D dissertation, Department of Nanotechnology Engineering, University of Waterloo, Waterloo, Canada, 2013.

[20] K. Y. Lau, "Structure and Electrical Properties of Silica-based Polyethylene Nanocomposites", Ph.D. dissertation, Faculty of Physical Sciences and Engineering, University of Southampton, Southampton, UK, 2013.

[21] B. Gunasekaran and P. Nirgude, "Optimization of grading rings for post insulators used in EHV/UHV transmission system", in 10th International Conference Properties and Applications of Dielectric Materias (ICPADM), Bangalore, pp. 1–4, 2012.

[22] "3FL Silicone Long Rod Insulators for Distribution and Transmission Overhead Power Lines – performance meets durability", Siemens AG, Energy Sector, Freyeslebenstrasse 1, 91058 Erlangen, Germany, 2012.

[23] A. Phillips, J. Kuffel and A. Baker, "Electric fields on AC composite transmission line insulators", in IEEE Transactions on Power Delivery, vol. 23, no. 2, pp. 823–830, 2008.

[24] R. Strobl, W. Haverkamp, G. Malin and F. Fitzgerald, "Evolution of stress control systems in medium voltage cable accessories", in IEEE/PES Conference and Exposition Transmission and Distribution, Atlanta, GA, vol.2, pp. 843–848, 2001.

[25] George V.Greshnyakov, Simon D.Dubitskiy and Nikolay V.Korovkin, "Capacitance And Impedance Methods of Electric Field Grading In Cable Joint And Terminations", in Energy, Environment And Materials, pp 95-99, 2014.

[26] Önneby et.al, "Field Grading Material", US Patent, No 7868079, Jan 2011.

[27] R. E. Newnham, "Smart,very smart and intelligent materials", in MRS Bulletin, vol.18, issue 4, pp. 24–26, published by Cambridge University, 1993.

[28] J. Pitha, "Non-linear resistance material", US Patent, No 3,291,759, pp. 1–3, 1966.

[29] A. Napierala, "Electrical behaviour of conducting current silicon rubber under short high current stress", in 9th International Conference on Environment and Electrical Engineering (EEEIC), pp. 459-460, 16-19 May 2010.

[30] E. Mårtensson, B.Nettelbled, U.Gafvert and L.Palmqvist, "Electrical Properties of Field Grading Materials With Silicon Carbide and Carbon Black", in 6th International Conference on Conduction Breakdown in Solid

Dielectric, Vasteras, pp. 548–552, 1998.

[31] S. M. Lebedev, O. S. Gefle and A. E. Strizhkov, "Novel polymeric composites with nonlinear current-voltage characteristic", in IEEE Transactions on Dielectrics and Electrical Insulation, vol. 20, no.1, pp. 289–295, Feb. 2013.

[32] W. T. Starr, "Polymeric outdoor insulation", in IEEE Transaction on Electrical Insulation, vol. 25, no. 1, pp. 125–136, 1990.

[33] S. Ishibe, M. Mori, M. Kozako and M. Hikita, "A New Concept Varistor With Epoxy/Microvaristor Composite", in IEEE Transactions on Power Delivery, vol.29, no. 2, pp.677-682, 2013.

[34] A. Haddad and P. Naylor, "Finite-element computation of capacitance networks in multiple-electrode systems: application to ZnO surge arresters", in IEE Proceeding - Science Measurement and Technology, vol.145, issue 4 pp. 129–135, July 1998.

[35] D. Warne and A.Haddad, Advances in High Voltage Engineering. The Institution of Electrical Engineers, London, 2004.

[34] T.K.Gupta, " Application of Zinc Oxide Varistors", in Journal of the American Ceramic Society, part 7, vol.73, pp.1817-1840, 1990.

[36] "Physical properties of zinc oxide varistors : Manufacturing of zinc oxide varistors", ABB Power Technology Products Surge Arresters, Ludvika, Sweden.

[37] A. S. Tonkoshkur, A. B. Glot and A. V. Ivanchenko, "Percolation effects in dc degradation of ZnO varistors", in Journal of Advanced Dielectrics, vol. 5, 2015.

[38] T. K. Gupta, "Microstructural engineering through donor and acceptor doping in the grain and grain boundary of a polycrystalline semiconducting ceramic", in Journal of Materials Research, vol. 7, no. 12, pp. 3280–3295, 1992.

[39] L. M. Levinson and H. R. Philipp, "The physics of metal oxide varistors", in Journal Applied Physics, vol. 46, no. 3, 1975.

[40] K. Eda, "Zinc Oxide Varistors", in IEEE Electrical Insulation Magazine, vol. 5, no. 6, pp. 28–30, 1989.

[41] J. Glatz.-Reichenbach, B.Meyer R. Strümpler, P. Kluge-Weiss and F.

Greuter, "New low-voltage varistor composites", in Journal of Materials Science, vol. 31, no. 22, pp. 5941–5944, November 1996.

[42] Maureen A.Boyle, C.J Martin and J. Neuner, "Epoxy Resins", ASM Handbook vol. 21, pp. 78–89, 2001.

[43] X. Yang, H. Kim, L. Yang, C. Cheng, and Y. Zhao, "Composite varistors based on epoxy resin/$La_{0.8}Sr_{0.2}Mn0_3$", in Journal of Composite Materials, 2013.

[44] D. Komesu, M. Mori, and S. Ishibe, "Simulation on the formation of microvaristor chains in liquid epoxy resin under electric field," in Conference of Electrical Insulation and Dielectric Phenomena (CEIDP), pp. 691–694, 2014.

[45] Seminar on adhesives : About epoxy resins [Online]. Available: https://www.threebond.co.jp/en/technical/seminar/epoxy.html, retrieved on 10th January 2014.

[46] J. M. Seifert, "New Concepts in Voltage Grading", INMR Transmission and Distribution, 2015. [Online]. Available: http://www.inmr.com/new-concepts-voltage-grading/, retrieved on 9th September 2015.

[47] Chemical structure. [Online]. Available : https://www.wacker.com/cms/media/publications/download/6709_EN.pdf, retrieved on 10th October 2013.

[48] J. Debus, V. Hinrichsen, J. M. Seifert, and M. Hagemeister, "Investigation of composite insulators with microvaristor filled silicone rubber components", in 10th IEEE International Conference on Solid Dielectrics, pp. 1–4,2010.

[49] R. Abd-Rahman, A. Haddad, N. Harid, and H. Griffiths, "Stress control on polymeric outdoor insulators using Zinc oxide microvaristor composites", IEEE Transaction on Dielectric Electrical Insulation, vol. 19, no. 2, pp. 705–713, April 2012.

[50] Laboratory mixer: Technical information. [Online]. Available: http://www.silverson.co.uk/en/products/laboratory-mixers/technical-information, retrieved on 6th June 2014.

[51] D. Weida, C. Richter, and M. Clemens, "Design of ZnO microvaristor material stress-cone for cable accessories", IEEE Transaction on Dielectrics Electrical Insulation, vol. 18, no. 4, pp. 1262–1267, August 2011.

[52]   N. H. Haddad, A, Rahisham Abd Rahman, "Performance of nonlinear grading coating on polymeric outdoor", in 21st International Conference on Electricity Distribution (CIRED), no.1276, Franfurt, Germany, 6-9 June 2011.

[53]   H. Ahmad, A. Haddad, H. Griffiths, S. Robson, T. Nishimura, and N. Tsukamoto, "Electrical characterisation of ZnO microvaristor materials and compounds", in 2015 IEEE Conference on Electrical Insulation and Dielectric Phenomena (CEIDP), Ann Arbor, Michigan, pp. 688–692, October 2015.

[54]   H. Ahmad, A. Haddad, H. Griffiths and S. Robson, "Electrical properties of field grading material", in 19th International Symposium on High Voltage Engineering (ISH), Pilsen, Czech Republic, August 2015.

[55]   D. Ryan and R.Allen Bernstorf, "Silicone Compounds for High-Voltage Insulators : Compounding Silicone Rubber", in Hubbel Power System, Inc, pp 1-8, 2007.

[56]   I. Ramirez, E. A. Cherney, S. Jarayam, and C. Palmira, "Comparison of the Erosion Resistance of Silicone Rubber and EPDM Composites Filled with Micro Silica and ATH", in IEEE Transactions on Dielectrics and Electrical Insulation, vol.19, no.1 pp. 218–224, February 2012.

[57]   Silicone Rubber ABB, Product Information 275051-131,2005-05-15. [Online].
Available:https://library.e.abb.com/public/b8f9ec30d6f91ec1c1256ffe004b
d405/2750%20515-131%20en%20Rev%201.pdf, retrieved on 3rd August 2014.

[58]   H. Matsuzaki, T. Nakano, and H. Ando, "Effects of second particles on nonlinear resistance properties of microvaristor-filled composites", in IEEE Conference on Electrical Insulation and Dielectric Phenomena (CEIDP), pp. 183–186, October 2012.

[59]   M. Reading, Z. Xu, A.S Vaughan, and P. L. Lewin, "On sample preparation and dielectric breakdown in nanostructured epoxy resins", in Journal of Physics, vol. 310, 2011.

[60]   L. F. Nielsen, "Composite Materials", published by Springer Berlin Heidelberg, 2005.

[61]   F. Ikazaki, A. Kawai, K. Uchida, T. Kawakami, K. Edamura, K. Sakurai, H. Anzai and Y. Asako, "Mechanisms of electrorheology: the effect of the

dielectric property", in Journal of Applied Physics, vol. 31, no. 3, pp. 336–347, 1999.

[62]   W. Wen, X. Huang and P. Sheng, "Electrorheological fluids: structures and mechanisms", in Journal for Royal Society of Chemistry, vol. 4, pp. 200–210, 2008.

[63]   I. Ramirez, E. A. Cherney, S. Jayaram, M. Gauthier and C. Palmira, "Nanofilled Silicone Dielectrics Prepared with Surfactant for Outdoor Insulation Applications", in IEEE Transactions on Dielectrics and Electrical Insulation, vol.5, no.1, pp. 228–235, 2008.

[64]   H. Matsuzaki, T. Nakano, H. Ando, and M. Takei, "Electrical properties of composite material containing microvaristor and semi-conductive whisker," in International Symposium on Electrical Insulating Materials, pp. 295–298, 2014

[65]   G. F. Robert Smith-Johannsen, "Silicone rubber compositions with heat-pre-treated fillers and silicate curing agents", US Patent, number US3325440, 13 June 1967.

[66]   V.K. V.N Morozov, G.A Voloskov, L.A Gorbanova, Yu.S.Zaitsev and V.V Kovriga, "Effect of heat treatment on the distribution of residual stresses and properties of epoxy polymers", in Journal of Mechanics Composite Material, vol. 22, no. 5, pp. 535–538, 1987.

[67]   T. Tada, "Degradation of ZnO varistors as estimated by aging tests", in Journal of Electrical Engineering Japan, vol. 170, no. 2, pp. 1–18, 2010.

[68]   A. Vicaud, "A.C. Voltage Aging of Zinc-Oxide Ceramics", in IEEE Power Engineering Review, vol. PER-6, no.4, pp. 30-30, April 1986.

[69]   K. L. Chrzan and Z. Wróblewski, "Degradation and destruction of ZnO varistors caused by current pulses", in International Conference on Advances in Processing, Testing and Application of Dielectric Materials, pp.217-220, 2001.

[70]   C. G. Shirley and W. M. Paulson, "The pulse-degradation characteristic of ZnO varistors", in Journal Applied Physics, vol. 50, no. 9, pp. 5782–5789, 1979.

[71]   J. Bak-Jensen, B. Bak-Jensen, S. Damsgaard Mikkelsen and J.Tolstrup Sørenson,"Examinations of ZnO varistors in the leakage region with regard to high frequency stresses", in 5th European Conference on Power

Electronics and Applications, vol.8, pp. 191-196, 13-16 September 1993.

[72] X. Zhao, J. Li and S. Li, "DC Degradation of ZnO Varistor and Its Restorability by Heat-Treatment", in International Conference on Condition Monitoring and Diagnosis, Bali, Indonesia, pp. 1093-1096, September 2012.

[73] H.Kawamura and M.Nawata, "Influence of dc pre-stress on electrical and dielectric properties of zinc oxide ceramics", in 11th International Symposium on High Voltage Engineering, vol.2, pp. 325–328, 1999.

[74] A.Kheirman and M .Leijon , " Continous On-Line Partial Discharge Monitoring of Power Generators'', in Conference on Electrical Insulation and Dielectric Phenomena (CEIDP), San Francisco, Oct 20-23,1996.

[75] J. Lundquist, L.Stenström, A.Schei and B.Hansen , "New method for measurement of the resistive leakage currents of metal-oxide surge arresters in service", in IEEE Transactions on Power Delivery, vol. 5, no. 4, pp. 1811–1822, 1990.

[76] X. Yan, Y. Wen and X. Yi, "Study on the resistive leakage current characteristic of MOV surge arresters", in IEEE/PES Conference and Exhibition of Transmission and Distribution, vol. 2, pp. 683–687, 2002.

[77] A. Novizon, Zulkurnain Abdul Malek, Nouruddeen BAshir, "A new method to extract the resistive component of the metal oxide surge arrester leakage current", in 2nd IEEE International Conference on Power and Energy, pp. 399–402, 2008.

[78] Z. Abdul-Malek, N. Yusoff, M. Fairouz and M. Yousof, "Field experience on surge arrester condition monitoring - modified shifted current method", in 45th International Universities Power Engineering Conference (UPEC), pp. 1-5, 2010.

[79] R. Omranipour and S. Haq, "Evaluation of grading system of large motors AC stator windings," in IEEE International Symposium on Electrical Insulation (ISEI),Vancouver,BC, pp. 158–161, 2008.

[80] D. I. Kovalev, "Calculation of electric fields in electrical high-voltage equipment", in Journal of Russian Electrical Engineering, vol. 86, no. 10, pp. 579–582, December 2015.

[81] D. Weida, "Electro-Quasistatic High-Voltage Field Simulations of Insulator Structures Covered with Thin Resistive Pollution or Nonlinear Grading Material", in IEEE International Power Modulators and High Voltage

Conference, Las Vegas, NE, pp. 580–583, 2008.

[82]   D. Stefanini and J. Seifert, "Three dimensional FEM electrical field calculations for EHV composite insulator strings," in IEEE International Power Modulators and High Voltage Conference, Atlanta,GA,pp. 238–241, 2010.

[83]   F. Tighilt, A.Bayadi and A.Haddad "Voltage Distribution on ZnO Polymeric Arrester Under Pollution Conditions," in 45th International Universities Power Engineering Conference (UPEC), Cardiff, Wales, pp 1-5,2010.

[84]   S. Ilhan, A. Ozdemir, S. H. Jayaram and E. A. Cherney, "AC and Transient Electric Field Distributions along a 380 kV V-String Insulator", in IEEE International Symposium on Electrical Insulation, pp. 399–403, 2012.

[85]   J. Rivenc, S. Dinculescu and T. Lebey, "Suitable properties of stress grading materials", in 11th Symposium on High Voltage Engineering (ISH), London, pp. 22–25, 1999.

[86]   N. Li and Z. Peng, "Modeling of electric stress control in HV bushing using field grading material", in IEEE Conference on Electrical Insulation and Dielectric Phenomena (CEIDP), Des Moines, no. 1, pp. 550–553, 2014.

[87]   M. L. Clingerman, "Development and Modelling of Electrically Conductive Composite Materials", Ph.D dissertation, Chemical Engineering Department, Michigan Technological University, 2001.

[88]   M.Khalifa, " High Voltage Engineering Theory and Practice", published by Marel Dekker,Inc (New York and Basel), 1990.

[89]   E. Al Murawwi and A. El-Hag, "Corona ring design for a 400 kV non-ceramic insulator", in 2nd International Conference on Electric Power and Energy Conversion Systems (EPECS), pp. 1–4, November 2011.

[90]   B. F. Hampton, "Flashover mechanism of polluted insulation", in Proceeding of The Institution of Electrical Engineers, vol.111, no.5, pp. 985–990, May 1964.

[91]   L. L. Alston and S. Zoledziowski, "Growth of discharges on polluted insulation", in Proceedings of the Institution of Electrical Engineers, vol. 110, no. 7, pp. 1260–1266, 1963.

[92]   R. Waters, A. Haddad, H. Griffiths, N. Harid, P. Charalampidis and P. Sarkar, "Dry-band discharges on polluted silicone rubber insulation: control

and characterization", in IEEE Transactions on Dielectric Electrical Insulation, vol. 18, no. 6, pp. 1995–2003, December 2011.

[93] B. Boettcher, G. Malin and R. Strobl, "Stress control system for composite insulators based on ZnO-technology", in IEEE/PES Transmission and Distribution Conference and Exposition, Atlanta, vol. 2, pp. 776–780, 2001.

[94] D. Clark, "Exported Potentials and Profiles Around Earth Electrodes and Opposite Side Injection for Large-Area Earthing Systems", Advanced High Voltage Engineering Research Centre, Cardiff School of Engineering, January 2014.

[95] C. Spellman, "A Technique for on-Line Monitoring of ZnO Surge Arrester", 10th International Symposium on High Voltage Engineering (ISH),Canada, 1997.

[96] E. Kuffel, W. S. Zaengl and J. Kuffel, "High Voltage Engineering Fundamentals", 2nd edition, published by Butterworth-Heinemann, 2000.

[97] E. Dokur, "Matlab GUI based data acquisition and processing of lightning impulse voltages", in International Conference on High Voltage Engineering and Application (ICHVE), Poznan, Poland, pp.1-4, September 2014.

[98] Bahruji.H, "Photocatalytic reforming of oxygenates on Pd/TiOs catalysts", Ph.D dissertation, School of Chemistry, Cardiff University, 2011.

[99] Paul Van der Heide, "X-ray photoelectron spectroscopy an introduction to principles and practices", published by John Wiley & Sons, 2012.

[100] Axio Observer Inverted Microscope for Materials Research [Online]. Available:http://www.zeiss.com/microscopy/en_de/products/light-microscopes/axio-observer-for-materials.html, retrieved by 14th December 2014.

[101] H. Gramespacher, L. Donzel, T. Christen and F. Greuter, "Microvaristor based field grading elements for HV terminations", in 13th International Symposium on High Voltage Engineering (ISH), Delft, Netherlands, 2003.

[102] L. Saint Macary, M. L. Kahn, C. Estournès, P. Fau, D. F. Flash, D. Trémouilles, M. Bafleur, P. Renaud and B. Chaudret, "Size effect on properties of varistors made from zinc oxide nanoparticles through low temperature spark plasma sintering", in Journal of Advanced Functional Materials, vol. 19, no. 11, pp. 1775–1783, 2009.

[103] M-S Wang, S-H Oh, C-B Park, " Effect of thermal distribution for ZnO nano powder Bi-based varistors", in IEEE Conference of Nanotechnology Materials and Devices (NMDC), 22-25 October 2006.

[104] J. E. White and L. Jackson, "Polymer microfiller composites", US Patent, No. US 2010/0137478 A1, 2010.

[105] M. Bumiller, "Dispersing Powders in Liquid", HORIBA, 2013, [Online]. Available:http://www.horiba.com/fileadmin/uploads/Scientific/Documents/ PSA/Webinar_Slides/TR016.pdf, retrieved by 1st June 2014.

[106] J. E. White, H. Parvatareddy, F.Achille, Leonardo C.Lopez, Rudolf J.Koopmans, Rene Broos, Scott T.Matteucci and Steven R.Lakso, "Polymer microfiller composites", US Patent, number 12 623 316, 17th December 2013.

[107] Donald R.Askeland, "The science and engineering of materials", 3rd edition published by Chapman & Hall, 1996.

[108] M. Sumita, K. Sakata, S. Asai, K. Miyasaka and H. Nakagawa, "Dispersion of fillers and the electrical-conductivity of polymer blends filled with carbon-black", in Polymer Bulletin, vol. 25, no. 2, pp. 265–271, February 1991.

[109] P. V. B. Pulickel M.Ajayan and Linda S.Schadler, "Nanocomposite science and technology", 1st edition, published by Wiley-VCH, 2004.

[110] A. B. Balashov, N. P. Golubeva and B. S. Skidan, "Oxide Zinc Ceramics for Varistor", in Journal for Glass and Ceramics, vol. 56, pp. 58-60, January 1999.

[111] N. K. Reddy, K. B. Reddy, and V. N. Mulay, "Synthesis of zinc oxide varistors with bismuth oxide additive by the sol-gel route", in Journal of Materials Science Letters, vol. 18, no. 14, pp. 1167–1169, 1999.

[112] Relva C.Buchanan, "Ceramic Materials for Electronics", 3rd edition, published by New York: CRC Press, 2004.

[113] R. R. Patel, N. Gupta and S. Basu, "A quantitative method for characterising dispersion in nanocomposites", in Journal of Nanostructured Polymers and Nanocomposites, vol. 9, no. 4, pp. 108–113, 2014.

[114] F. Greuter and G. Blatter, "Electrical properties of grain boundaries in polycrystalline compound semiconductors," in Semiconductor Science and

Technology, vol. 5, no. 2, 1990.

[115] K. Mukae, K. Tsuda and I. Nagasawa, "Capacitance-vs-voltage characteristics of ZnO varistors", in Journal of Applied Physics, vol. 50, no. 6, p. 4475, 1979.

[116] K. Eda, "Transient conduction phenomena in non-ohmic zinc oxide ceramics", in Journal of Applied Physics, vol. 50, no. 6, p. 4436, 1979.

[117] C.Dang, T. M. Parnell and P. J. Price, "The Response of Metal Oxide Surge Arresters to Steep Fronted Current Impulses", in IEEE Transactions on Power Delivery, vol.1, no.1, pp 157-163, January 1986.

[118] W.Schmidt, J.Meppelink, B.Richter, K.Feser, L.E Kehl and D.Qui, "Behavior of MO-surge arrester blocks for fast transients", in IEEE Transactions on Power Delivery, vol.4, issue.1, pp.292-300, January 1989.

[119] A.Haddad, P.Naylor, I.A.Metwally, D.M.German and R.T Waters, "An improved non-inductive impulse voltage measurement technique for ZnO surge arresters", in IEEE Transactions on Power Delivery, vol.10, no.2, pp.778-785, April 1995.

[120] H.Fan and D.B Miller, "Transition of MOV distribution arresters from capacitive to resistive during steep-front impulse", in IEEE International Symposium on Electrical Insulation, pp. 452–455, 7-10 June 1992.

[121] L. P. Carina Onneby, Eva Martensson, Uno Gafvert and Anders Gustafsson, "Electrical properties of field grading materials influenced by the silicon carbide size", in 7th International Conference on Solid Dielectrics, pp.43–45,2001

[122] F.Schmuck, J.Seifert, I.Gutman and A.Pigini, "Assesment of the condition of overhead line composite insulators", B2-214 CIGRE 2012.

[123] D.A.Swift, "Insulators for outdoor applications," in Advances in High Voltage Engineering, pp. 257, 2004.

[124] C. Spellman, A.Haddad, A.R.Rowlands and H.M. Young, "Survey of polymeric insulator ageing factors", in 11th International Symposium on High Voltage Engineering (ISH), London, vol.4, no.467, pp.160-163, 1999.

[125] A. Phillips, "Electric Field Distribution and their Impact on Transmission Line Composite Insulators", in IEEE Transmission and Distribution Conference and Exposition, Orlando, FL, pp. 1-3, 7-10 May 2012.

[126] S. M. Gubanski, "Outdoor Polymeric Insulators : Role of Corona in Performance of Silicone Rubber Housings", in Conference on Electrical Insulation and Dielectric Phenomena (CEIDP), Michigan,USA, pp. 1–9,2015.

[127] F. Aouabed, B.Abdelhafid, S.Satta and B.Rabeh, "Conductivity Effect On The Flashover Voltage Of Polluted Polymeric Insulator Under AC Voltage", in Universities Power Engineering Conference (UPEC), 31st August-3rd September 2010.

[128] R. Hernanz, A. José, C. Martín, J. José, M. Gogeascoechea and Z. Belver, "Insulator pollution in transmission lines", in International Conference on Renewable Energies and Power Quality (ICREPQ), 2006.

[129] Y.Khan, "Degradation of High Voltage Polymeric Insulators in Arid Desert ' s Simulated Environmental Conditions", in American Journal of Engineering and Applied Sciences, vol. 2, no. 2, pp. 438–445, 2009.

[130] S. A. Sebo and W.Que, "Electric field and potential distributions along dry and clean non-ceramic insulators", in Conference of Electrical Insulation and Electrical Manufacturing (Cat. No.01CH37264), pp. 437–440, 2001.

[131] C. Muniraj and S. Chandrasekar, "Finite Element Modeling for Electric Field and Voltage Distribution along the Polluted Polymeric Insulator", in World Journal of Modelling and Simulation, vol. 8, no. 4, pp. 310–320, 2012.

[132] Introduction to COMSOL Multiphysics [Online]. Available: https://cdn.comsol.com/documentation/5.2.1.262/IntroductionToCOMSOL Multiphysics.pdf, retrieved by July 2013.

[133] H. Cho and U. Lee, "Electrical properties of polymer insulator with end-fitting design", in IEEE International Symposium on Electrical Insulation, Indianapolis, USA, pp. 296–299, 19-22 September,2004.

[134] D. Weida, J. Nevoigt, M. Clemens, D.- Wuppertal, D. Stefanini and J. Seifert, "Effects of Microvaristor Material on the Occurrence of Partial Discharges upon Insulators in Rain Test", in IEEE International Power Modulator and High Voltage Conference (IPMHVC), pp. 505–508, 23rd -27th May 2010.

[135] Arshad, A.Nekahi, S.G. McMeekin and M.Farzaneh, "Effect of Dry Band Location on Electric Field Distribution along a Polymeric Insulator under Contaminated Conditions", in 50th International Universities Power Engineering Conference (UPEC), Stoke on Trent,UK, pp.1-4, 2015.

[136] M. Albano, R. T. Waters, P. Charalampidis, H. Griffiths, and A. Haddad, "Infrared analysis of dry-band flashover of silicone rubber insulators", in IEEE Transaction on Dielectric Electrical Insulation, vol. 23, no. 1, pp. 304–310, 2016.

[137] V. K. Naidu, M S, " High Voltage Engineering" 3rd edition, published by Tata McGraw-Hill Education, 2004.

a) 1 mm sample
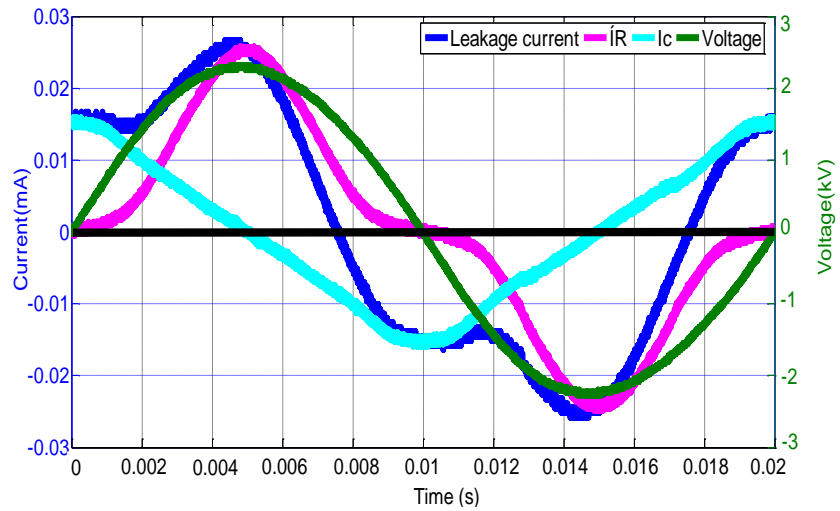
A-1: The voltage and current waveform of 1 mm microvaristor filled with silicone rubber at 60 wt. %.
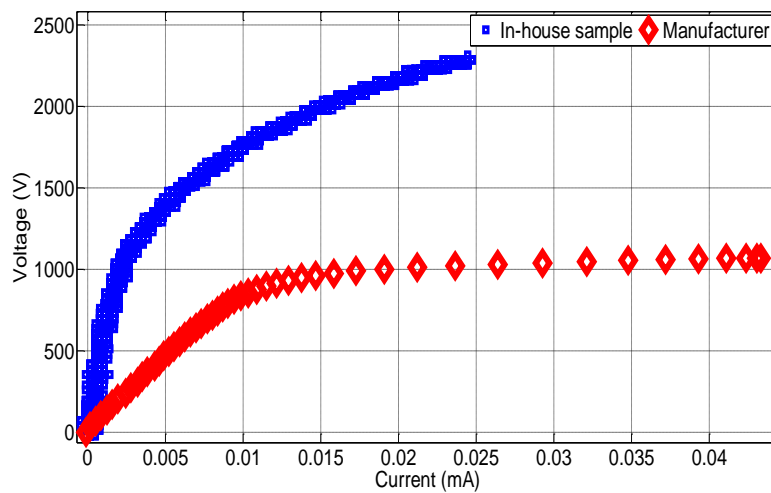

A-2: The comparative V-I characteristics of 60 wt. % of in-house field grading layer and the manufacturer's sample.

b) 5 mm sample at different microvaristor loadings
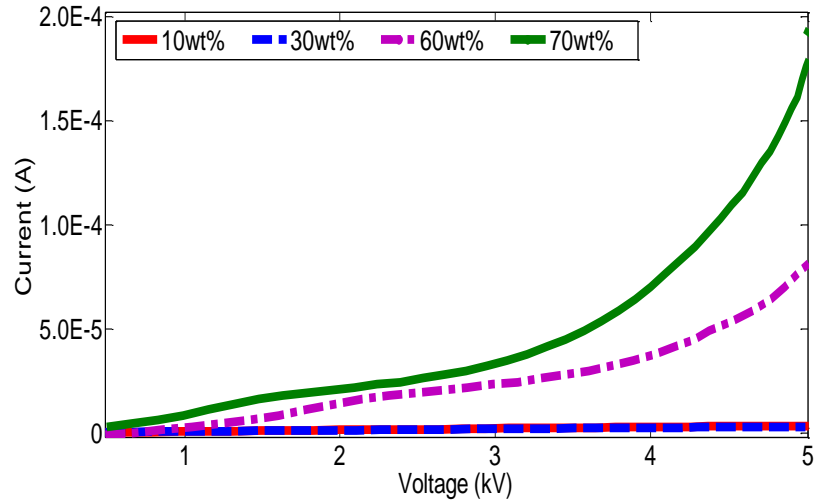
A-3: The voltage and current profiles at different microvaristor loadings in the composite samples.
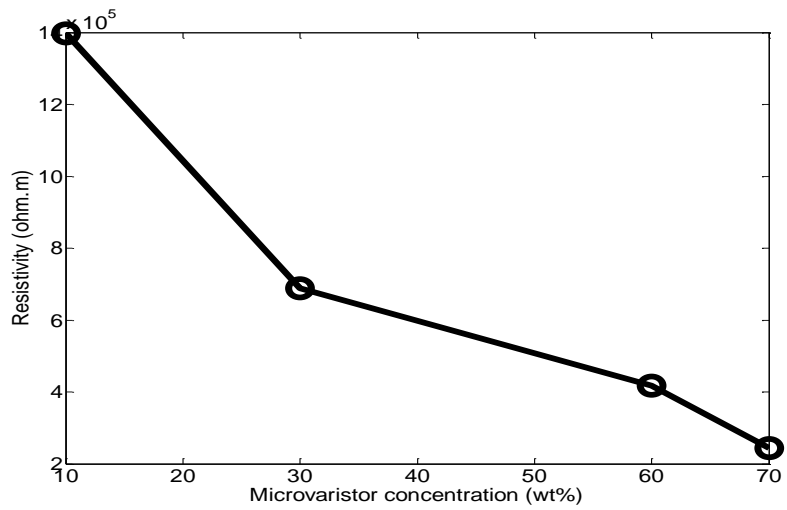
A-4: The resistivity of silicone rubber filled with microvaristor against filler concentrations at 10 kV/cm.
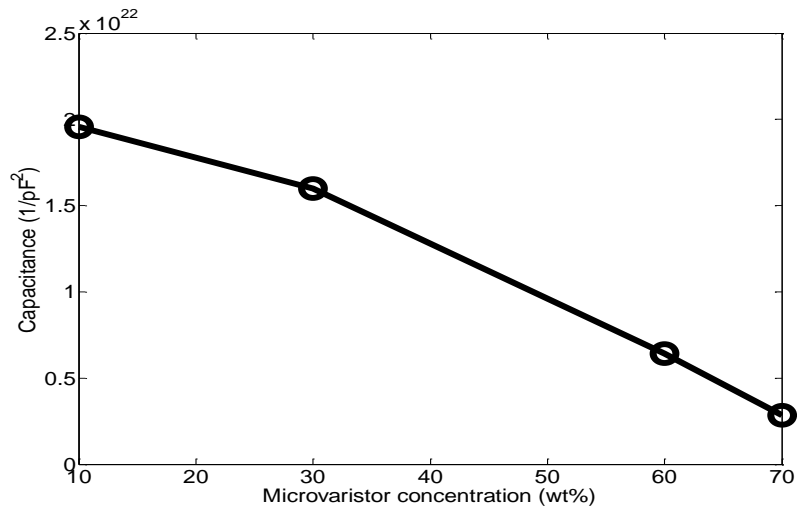
A-5: The capacitance profile against different microvaristor loadings at 10 kV/cm.
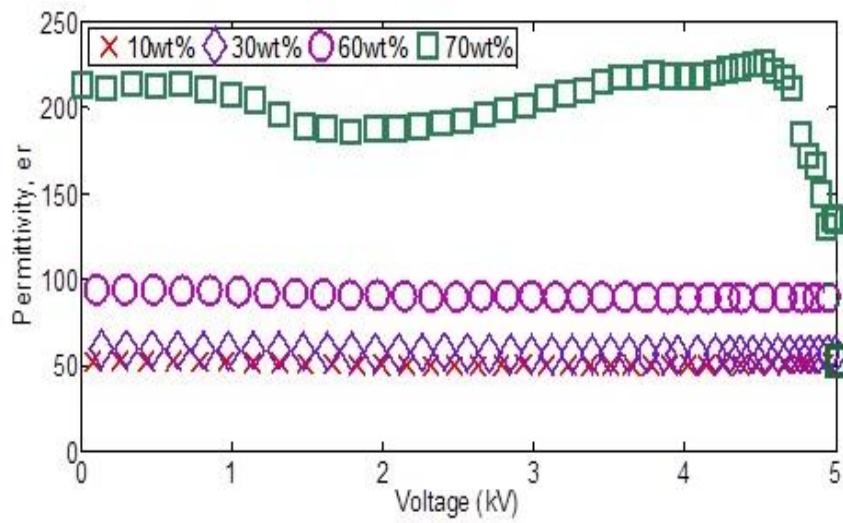
A-6: Relative permittivity as a function of voltages applied when all samples reached 10 kV/cm.

Appendix B

Mathematical equations

$$Resistivity, \rho\,(\Omega.m) = \frac{Resistance \; x \; A}{d}$$

$$Relative \; permittivity, \varepsilon_r = \frac{d \; x \; Capacitance}{\varepsilon_o \; x \; A}$$

$$Current \; density, J \; (A/cm^2) = \frac{Resistive \; current, I_r}{A}$$

$$Conductivity \, , \sigma \, (S/m) = \frac{1}{Resistivity, \rho}$$
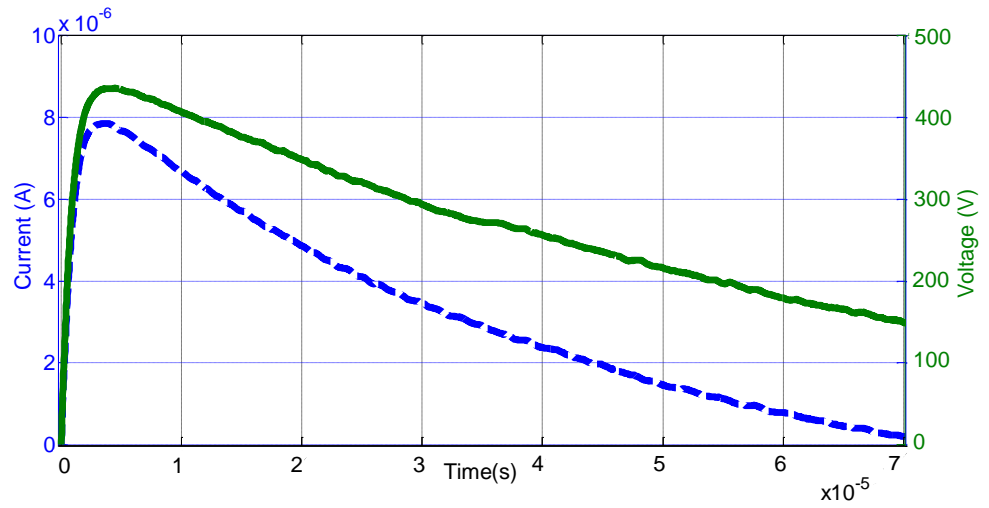
C-1: Voltage and current signals for microvaristor *A* composites in low voltage impulse tests.
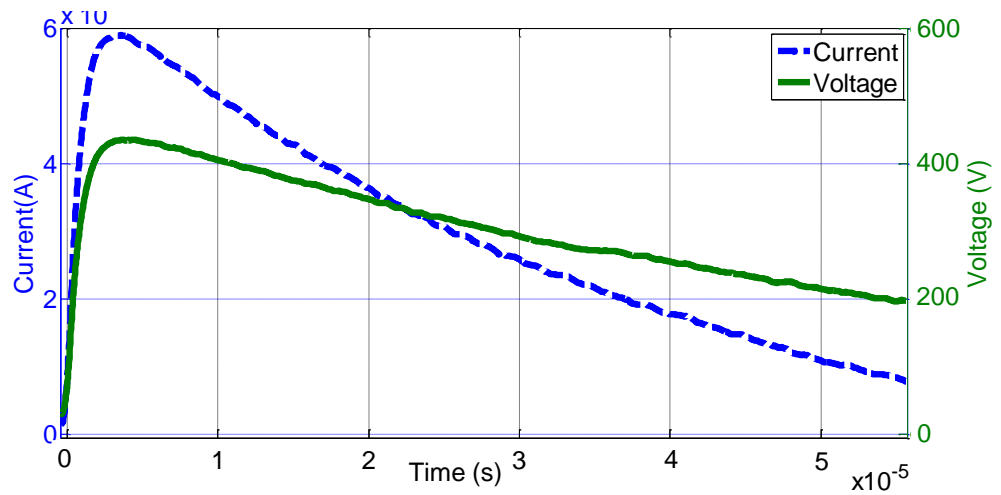
C-2: Voltage and current signals for microvaristor *B* composites in low voltage impulse tests.

Appendix D : Silicone rubber Powersil 600-A /600-B

WACKER

POWERSIL®

Product data

Typical general characteristics	Inspection Method	Value
Product data (uncured)		
Color		Light Grey
Mixing ratio	A : B	9 : 1
Viscosity of mix (shear rate 10 s⁻¹)	ISO 3219	10000 mPa s
Pot life at 23 °C		70 min
Product data (cured)		
Test samples press cured		10 min / 100 °C
Density	ISO 1183-1 A	1,13 g/cm³
Hardness Shore A	ISO 868	30
Tensile strength	ISO 37	6,5 N/mm²
Elongation at break	ISO 37	500 %
Tear strength	ASTM D 624 B	20 N/mm
Dielectric strength (1 mm)	IEC 60243	> 23 kV/mm
Volume resistivity	IEC 60093	10^{15} Ω cm
Permittivity (50 Hz)	IEC 60250	2,9 εr
Dissipation factor (50 Hz)	IEC 60250	3×10^{-4}
Arc resistance	IEC 61621	> 300 s
Tracking resistance	IEC 60587	1A 3.5
Flammability	IEC 60707	FV 0

These figures are only intended as a guide and should not be used in preparing specifications.